AN ANALYSIS OF MODELS FOR ESTIMATING SURFACE NET RADIATION FROM INCOMING SOLAR RADIATION

By

ANTHONY JOHN ARNFIELD, B.A., M.A.

A Thesis

Submitted to the School of Graduate Studies

in Partial Fulfilment of the Requirements

for the Degree

Doctor of Philosophy

McMaster University

May 1973

MODELS FOR ESTIMATING

SURFACE NET RADIATION

DOCTOR OF PHILOSOPHY (1973)
(Geography)

McMASTER UNIVERSITY
Hamilton, Ontario

TITLE: An Analysis of Models for Estimating Surface Net Radiation from Incoming Solar Radiation

AUTHOR: Anthony John Arnfield, B.A. (University of Wales)
M.A. (McMaster University)

SUPERVISOR: Dr. W. R. Rouse

NUMBER OF PAGES: xiv, 241

ABSTRACT

The importance of surface net radiation to several branches of physical environmental research is stressed and the dependence of this flux on surface controls is explored. An analysis of a group of models, employing incoming solar radiation to estimate net radiation, is presented, including a new approach which utilises parameters of greater specificity than appear in previous models. Potentially, this model is applicable in both clear and cloudy conditions. An expression for the parameter representing the intensity of the thermal response of a surface to radiant energy input is obtained analytically for some surfaces and the factors in this expression are discussed for all surfaces.

The diurnal regimes of the radiation budget components for three surfaces - grass, bare soil and a cornfield - are presented in both graphical and tabular form for several days over a growing season. Differences in net radiation totals are shown to be the result of both short- and longwave factors. An analysis of this data reveals that the "heating coefficient" concept is unlikely to be a useful one for estimating net radiation on a routine basis, but that the resolution of the net longwave coefficients into unidirectional components holds some promise. The effect of surface dessication on the thermal response of a surface (and, hence, on net radiation) is apparent in the seasonal behaviour of the outgoing longwave parameters. This behaviour is different for each surface and, for the soil, is

analysed in terms of the thermal and radiative properties specified in the theoretical analysis. Reflection coefficient differences were marked and the seasonal regimes of this parameter differed for each surface. Difficulty was encountered, however, in adequately predicting the parameters representing the influence of variations in atmospheric longwave emission on net radiation totals.

The data collected were used to assess the predictive accuracy of various net radiation equations, over the period of a growing season. It was found that simple linear regression equations with insolation performed as well, in this respect, as the more sophisticated models. The potentially large errors associated with the use of equations derived for different surfaces or locations is demonstrated. The model introduced in this study, however, represents more explicitly the controls on net radiation and could conceivably provide superior estimates of the flux when daily totals are required over periods of time longer than a growing season. Some suggestions for future studies of radiation exchange at the earth-atmosphere interface are presented.

ACKNOWLEDGEMENTS

I would like to express my gratitude to the many people whose advice and assistance were freely given during the field investigation and the preparation of this thesis.

Partic lar thanks are due to Dr. Wayne Rouse, for his advice in supervising the research and revising the text, and for his boundless patience; to Dr. George Collin and his co-workers at the Simcoe Horticultural Experiment Station for providing the site, laboratory facilities and assistance during the field season; to the other members of my supervisory committee, Drs. J.A. Davies, P.J. Howarth and R.L. Judd, for their helpful criticism of earlier drafts; to Mr. J.R. Latimer and his staff at the National Atmospheric Radiation Centre, Scarborough, for their thoroughness in calibrating the sensors; to fellow graduate students in the McMaster and McGill University programmes in microclimatology for help in the field; to Sherry Barhorst for drawing the diagrams; to the Instructional and Research Computing Center of the Ohio State University for providing free computer time.

Finally, I would like to acknowledge the support given me by my friends at McMaster and Ohio State Universities, and, in particular, by my wife, Joan, not merely for typing the final draft of this thesis, but for her fortitude, patience and encouragement during my graduate studies.

TABLE OF CONTENTS

LIST OF PLATES

LIST OF TABLES

LIST OF FIGURES

CHAPTER 1

INTRODUCTION

1.1: Nature of Research Problem.

Net radiation (R_n) is defined as the difference between the sum of the radiant energy inputs to a landscape surface and the sum of its radiant energy losses, i.e.

$$R_n = Q_{\downarrow} + L_{\downarrow} - Q_{\uparrow} - L_{\uparrow} \qquad (1.1)$$

where $Q_{\downarrow}$ is the incoming shortwave[1] (global solar) radiation flux,

$L_{\downarrow}$ is the longwave flux from the atmosphere,

---

1. The terms used to designate the two major spectral regions which may be distinguished within the energetically-important radiation present at the earth's surface are as follows:

   (i) "shortwave radiation" is of solar origin. After being filtered by the atmosphere, the short- and longwave limits, chosen so as to exclude less than one percent of the total flux, are 0.29 μm and 4.00 μm respectively.

   (ii) "longwave radiation" originates within the earth-atmosphere system. Black bodies at a wide range of representative temperatures will radiate between the spectral limits chosen to fulfill the previously mentioned criterion, of 4 and 100 μm.

Fortunately, the discriminant wavelength, 4 μm, corresponds to the longwave cut-off of the glass filters generally used to cover radiometer elements, providing a practical method of separating the two spectral regions. (Special Committee for the International Geophysical Year, 1958; Gates, 1965; World Meteorological Organisation, 1965.)

$Q_{\uparrow}$ is the reflected shortwave radiation and

$L_{\uparrow}$ is the outgoing longwave flux, comprising both emitted and reflected portions.

Net radiation is a term of considerable micrometeorological significance since, in non-advective situations, it represents the sole energy source for the turbulent and conductive energy exchanges at the earth-atmosphere interface. In particular, where soil moisture is non-limiting, evaporation is largely determined by net radiation. Indeed, Thornthwaite and Hare (1965) have suggested that the water equivalent of the net radiation provides an attractive "energetic" definition of the concept of "potential evapotranspiration". Even when evapotranspiration is proceeding at a sub-potential rate, the net radiation is an important term in the "energy balance" (e.g. Tanner, 1960) and "combination model" (Penman, 1948; Slatyer and McIlroy, 1961; Monteith, 1964; Tanner and Fuchs, 1968) approaches to its evaluation. Considerable research effort has been invested in the problem of modelling the surface sensitivity of the evaporative flux, as an aerodynamic and plant physiological process, but scant attention has been paid to spatial variations in the energy supply. Moreover, differences in the radiant energy retention of adjacent landscape elements can give rise to the horizontal gradients of atmospheric properties which initiate advective mass and energy exchanges.

Furthermore, the importance of the role played by the

surface boundary layer in larger-scale atmospheric processes is increasingly being recognised. Computations of the turbulent fluxes of sensible and latent heat at the surface, as lower boundary conditions for models of the free atmosphere, require net radiation data (e.g. Gadd and Keers, 1970). Priestley and Taylor (1972) have stressed the importance of net radiation as a basic synoptic variable and have suggested that estimation procedures should be applicable on a daily basis (a period for which evapotranspiration estimates are also frequently required in agricultural and hydrological studies).

Any attempt to consider the spatial variation of R_n must recognise the surface sensitivity of this flux. Rewriting (1.1) in terms of surface properties,

$$R_n = (1 - \alpha)Q_\downarrow + \left[L_\downarrow - (1 - \epsilon)L_\downarrow - \epsilon\sigma T_s^4\right], \quad (1.2)$$

where α is the shortwave reflection coefficient,

ϵ is the longwave emissivity (and absorptivity),

T_s is the surface temperature and

σ is the Stefan-Boltzmann constant.

Both α and ϵ are functions of the surface material and its configuration, while T_s is related to the thermal properties of the substrate and/or biomass and the relationship between the components of the surface's energy budget.

Unfortunately, despite the availability of a reliable and robust instrument (Funk, 1959), net radiation measurements on a routine basis are scarce. Only nineteen stations regularly measure and report this flux in Canada (Canada, Environment Canada, Atmospheric Environment Service, 1972) and only one in the United States (U.S., Department of Commerce, NOAA, 1972). Moreover, following international meteorological practice, most measurements of R_n are made over a short grass surface (though this may be snow-covered in some areas in winter), the only exceptions being those made in the Canadian Arctic, where a representative non-vegetated surface is used. Accurate extrapolations cannot be made to other surfaces owing to spatial variability in α, ϵ and T_s. Equations (1.1) and (1.2) are of very limited climatological use, since routine measurements of $Q_{\uparrow}$, $L_{\uparrow}$ and $L_{\downarrow}$ are not available and data on the spatial and temporal variation of ϵ are scarce. The concept of "surface temperature" is poorly defined for all but the simplest (planar) surfaces and the sampling and exposure problems posed by direct thermometry are virtually prohibitive. Indeed, the most practical method of estimating T_s for plant canopies and similar complex landscape units is by radiative means.

The only term in (1.2) for which data are available on a routine basis is $Q_{\downarrow}$. Forty-five stations in Canada (Canada, Environment Canada, Atmospheric Environment Service, 1972) and eighty in the United States (U.S., Department of Commerce, NOAA, 1972) regularly measure and report this flux. Consequently,

several empirical models have been proposed for the estimation of R_n, using $Q_\downarrow$ as the principal predictive variable.

1.2: Modelling of Net Radiation.

The discussion of the previous section suggests, in the opinion of the author, that a microclimatological model for the estimation of net radiation might usefully satisfy the following criteria. It should:

(i) preserve a degree of surface sensitivity appropriate to the scale of application,

(ii) use $Q_\downarrow$ as the major predictive variable,

(iii) be applicable on a daily basis and

(iv) use, wherever possible, readily available input data.

However, since neither $Q_\downarrow$ nor the types of data referred to in (iv) are strongly surface sensitive, (i) can be satisfied only by the inclusion of appropriate surface dependent parameters.

Shortwave behaviour is conveniently characterised by the reflection coefficient. However, in the longwave spectral region, the problem is more complex, since a surface will not only reflect but also emit. Moreover, variations in the incoming component cannot be explicitly incorporated. Clearly, parameters defined for use in any predictive model must exhibit properties appropriate to this function. Either they must be constant or they must vary in a manner which is predictable from data which are more readily obtained than is the predictand.

The problem of finding parameters which satisfy these criteria is hampered by the scarcity of information on the components of the radiation budget, especially on the partitioning of the net longwave flux. In this study, careful measurements were made of a number of these components, for each of three dissimilar surfaces, from which all of the terms in (1.1) could be derived. The investigation was conducted on the Ontario Horticultural Experiment Station at Simcoe, Southern Ontario (42^{o} 50' N, 80^{o} 19' W), during July, August and September, 1969. These measurements provided the basic data for subsequent investigation of the surface dependence of net radiation.

CHAPTER 2

THEORY, LITERATURE REVIEW AND RESEARCH OBJECTIVES

In the previous chapter, reference was made to a group of net radiation estimation models using $Q_{\downarrow}$ as the principal predictive variable. The members of this group are as follows:

(i) simple linear regression models,

(ii) the "clear sky" models of Monteith and Szeicz (1961) and Gay (1971),

(iii) models, derived from those in (ii), in which surface and atmospheric influences on the longwave regime are incorporated separately.

Since these are essentially first, second and third generation applications of the same fundamental concept, the characteristics and limitations of the linear regression and "clear sky" models will be reviewed, prior to the development and description of those, in category (iii), which are the major concern of this investigation.

2.1: Linear Regression Models.

Since Fleischer (1953/54) drew attention to the good linear relationships which exist between R_n and $Q_{\downarrow}$, numerous determinations of the parameters of

$$R_n = BQ_{\downarrow} + a \qquad (2.1)$$

have been made. The table in Appendix 1 lists the sources of such analyses. The correlation between these two variables is high, generally exceeding 0.98, even when data from cloudy periods are included. This implies that the residual components of R_n are either constant over the period of analysis or that they also are highly correlated with $Q_{\downarrow}$. Nevertheless, the longwave terms, as a result of their dependence on surface heating, exhibit a slight phase lag behind $Q_{\downarrow}$, which also effects R_n. Hence, for a given value of $Q_{\downarrow}$, R_n is larger in the morning than in the afternoon. Occasionally, this phenomenon is indistinct or even reversed, and is most likely to owe its origin to the development of cloud, which disturbs the diurnal cycles of solar radiation and surface heating, and gives rise to large fluctuations in atmospheric longwave emission which are not closely related to atmospheric temperature. The high correlations mentioned, however, indicate the small magnitude of the phase lag effect. Nevertheless, the non-random nature of the distribution of the deviations from the regression line precludes the use of the standard error of the estimate in an inferential sense.

The parameters of (2.1) are frequently evaluated from instantaneous flux data, even when the net radiation estimates

required are daily totals or daily means. A brief discussion of the validity and implications of this procedure is appropriate at this point. Equation (2.1) may be most properly written, in its exact form, as

$$R_n = BQ_{\downarrow} + a + E \ , \qquad (2.2)$$

where E is an "error" term associated with the phase lag between the incoming shortwave radiation and the longwave fluxes, plus instrumental and sampling errors. The models discussed in this investigation are primarily intended for the estimation of total net radiation during a daylight period. Integrating (2.2) over a period $(t_2 - t_1)$ gives

$$\int_{t_1}^{t_2} R_n \, dt = B \int_{t_1}^{t_2} Q_{\downarrow} \, dt + \int_{t_1}^{t_2} a \, dt + \int_{t_1}^{t_2} E \, dt \ .$$

If the period of integration extends over a whole daylight period, or over any sufficiently long interval that both surface heating and cooling phases are encountered and are approximately of equal length,

$$\int_{t_1}^{t_2} E \, dt \longrightarrow 0 \ .$$

Denoting integrated totals by brackets[1] gives

$$\left[R_n\right] = B\left[Q_{\downarrow}\right] + Pa \ , \qquad (2.3)$$

where $P = t_2 - t_1$. If $Q_{\downarrow}$ is daily total insolation, P is day length and may be calculated from solar declination and station latitude (Sellers, 1965). Since insolation will generally be expressed as a daily total or as the integral mean $\left[Q_{\downarrow}\right]/P$, (2.3) is potentially the most useful form of the equation for routine use.

B values reported in the literature range from 0.326 to 1.350, with a mean of 0.759. Variation in this term can be expected since both the absolute magnitude and diurnal fluctuation of α, $L_{\downarrow}$ and $L_{\uparrow}$ will determine its value. Even for a single surface, variations in plant height, moisture stress, vegetation ground cover and atmospheric emission may be expected to influence the magnitude of the coefficient.

A potentially more stable relationship results from the use of the net shortwave radiation, rather than $Q_{\downarrow}$, as the independent variable, thus eliminating the shortwave influences on the regression coefficient. Relationships of the form

---

1. This convention is followed henceforth. All bracketed quantities will be expressed in J m^{-2}.

$$R_n = b(1 - \alpha)Q_{\downarrow} + a \qquad (2.4)$$

exhibit the same high correlations and phase lag effects which were noted for (2.1). For daily estimates, (2.4) becomes

$$\left[R_n\right] = b(1 - \alpha)\left[Q_{\downarrow}\right] + Pa \ . \qquad (2.5)$$

Sources of regression coefficient data are listed in Appendix 1.

Values of b reported in the literature range from 0.663 to 1.610, with a mean of 0.949. The coefficient of variation is slightly smaller than that of B (Table 2.1), signifying a more stable term, though this characteristic is more clearly illustrated if the extreme range of published values is expressed as a percentage of the mean.

Nevertheless, variations in the term b are large, even when the individual determinations are grouped by surface type and/or sky condition. For example, clear sky evaluations for grass range between 0.720 and 1.198; those for bare soil, between 0.696 and 0.97. Much of this variation is due to the influence of surface properties and atmospheric behaviour on the diurnal course of the net longwave radiation.

Linacre (1968) attempted to show that the coefficients of such models could be obtained <u>a priori</u>, but was successful in his aim only for a very limited set of surfaces, and then only by

TABLE 2.1

VARIATION OF THE COEFFICIENTS B AND b.

Coefficient	Mean	Standard Deviation	Maximum Value	Minimum Value	Total Range	Percent of Mean	
						Standard Deviation	Total Range
B	0.759	0.131	1.350	0.326	1.024	17	135
b	0.949	0.139	1.610	0.663	0.947	15	100

making use of a number of empirical relationships, the coefficients of which were functions of surface type, surface condition, climate and season.

2.2: The "Clear Sky" Models of Monteith and Szeicz (1961) and Gay (1971).

Variations in the diurnal behaviour of the net longwave radiation may thus be responsible for observed differences in the coefficient b. This dependence is made explicit in the concept of the "heating coefficient", introduced by Monteith and Szeicz (1961).

The defining radiation balance equation (1.1) can be stated in terms of the net shortwave (Q_n) and net longwave (L_n) fluxes as

$$R_n = Q_n + L_n \,, \tag{2.6}$$

which satisfies the regression relation (2.4) only when L_n is a linear function of R_n, of the type

$$L_n = \frac{a}{b} - R_n \left(\frac{1 - b}{b}\right)$$

$$= \frac{a}{b} - R_n \beta' \,.$$

The term β' is thus $-dL_n/dR_n$, the change in net longwave loss per unit change in net radiation input. Under clear sky conditions, Monteith and Szeicz postulated that $L_{\downarrow}$ would be virtually constant on a diurnal basis. The fluctuation in L_n would then be entirely determined by the diurnal changes in $L_{\uparrow}$. Since the amplitude of $L_{\uparrow}$ is a function of the daily wave of surface temperature, they regarded β' as a "heating coefficient", a measure of the magnitude of the thermal response of a surface to unit net radiation input..

It should be noted that the direct regression of L_n on R_n will yield a slightly different value of $-dL_n/dR_r$ (termed β henceforth) from that computed from b. The relationship between β' and β is clarified if the definition of the former parameter is expanded in terms of the component net fluxes of R_n, i.e.

$$\beta' = (1 - b)/b$$

$$= \frac{\left(\sum(Q_n^2) - n\bar{Q}_n^2\right) - \left(\sum(Q_n R_n) - n\bar{Q}_n\bar{R}_n\right)}{\left(\sum(Q_n R_n) - n\bar{Q}_n\bar{R}_n\right)},$$

where the bar denotes a mean flux and n is the number of data points. Since $Q_n = R_n - L_n$

$$\beta' = -\frac{\left(\sum(L_n R_n) - n\bar{L}_n\bar{R}_n\right) + \left(\sum(L_n^2) - n\bar{L}_n^2\right)}{\left(\sum(R_n^2) - \bar{R}_n^2\right) - \left(\sum(L_n R_n) - n\bar{L}_n\bar{R}_n\right)}.$$

By definition,

$$\beta = -\frac{\sum(L_n R_n) - n\bar{L}_n\bar{R}_n}{\sum(R_n^2) - n\bar{R}_n^2} ,$$

therefore,

$$\beta - \beta' = \beta\beta' - \frac{\sum(L_n^2) - n\bar{L}_n^2}{\sum(R_n^2) - n\bar{R}_n^2} . \qquad (2.7)$$

The second term on the right-hand side of (2.7), which is equivalent to the ratio of the variance of L_n to that of R_n, is always positive and larger than $\beta\beta'$. Hence, $(\beta - \beta') < 0$. This difference is, moreover, variable and bears no unique relationship to either β or β', since these parameters are also determined by the covariance of L_n and R_n. The two methods of obtaining $-dL_n/dR_n$ will give the same results only in the trivial (and physically improbable) case when L_n is diurnally constant and $\beta = \beta' = 0$. Some implications of this inequality will be treated in section 2.5.

Since $b = 1/(1 + \beta')$, (2.5) becomes the Monteith and Szeicz form of the radiation balance equation,

$$\left[R_n\right] = \frac{(1 - \alpha)}{(1 + \beta')}\left[Q_{\downarrow}\right] + PL_o , \qquad (2.8)$$

in which L_o replaces a, to emphasise that, at zero insolation, R_n consists solely of the net longwave term.

Monteith and Szeicz hypothesised that, for clear days, α and β' would be surface-sensitive parameters and L_o could be approximately computed using an empirical relationship for L_n, such as that of Brunt (1932). Since the absolute magnitude of L_o is much smaller than the first term, a relatively large error in its calculation would not unduly effect the estimate of R_n. However, it is again worth emphasising that if (2.8) is to be generally useful for routine calculations of R_n, the parameters α, β' and L_o must be known a priori.

Monteith and Szeicz suggest that, for most agricultural and similar natural vegetation, $\beta' \approx 0.1$ if a complete ground cover exists and the plants are never short of water. If evapotranspiration is sub-potential, either as a result of incomplete ground cover or the physiological restriction of transpiration, $0.1 < \beta' < 0.2$. For very dry soils, $0.3 < \beta' < 0.4$.

The model of Gay (1971) is essentially identical to the previous one, though he chose to solve (2.4) and (2.6) for dL_n/dQ_n, which he denotes λ and calls the "longwave exchange coefficient". He argues its superiority over the β' coefficient from a statistical standpoint. It is appropriate at this point to examine the validity of Gay's criticism of the Monteith and Szeicz approach, which concerns the practice of performing regression and correlation analysis between two variables, one of which is, by

definition, a component of the other. Much of his discussion centres on the use of correlation analysis. Clearly, to use the correlation of R_n and $Q_{\downarrow}$ as an example, since $Q_{\downarrow}$ is a major component of the dependent variable, a certain inherent linearity is assured. While this characteristic could be disturbed by random fluctuations or non-linear behaviour of the residual terms ($Q_{\uparrow}$, L_n), it is nevertheless a matter of observation that surface temperature (and, hence, $L_{\uparrow}$), the incoming longwave flux and the reflection coefficient tend to be serially correlated with $Q_{\downarrow}$, though small phase differences may exist. It is, thus, virtually inevitable that the correlation between R_n and $Q_{\downarrow}$ will be high, though this in no way invalidates the procedure of computing r, which has value as a purely descriptive statistic. Even less does this argument invalidate the use of the regression slope as an estimate of the change in R_n, per unit change in $Q_{\downarrow}$. These remarks are equally relevant to the practice of computing β by the regression technique.

Both the direct and indirect methods of calculating λ will give identical results since, from the definitions of λ and b and setting $Q_n = R_n - L_n$,

$$\lambda = b - 1$$

$$= \frac{\sum(L_n Q_n) - n\bar{L}_n\bar{Q}_n}{\sum(Q_n^2) - n\bar{Q}_n^2} . \qquad (2.9)$$

The expression on the right-hand side of (2.9) is the slope of the regression line of L_n on Q_n.

Substitution for b in terms of λ in (2.5) yields the Gay form of the radiation balance equation,

$$\left[R_n\right] = (1 + \lambda)(1 - \alpha)\left[Q_{\downarrow}\right] + PL_o \; . \qquad (2.10)$$

λ is an expression of the same surface response as β', providing that the same assumption is made concerning the diurnal behaviour of $L_{\downarrow}$, large negative values denoting a marked thermal response to radiant energy input. Since both parameters are derived from the coefficient b, they may be related by

$$\lambda = - \beta' / (1 + \beta') \; . \qquad (2.11)$$

However, determinations of the net longwave parameters β' and λ by numerous authors, using data collected for several different surfaces, have revealed a number of major problems in their interpretation, which are explored in detail in section 2.4. Prior to this, consideration will be given to some aspects of the behaviour of the reflection coefficient.

2.3: The Reflection Coefficient.

Many determinations of α values for numerous landscape surfaces have been made since the classic measurements of

Ångström (1925). Consideration, therefore, will be restricted primarily to data relevant to the three surfaces used in this investigation - grass, soil and corn. Table 2.2 lists a number of α evaluations which have been made for these surfaces. In each case it is clear that α is not a stable term.

There are two major categories of factors which have been shown to influence the reflection coefficient:

(i) environmental factors, which may be expected to effect all surfaces similarly,

(ii) surface factors, which depend upon the particular physical and biotic characteristics of a landscape element and will not necessarily be generally significant.

In either case, a knowledge of such dependencies is necessary for successful a priori estimation of the α parameter.

The diurnal dependence of α on solar zenith angle has been noted by many workers, including Graham and King (1961), Davies (1967), Davies and Buttimor (1969), Kyle (1971) etc. Two reasons have been cited for this. Firstly, with decreasing zenith angle, a larger proportion of the direct beam radiation penetrates into a vegetation canopy, and is absorbed in the process of multiple reflection within it. Secondly, with increasing optical air mass, a larger proportion of the incoming solar radiation is found in the near infra-red region (Kondrat'yev, 1969), in which the reflectance of plant tissues is considerably higher than that in the visible and ultra-violet portion of the solar spectrum (Gates, 1965).

TABLE 2.2

REFLECTION COEFFICIENTS FOR GRASS, BARE SOIL AND CORN

Source	Grass α	Bare Soil α	Cornfield α
Allen and Brown (1965)			0.235
Allen et al (1964)			0.17
Ångström (1925)	0.25 -0.33	0.09 -0.18	
Barry and Chambers (1966)	0.223-0.263	0.184	
Brown and Covey (1966)			0.17
Budyko (1956)	0.15 -0.25	0.05 -0.45	
Davies (1967)	0.25		
Davies and Buttimor (1969)	0.20 -0.25	0.199	0.22 -0.26
de Boer (1959)	0.20		
Decker (1966)	0.132-0.244		
Ekern (1965)	0.16	0.08	
Fritschen (1967)		0.14 -0.24	
Fritz (1948)		0.08 -0.12	
Graham and King (1961)			0.17 -0.19
Haise et al (1967)			0.17 -0.18
Idso (1971)	0.140-0.243	0.143-0.244	
Idso et al (1969)	0.26 -0.27	0.28 -0.29	
Impens and Lemeur (1969)			0.2
Kalitin (1930)	0.14 -0.37		
Kondrat'yev (1969)	0.26		
Kuhn and Suomi (1958)	0.17 -0.21		
Kung et al (1964)			0.12 -0.14
Kyle (1971)			0.213-0.240
Lemon (1963)			0.21
Monteith (1959)	0.24 -0.26	0.11 -0.18	
Monteith and Szeicz (1961)	0.25 -0.27	0.17	
Oguntoyinbo (1970)		0.09 -0.17	
Polavarapu (1970)	0.211-0.214		
Rider and Robinson (1951)	0.208		
Scholte Ubing (1961)	0.20		
Shinn and Lemon (1962)			0.20
Stanhill and Fuchs (1968)		0.13	
Stanhill et al (1968)		0.10 -0.11	0.153-0.210

Nevertheless, Fritschen (1967) has denied the reality of the phenomenon, suggesting that the interception and refraction of the incoming solar beam by the dome of an inverted pyranometer measuring $Q_{\uparrow}$ may give rise to spuriously high reflection coefficients at high zenith angles. Brown et al (1970) found that the use of a shading ring, designed to prevent any such error, reduced significantly the apparent reflected flux but failed to eliminate the diurnal pattern. Stanhill et al (1966) could detect no strong dependence of α on zenith angle for eleven natural and agricultural vegetation associations in Israel and Kuhn and Suomi (1958) found no diurnal pattern in evaluations of the parameter from aircraft-based measurements of reflected radiation, using a beam reflector. However, both Monteith and Szeicz (1961) and Davies (1967) have found the dependence of α on zenith angle to be more pronounced for rough surfaces, suggesting that measurement errors cannot entirely explain this phenomenon. If such a pattern exists on a diurnal basis, any dependence on the annual course of mean daily zenith angle must be considered in selecting an appropriate value of α for use in a net radiation estimation equation.

The second major environmental influence is that of cloud and atmospheric haze or, more specifically, the proportion of $Q_{\downarrow}$ that is diffuse. This has been shown to have two main effects. Firstly, the magnitude of daily mean α may be influenced by the presence of cloud cover. Rijks (1967), Grulois (1968), Impens and

Lemeur (1969) and Kalma and Stanhill (1969) have measured higher reflection coefficients in cloudy conditions, although Stanhill et al (1966) and Stanhill and Fuchs (1968) could detect no clear trend in this respect. Secondly, the presence of cloud will reduce the dependence of α on zenith angle, since radiation penetration into a crop canopy will be less a function of solar elevation with diffuse radiation (Graham and King, 1961; Impens and Lemeur, 1969; Kyle, 1971).

Although environmental influences are clearly of significance, undoubtedly part of the variance in α determinations can be attributed to diurnal or seasonal changes in the radiative properties of the surfaces themselves. This is particularly significant with bare soils, which exhibit considerable variations in component materials and in surface roughness, both factors which may be expected to influence a soil's reflective properties (Budyko, 1956; Kondrat'yev, 1969). Water is, of course, a variable constituent of soils and has a lower reflectivity over the solar spectrum than that of organic and mineral soil constituents. Many investigations have drawn attention to the inverse relationship which exists between α and soil moisture content (Monteith, 1959; Fritschen, 1967; Oguntoyinbo, 1970; Idso, 1971).

Monteith (1959) has noted the apparent uniformity, around 0.26, of the reflection coefficient for short, green agricultural crops and similar natural vegetation, with a complete ground cover. He argues that, since the spectral properties of most leaves will

be similar, α must be primarily a function of the disposition of plant material within the canopy and will, therefore, be virtually identical for vegetation with similar growth habits. Since most soils are less efficient reflectors than plant canopies, α will increase with ground cover, until a maximum is reached when the soil is virtually obscured. The values in column one of Table 2.2, with the exception of the early data of Ångström (1925) and Kalitin (1930), support Monteith's contention.

Monteith also notes that the reflection coefficients of several crops are independent of crop colour. This is attributable to the relatively large proportion of $Q_{\downarrow}$ which lies outside the visible wavelengths. Also of note in this respect is the eye's inefficiency in judging the comparative reflectivity of surfaces of different colours.

Dew deposition has been shown to increase α (Monteith, 1959; Monteith and Szeicz, 1961; Oguntoyinbo, 1970), though this can hardly be expected to significantly influence the daily mean. An inverse relationship between α and crop height has been noted by Kalma and Stanhill (1969) and Oguntoyinbo (1970), for a number of vegetation types. The reflection coefficient evaluations of Idso (1971), for grass, appear to confirm this trend, for a plant height range between 0.1 and 1.04 m.

Corn exhibits a lower α than grass (Table 2.2), presumably since its open structure and greater height permit a more

efficient multiple reflection process within its canopy. Despite the inverse relationship of α with crop height, Graham and King (1961) and Davies and Buttimor (1969) have noted an increase in reflection coefficient over the growing season, suggesting that the increasing ground cover and decreasing daily mean solar zenith angle factors outweigh the effect of crop height. Stanhill et al (1968) draw attention to the good linear relationship which exists between corn α and crop leaf area index. They feel, however, that this is due primarily to the mutual dependence of both variables on ground cover. Their investigation also noted an initial increase in α over the season, followed by a gradual decrease as canopy structure degenerated.

Asymmetry in the diurnal pattern of α has been noted for corn, by Graham and King (1961), Stanhill et al (1968) and Impens and Lemeur (1969), and for other vegetation types, by Kalma and Stanhill (1969) and Oguntoyinbo (1970), larger values being detected in the afternoon at a given solar zenith angle. Possible explanations of this behaviour are:

(i) a crop row orientation which is neither parallel nor orthogonal to the N-S line,

(ii) a change in the spectral properties of leaves during the day and/or

(iii) a diurnal change in the disposition of the leaves within the canopy.

Asymmetry in the diurnal course of α has been recorded for a crop

planted in rows oriented N-S (Stanhill et al, 1968), suggesting that (ii) and/or (iii) must be significant.

Since the effects of water stress could be expected to effect the spectral properties of individual leaves and to influence the disposition of leaves within the canopy, a dependence of mean daily α on soil moisture content might be expected. However, Stanhill et al (1968) could detect no significant difference between the reflection coefficients of corn crops subjected to different irrigation treatments and Kalma and Stanhill (1969) found no dependence of orange orchard α on soil moisture. On the contrary, Rijks (1967) measured differences of 0.02 between cotton crops subjected to different levels of moisture stress. Since the reflection coefficients of individual leaves were shown to be identical, such a phenomenon must be attributed to the change in orientation of the leaves within the canopy, as a result of wilting.

Graham and King (1961) and Stanhill et al (1968) could detect no effect on corn α of the appearance of male inflorescences, despite the colour change which this induces. The former study also revealed no significant change in α when frost damage caused the crop to turn brown.

2.4: The Net Longwave Coefficients.

Appendix 1 lists the sources of almost four hundred evaluations of the coefficient b, for each of which can be

computed a corresponding β' or λ value. However, attempts to derive representative and predictively useful values of these parameters have met with little success. For convenience, the following discussion will make explicit mention of the term β' only. Since λ is uniquely related to β' by (2.11), the implications of the behaviour of these two parameters are identical.

The major difficulty associated with the net longwave coefficients lies in their apparent instability. β' values for alfalfa, for example, fall between 0.358 and -0.082, with a coefficient of variation of 90% (Fritschen, 1967; Idso et al, 1969; Idso, 1971). Even greater instability is indicated for grass and corn in Table 2.3.

A further complication arises since many evaluations of β' have been made for days on which cloud was present. Since Monteith and Szeicz's interpretation of β' as a surface parameter is justified only when $L_{\downarrow}$ is diurnally constant, any correlations established between β' values derived on such days and surface characteristics must imply that:

(i) only small changes in $L_{\downarrow}$ took place, which were unable to mask the dependence of L_n on surface heating or

(ii) the diurnal pattern of $L_{\downarrow}$ is a relatively constant feature of successive days, leaving daily variations in $L_{\uparrow}$ to explain the variance in β'.

The effect of the inclusion of data derived from cloudy periods on the magnitude of β' is rather indeterminate. Impens

TABLE 2.3

PUBLISHED VALUES OF β' FOR GRASS, BARE SOIL AND CORN

Surface	Data Set	Maximum Value	Minimum Value	Mean	Median	Standard Deviation	Coefficient of Variation x 10^2	Number of Determinations	Percentage of Values < 0	Sources*
Grass	C	0.390	-0.165	0.055	0.044	0.122	222	78	41	1,5,6,7,8,9,12,13,14,19,23,24,25,26,30..
	A	0.459	-0.326	0.043	0.010	0.141	327	160	47	
Bare Soil	C	0.438	0.030	0.246	0.220	0.111	45	21	0	5,8,13,14,19,28.
	A	0.438	0.030	0.245	0.220	0.110	45	23	0	
Corn	C	0.280	0.030	0.127	0.099	0.118	93	4	0	5,15,17,18,27.
	A	0.308	-0.250	0.138	0.150	0.136	99	23	13	

C - clear conditions only.
A - all data.
* - numbers refer to references listed in Appendix 1.

and Lemeur (1969), in a study of the radiation balance of field crops, measured lower β' values for cloudy weather than for clear, whilst Shaw (1956) and Kyle (1971) found the opposite effect. Davies and Buttimor (1969) and Kalma and Stanhill (1969) could find no correlations between β' and cloud cover. In Table 2.3, mean β' is lower for grass, when evaluations from cloudy periods are included, but corn exhibits the opposite trend. In both cases where all data are used, however, a larger proportion of determinations is negative.

Large deviations exist between the magnitude of the evaluations presented in the literature and the values which Monteith and Szeicz (1962) suggest might be typical of common surface types. In particular, the large proportion of very small or negative determinations should be noted. Of the 391 evaluations available for all surfaces, 63% are less than 0.1, which was suggested would be typical of short vegetation transpiring at the potential rate, and 35% are negative. If the assumption of a constant atmospheric longwave emission may be regarded as valid, near zero values of the β' parameter suggest that surface temperature is virtually independent of radiant energy input, implying that the atmosphere must be an extremely efficient convective heat sink or that the substrate is equally effective in conducting absorbed radiant energy to depth. A negative value implies that surface temperature is inversely related to net radiation, an unlikely situation for many of the surfaces for which such

values have been found, where aridity precludes even the possibility of strong evaporative cooling.

Table 2.4 lists β' values for a number of surfaces, derived from clear sky measurements only, and ranked from largest to smallest. No explanation may be offered for the order of the ranking, though it is noteworthy that the surfaces whose daily amplitude of surface temperature might be expected to be extreme (bare soil, desert and lava) are in the top half of the table. Why the thermal response of wheat should equal that of lava or why sugar beet should fall between desert and bare soil, is, however, inexplicable. Stanhill et al (1966) could find no relationship between the botanical or ecological features of vegetation surfaces and β' and Davies and Buttimor (1969) could detect no significant difference between β' values for a number of field crops.

Nevertheless, some success has been achieved in relating fluctuations in β' to surface characteristics, suggesting that the apparent instability of the parameter is, in part, related to real changes in surface properties. The most commonly sought relationship, in agricultural crop studies, has been that between β' and evaporation rate. However, since the latter variable is not measured on a routine basis in most locations and data is frequently not available, even in an experimental investigation, the following surrogates have been used:

(i) irrigation cycles and precipitation regime (representing soil moisture),

TABLE 2.4

PUBLISHED CLEAR SKY EVALUATIONS OF β' FOR A NUMBER OF SURFACES

Surface	Mean	No. of Determinations
Bare soil	0.246	21
Sugar beet	0.210	1
Desert, with dwarf shrubs	0.180	1
Wheat	0.150	1
Lava	0.150	2
Corn	0.127	4
Alfalfa	0.103	51
Orange orchard	0.070	1
Grass	0.055	78
Pine forest	0.030	1
Sugar cane	0.030	1
Pineapple	-0.015	2
Cotton	-0.060	1

(ii) percentage ground cover,

(iii) windspeed (representing the intensity of atmospheric turbulent activity).

Stanhill and Fuchs (1968), evaluating β' for cotton from their own data and that of Zuev (1956), noted a tendency for lower values during the irrigation period. However, Kalma and Stanhill (1969) could find no relationship between β' and the seasonal distribution of precipitation and soil moisture.

A similar trend in the seasonal behaviour of β' for cotton is exhibited by the data of Zuev (1956), Fritschen (1967) and Stanhill and Fuchs (1968), with high values at the beginning of the season, when ground cover is incomplete, smaller, even negative, values when the crop reaches its maximum height, and some indication of a rise again toward the end of the season. This pattern is discernible in the mean values only, however, and is considerably disturbed by apparently random diurnal fluctuations. Davies and Buttimor (1969) detected no clear trend in time as the ground cover of a number of field crops increased.

The original evaluations of Monteith and Szeicz (1961) suggested an inverse relationship between β' and windspeed, more rapid air movement permitting a greater degree of turbulent mixing and greater convective heat loss from the surface. Davies and Buttimor (1969) and Kalma and Stanhill (1969), however, could detect no relationship of this type.

The only study in which evaporative rates were actually

measured is that of Idso (1971). Sudangrass, irrigated at the beginning of the study period and permitted to dry out subsequently, showed a general trend from low β' values (around -0.1) to high values (up to 0.123), but evaporation rates measured on days when $\beta' < 0$ were not significantly greater than those when β' exceeded zero. For regularly irrigated sudangrass, the correlation between β' and evaporation rate was 0.652, days with negative β' values having 50% more evaporation than those with $\beta' > 0$. Bare soil data, however, showed no relationship between β' and evaporation. For an alfalfa crop, there was a general trend, though with many individual exceptions, for β' to be inversely related to crop height, presumably because the increased surface roughness and larger leaf area index of the taller crop result in a larger vapour flux and, hence, increased evaporative cooling. For sudangrass, the same relationship between crop height and β' was noted, except for two days on which inflorescences were present on the taller crop, when the reverse was true. Idso postulates that a significant proportion of the incoming shortwave flux will be intercepted by the inflorescences and converted to sensible heat, since the flower parts are not capable of transpiring to the same degree as the leaves. In addition, Fritschen and van Bavel (1964) hypothesise that the seedheads may constitute a barrier to the aerodynamic transport of sensible and latent heat. Both processes would tend to increase the surface temperature of the crop and, hence, increase β'. Despite these broad trends,

however, daily β' values were extremely variable and the selection of an appropriate value of the parameter to represent a given crop and crop condition would necessarily be largely arbitrary.

The problem of very small and negative β' determinations remains largely unresolved, although Kalma and Stanhill (1969) have suggested that such values may be related to the diurnal pattern of shortwave absorbtion, in canopies having a considerable vertical development and an open structure. At maximum $Q_{\downarrow}$, radiation will penetrate into the canopy and the major zone of absorption will be in the lower layers, thus reducing the direct solar heating of the upper surface and, hence, $L_{\uparrow}$. At low $Q_{\downarrow}$, absorption is at the surface of the canopy. Such a pattern would tend to reduce the diurnal change in $L_{\uparrow}$ and, in the extreme case, could even invert the familiar daily wave of surface radiative temperature. Nevertheless, this explanation could hardly be invoked to account for the small β' values found for such surfaces as grass and bare soil.

The major conclusion to emerge from the published values of β' is that the assumption of diurnal $L_{\downarrow}$ constancy for clear days cannot be accredited general validity. Fig. 2.1 presents data, from several authors, on the diurnal fluctuation of $L_{\downarrow}$ that may be expected in cloudless conditions. Not only can this fluctuation be large, but the diurnal pattern is very variable. The dependence of atmospheric emission on cloud type and amount is well known (Sellers, 1965; Kondrat'yev, 1969). Stanhill et al (1966 and 1968)

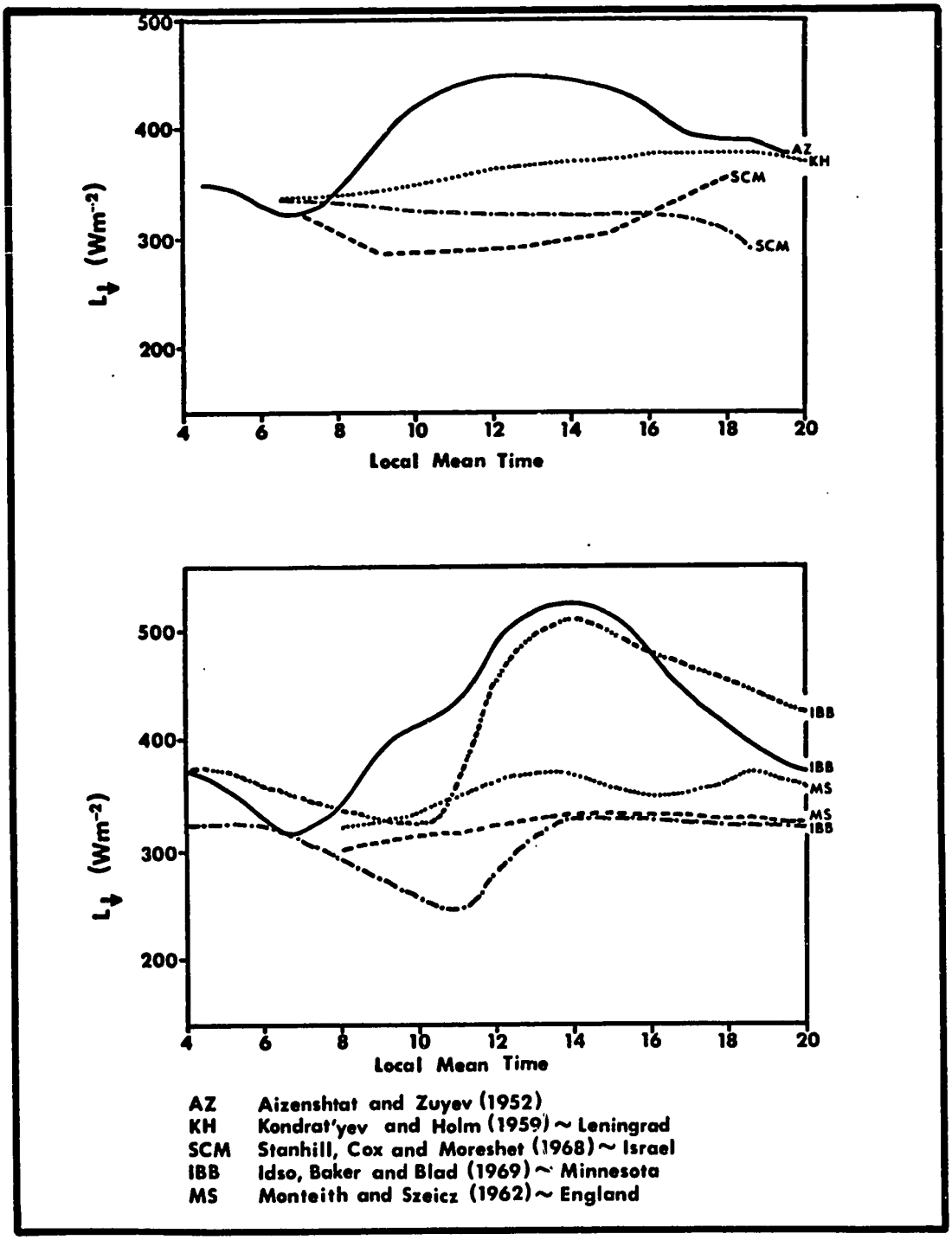

Figure 2.1: The diurnal fluctuation of atmospheric longwave emission on clear days.

found fluctuations of up to 280 W m^{-2} due to the onset of cloudy conditions. Clearly, whenever the amplitude of the diurnal wave of incoming longwave radiation is similar to that of $L\uparrow$, L_n will be virtually constant and $\beta' \approx 0$. When a surface does not exhibit a strong thermal response to radiation input, as with irrigated agricultural crops, the diurnal fluctuation of $L\downarrow$ may exceed that of $L\uparrow$ and negative values of β' will ensue. On the other hand, when the daily curve of $L\downarrow$ is concave upwards (e.g. that of Stanhill et al in Fig. 2.1), the amplitude of the wave of L_n will be increased and β' will tend to be larger. Stanhill et al (1966) postulate that strong fluctuations in $L\downarrow$ on clear days may be linked to diurnal changes in atmospheric dust content, in phase with surface heating and turbulent activity. Idso et al (1969) reject this hypothesis and suggest, with Hall (1968), that large variations in emission in the 8 - 13 μm band, linked with cirrus cloud development, undetectable to the ground-based observer, may be responsible.

It is apparent that considerable confusion exists regarding the meaning of the net longwave coefficients β' and λ. Clearly, the tabulation of representative values of these parameters for different surface types is not yet feasible. Indeed, since they have been shown to be as much dependent on atmospheric behaviour as on surface properties, such a tabulation cannot be regarded as a valid objective of research in this field. In an attempt to clarify this situation and to formalise the separation of the

atmospheric and surface influences, the models described in the following section are proposed. A study of the characteristics of these models is the prime purpose of this investigation.

2.5: Generalisation of the Net Longwave Coefficients and Modified Models.

Since, by definition, $\beta = -dL_n/dR_n$, $\lambda = dL_n/dQ_n$ and $L_n = L_\downarrow - L_\uparrow$, the net longwave coefficients may be simply expressed in terms of their components and the following new parameters defined:

$$\beta = -dL_n/dR_n = -(dL_\downarrow/dR_n - dL_\uparrow/dR_n) = \beta_\uparrow - \beta_\downarrow \qquad (2.12)$$

and

$$\lambda = dL_n/dQ_n = dL_\downarrow/dQ_n - dL_\uparrow/dQ_n = \lambda_\downarrow - \lambda_\uparrow \ . \qquad (2.13)$$

The parameters $\beta_\downarrow$ and $\lambda_\downarrow$ are partially dependent upon surface characteristics, since surface-dependent fluxes (R_n and Q_n) enter into their calculation. An investigation of the degree to which they vary between surfaces is one of the purposes of this study. Furthermore, for any surface with an emissivity significantly less than unity, $\beta_\uparrow$ and $\lambda_\uparrow$ will be partially influenced by atmospheric behaviour, through longwave reflection. However, in general, $\beta_\uparrow$ and $\lambda_\uparrow$ may be regarded as surface parameters and $\beta_\downarrow$ and $\lambda_\downarrow$

characterise atmospheric behaviour.

The assumption of a constant incoming longwave flux is clearly equivalent to the condition that $\beta_{\downarrow} = 0$ and $\lambda_{\downarrow} = 0$. Then, $\beta = \beta_{\uparrow}$ and $\lambda = -\lambda_{\uparrow}$; that is, the net longwave coefficients are determined entirely by surface response. Any non-random diurnal pattern in $L_{\downarrow}$ will result in a non-zero value of $\beta_{\downarrow}$ and $\lambda_{\downarrow}$ and β and λ can no longer be regarded solely as surface characteristics. Both positive and negative values of the incoming longwave parameters are conceivable. However, in view of the usual diurnal temperature regime and the tendency for convective activity to enhance the radiative efficiency of the atmosphere roughly in phase with R_n and Q_n, by the addition of particulate matter and the development of cloud, positive values are most likely.

An inspection of Fig. 2.1 reveals that the magnitude of $\beta_{\downarrow}$ and $\lambda_{\downarrow}$ can vary considerably. A very approximate calculation may be made for the data of Idso et al (1969), Fig. 2.1. The total diurnal change in $L_{\downarrow}$($\Delta L_{\downarrow}$) amounts to some 210 W m^{-2}. For the same day, the difference between maximum and minimum net radiation for bare soil (ΔR_n) was 551 W m^{-2} and a β' value of 0.05 was computed. Assuming $\beta' = \beta$, $\beta_{\uparrow} = \beta' + \beta_{\downarrow} = 0.43$, where $\beta_{\downarrow}$ is approximated as $\Delta L_{\downarrow}/\Delta R_n$. Such a value is approximately equivalent to a surface temperature fluctuation of 38C (at 17C), assuming an emissivity of 0.9 (Sellers, 1965), and this is in close agreement with the range of typical β' values for a dry

soil suggested by Monteith and Szeicz (1962). Actually, since $L_{\downarrow}$ is slightly out of phase with R_n, the $\beta_{\downarrow}$ value computed by the above method, and, hence, $\beta_{\uparrow}$, are probably a little too large.

Substituting (2.12) into (2.8), assuming $\beta = \beta'$, and (2.13) into (2.10) yields the generalised net radiation models,

$$\left[R_n\right] = \frac{(1 - \alpha)}{(1 + \beta_{\uparrow} - \beta_{\downarrow})}\left[Q_{\downarrow}\right] + PL_o \qquad (2.14)$$

and

$$\left[R_n\right] = (1 + \lambda_{\downarrow} - \lambda_{\uparrow})(1 - \alpha)\left[Q_{\downarrow}\right] + PL_o \,. \qquad (2.15)$$

The deviation between the two methods of calculating the net longwave coefficient must be regarded as a undesirable characteristic of (2.14), since it is β' which is related to the b term of the fundamental regression equation, but β which is given as $\beta_{\uparrow} - \beta_{\downarrow}$. A consideration of the magnitude of the error involved in equating them and the effect of this error on net radiation estimation is one of the objectives of this investigation.

2.6: An Analysis of the Outgoing Longwave Parameters for Simple Surfaces.

For a restricted range of landscape surfaces, an analysis of the dependence of $\beta_{\uparrow}$ and $\lambda_{\uparrow}$ on the relevant thermal and radiative properties of the surface is possible, if certain

simplifying assumptions are made. Though the derived expressions are unsuitable for the routine estimation of the outgoing long-wave parameters, they do provide some insight into the influences upon them. Moreover, they furnish a basis for speculation on the variables which are likely to exhibit correlation with $\beta\uparrow$ and $\lambda\uparrow$ for those more complex landscape elements which are not susceptible to theoretical treatment.

The analysis is applicable to any landscape element having a planar interface with the atmosphere and a substrate in which the thermal properties are independent of depth and conduction is the only process by which energy is transferred. These conditions are largely satisfied by soils, bare rock and certain urban surfaces. For ice and snow, in which radiative transfer plays a part in heating the substrate, and for water, in which both radiative and convective processes are important, a modification of the following analysis would be required.

For convenience, the major part of this analysis will be performed for the parameter $\beta\uparrow$ only. However, the equivalent expression for $\lambda\uparrow$ is given in (2.23).

By definition,

$$L\uparrow = \epsilon\sigma T_s^4 + (1 - \epsilon)L\downarrow .$$

Expressing the radiated portion of $L\uparrow$ as L_r yields

$$\frac{dL_{\uparrow}}{dR_n} = \frac{dL_r}{dR_n} + (1 - \epsilon)\frac{dL_{\downarrow}}{dR_n} . \qquad (2.16)$$

$\beta_{\uparrow}$ is defined only for complete daily periods; an instantaneous value of $dL_{\uparrow}/dR_n$ has no predictive value in the appropriate net radiation model, (2.14). Hence, it is convenient to identify derivatives characteristic of the daily period. In the following account, such derivatives are given the subscript d. Thus, (2.16) becomes

$$\beta_{\uparrow} = \left(\frac{dL_{\uparrow}}{dR_n}\right)_d = \left(\frac{dL_r}{dR_n}\right)_d + (1 - \epsilon)\left(\frac{dL_{\downarrow}}{dR_n}\right)_d . \qquad (2.17)$$

$(dL_{\downarrow}/dR_n)_d$ has been defined as $\beta_{\downarrow}$. The first term on the right-hand side of (2.17) may be expressed as the product of more tractable derivatives:

$$\beta_{\uparrow} = \left(\frac{dL_r}{dT_s}\right)_d \left(\frac{dT_s}{dG_o}\right)_d \left(\frac{dG_o}{dR_n}\right)_d + (1 - \epsilon)\beta_{\downarrow} , \qquad (2.18)$$

where G_o is the conductive heat flux at the earth-atmosphere interface. Since

$$L_r = \epsilon\sigma T_s^4$$

$$\frac{dL_r}{dT_s} = 4 \epsilon \sigma T_s^3 .$$

A convenient approximation is made by substituting mean daily surface temperature $\overline{T}_s$ to yield a daily mean value of dL_r/dT_s. This approximation is good when ΔT_s, the daily amplitude of surface temperature, is small relative to $\overline{T}_s$, an assumption which holds within the meteorological range of interest. Thus,

$$\left(\frac{dL_r}{dT_s}\right)_d = 4 \epsilon \sigma \overline{T}_s^3 . \qquad (2.19)$$

As an initial approximation, surface temperature may be expressed as a sine function of time t:

$$T_s = \overline{T}_s + \Delta T_s \sin(\omega t) ,$$

where ω is the radial frequency of the diurnal oscillation. With the above boundary condition, Sellers (1965) shows that the solution to the one-dimensional heat conduction equation (Carslaw and Jaeger, 1959) satisfies the relation

$$G_z = -k\frac{dT}{dz} ,$$

only when

$$G_z = \Delta T_s(\omega Ck)^{\frac{1}{2}} e^{-z(\omega/2D)^{\frac{1}{2}}} \sin\left[\omega t-(\omega/2D)^{\frac{1}{2}}z+(\pi/4)\right] , \qquad (2.20)$$

where G_z is the heat flux through depth z,

k is the substrate thermal conductivity,

T is the substrate temperature,

C is the substrate heat capacity and

D is the substrate thermal diffusivity (D = k/C).

At the surface, (2.20) simplifies to

$$G_o = \Delta T_s(\omega Ck)^{\frac{1}{2}} \sin\left[\omega t + (\pi/4)\right] .$$

Because of the phase lag between T_s and G_o, a plot of one against the other will yield a pattern similar to that depicted in Fig. 2.2, computed for data characteristic of a dry sandy soil ($\overline{T}_s$ = 289K; ΔT_s = 15K; C = 1.256 x 10^6 J m^{-3} K^{-1}; k = 0.293 W m^{-1} K^{-1}). The slope of the curve specified by the points plotted in Fig. 2.2 will vary both in sign and magnitude throughout the day. However, a general diurnal trend is defined by the major axis of the elliptical figure and the slope of this axis may be taken for $(dT_s/dG_o)_d$. This is given simply as the ratio of the diurnal range of T_s to that of G_o:

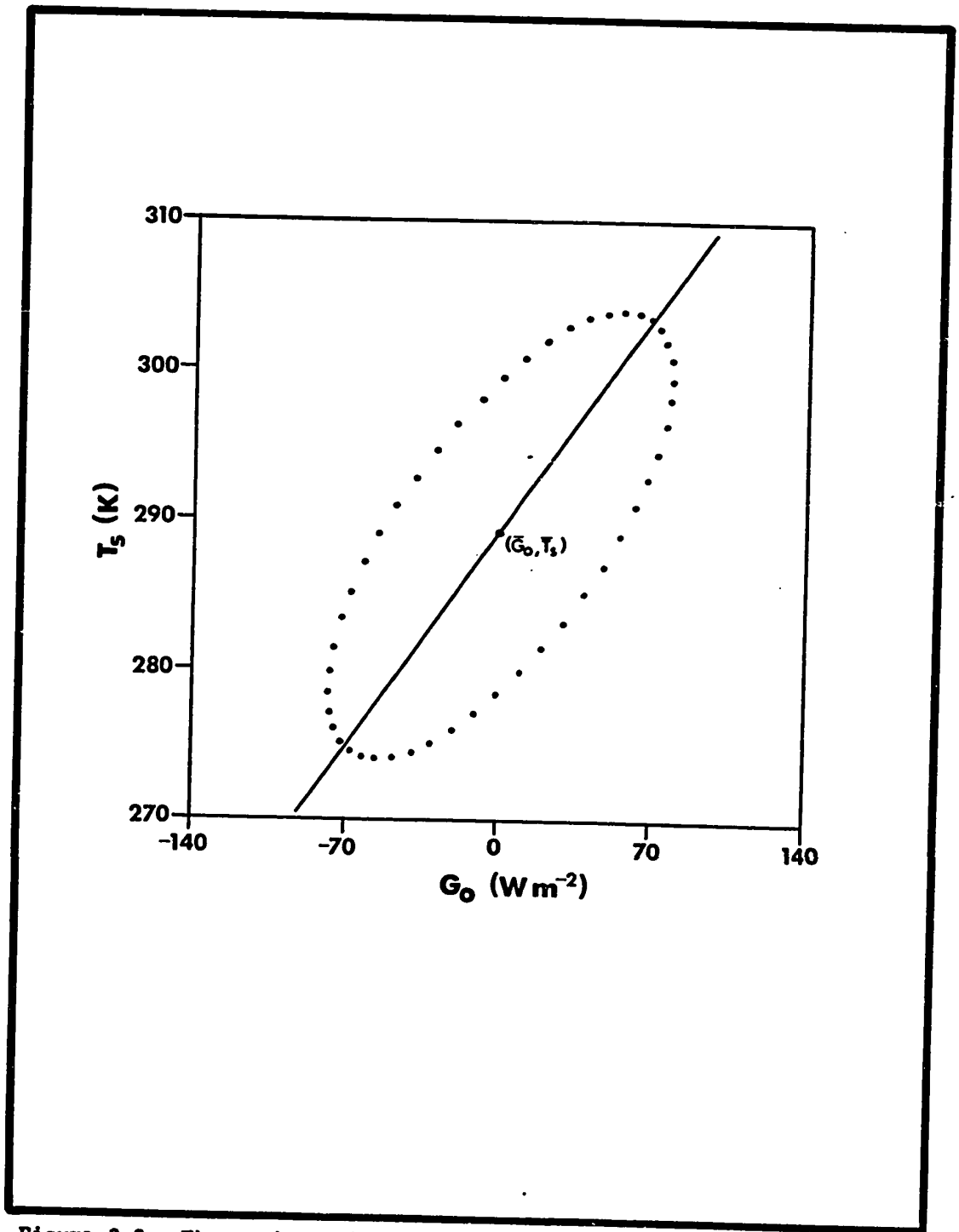

Figure 2.2: Theoretical diurnal relationship between T_s and G_o for a dry sandy soil.

$$\left(\frac{dT_s}{dG_o}\right)_d = \frac{1}{(\omega Ck)^{\frac{1}{2}}} . \qquad (2.21)$$

Plotted in Fig. 2.2 is the line of slope $1/(\omega Ck)^{\frac{1}{2}}$ which passes through the point $(\overline{G}_o, \overline{T}_s)$.

The simplest expression for $(dG_o/dR_n)_d$ results when the proportion of the net radiation used in the substrate heat flux is virtually constant thoughout the day, and G_o and R_n become negative simultaneously. Under these circumstances,

$$\left(\frac{dG_o}{dR_n}\right)_d = \frac{dG_o}{dR_n} = \frac{G_o}{R_n} .$$

Other non-linear relationships between G_o and R_n are, of course, possible and will necessitate more complex expressions for $(dG_o/dR_n)_d$, which may be designated g_β for convenience.

Substituting (2.19) and (2.21) into (2.18), and grouping the surface dependent terms, yields

$$\beta_\uparrow = \frac{4\sigma}{\omega^{\frac{1}{2}}} \frac{\epsilon \overline{T}_s^{\,3} g_\beta}{(Ck)^{\frac{1}{2}}} + (1 - \epsilon)\beta_\downarrow . \qquad (2.22)$$

Similarly,

$$\lambda_{\uparrow} = \frac{4\sigma}{\omega^{\frac{1}{2}}} \frac{\epsilon \bar{T}_s g_{\lambda}}{(Ck)^{\frac{1}{2}}} + (1 - \epsilon)\lambda_{\downarrow}, \qquad (2.23)$$

where $g_{\lambda} = (dG_o/dQ_n)_d$. The value of the constant term $4\sigma/\omega^{\frac{1}{2}}$ is 2.661×10^{-7} J $s^{-\frac{1}{2}}$ m^{-2} K^{-4}.

Evaluations of (2.22) are presented in Fig. 2.3 for a number of surfaces, represented by C, k and ϵ, at different temperatures and for various values of g_{β}. A constant $L_{\downarrow}$ flux ($\beta_{\downarrow} = 0$) is assumed for convenience.

Though not directly applicable to surfaces other than those which satisfy the theoretical requirements, the form of (2.22) and (2.23) is suggestive of the types of factors which might be expected to influence the magnitude of the $L_{\uparrow}$ parameters. These are:

(i) a radiative efficiency factor - ϵ

(ii) a temperature factor - $\bar{T}_s^3$

(iii) an energy input factor - g_{β} or g_{λ}

(iv) a substrate thermal property term - $(Ck)^{\frac{1}{2}}$

These factors are amplified below.

Factor (i): when $L_{\downarrow}$ is diurnally constant ($\beta_{\downarrow} = 0$), $\beta_{\uparrow}$ will increase as ϵ increases. However, as $\beta_{\downarrow}$ increases, the degree of dependence will lessen.

Factor (ii): since the relationship between emitted radiation and T_s is not linear, the temperature factor establishes the magnitude of the change in L_r per unit increment of

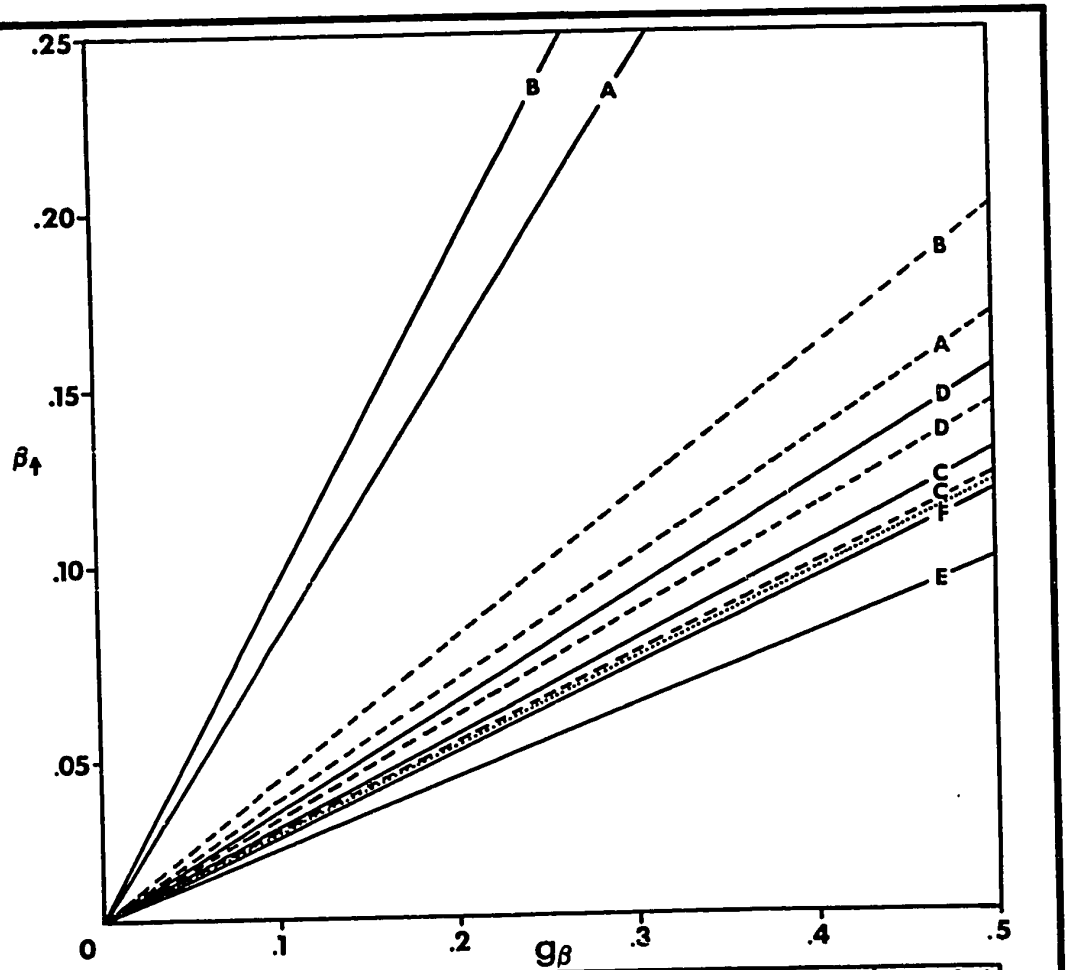

	SURFACE	ϵ	$\bar{T}_s$ (K)	k ($Wcm^{-1}K^{-1}$)	C ($Jcm^{-3}K^{-1}$)
—A—	Sand, Moisture Content = 0	.9	273	.00293	1.256
—B—	" " " 0	.9	289	.00293	1.256
—C—	" " " .2	.92	273	.01758	2.093
—D—	" " " .2	.92	289	.01758	2.093
—E—	" " " .4	.95	273	.02260	2.930
—F—	" " " .4	.95	289	.02260	2.930
--A--	Clay, " " .2	.97	273	.01172	2.093
--B--	" " " .2	.97	289	.01172	2.093
--C--	" " " .4	.97	273	.01590	2.930
--D--	" " " .4	.97	289	.01590	2.930
.....	Concrete	.8	289	.00921	1.925

Data from List (1966), Sellers (1965), and van Wijk (1965)

Figure 2.3: Evaluations of (2.22) for a number of surfaces.

T_s. Thus, the higher the mean daily temperature of a surface, the larger will be $\beta\uparrow$. It should be noted that $\beta\uparrow$ is independent of ΔT_s. Hence, other factors remaining constant, $\beta\uparrow$ might be expected to be the same on a completely overcast day ($\beta\downarrow = 0$) as on a clear day ($\beta\downarrow = 0$). However, since $\overline{T}_s$ is likely to be inversely related to cloud amount, this equality is probably not realised in practice.

Factor (iii): the greater the proportion of R_n used in heating the substrate, the larger will be $\beta\uparrow$. For many landscape elements, processes other than conduction might be important in this respect. Turbulent transfer might be significant in a water body or in the air of a plant canopy, while radiative fluxes will heat the substrate in lakes, snow and ice.

For plant canopies, when moisture is non-limiting, most of R_n will be consumed in the evaporative flux and $g_\beta \longrightarrow 0$. For this reason, an inverse dependence of $\beta\uparrow$ on soil moisture might be expected. This tendency is enhanced by the fact that $\overline{T}_s$ would tend to be higher when evaporative cooling is impeded.

Factor (iv): when C and k are small, the energy input will be confined to the near-surface layers and strong surface heating, and longwave emission, will take place. The term $(Ck)^{\frac{1}{2}}$, which figures in many analyses of the temperature response of surfaces, has been called variously the "thermal contact coefficient" by Businger and Buettner (1961) and van Wijk and Derksen (1963), the "soil product" by Haltiner and Martin (1957),

the "thermal property" by Johnson (1954) and Sellers (1965), the "thermal admittance" by Lettau (1959) and Turner (1968) and the "conductive capacity" by Priestley (1959) and Petterssen (1959). In a plant canopy, where only part of the energy transfer away from the "active surface" is by conduction, the eddy diffusivity of the air could be as important as the heat capacity and thermal conductivity of the biomass. As such, a negative dependence of $\beta\uparrow$ on windspeed might be found. For soil, C and k are functions of the volume fraction of water, and an inverse relationship between $\beta\uparrow$ and soil moisture will result.

2.7: Objectives of Research.

The primary objectives of this investigation are as follows:

Objective 1: Data Acquisition. To measure the components of the radiation budget for three dissimilar surfaces and to determine the degree to which these components, and, hence, net radiation, differ under identical incident long- and shortwave radiation fluxes (i.e. to make simultaneous radiation budget evaluations).

> Objective 1.1: Implicit in the successful prosecution of this objective is an investigation of error propagation in the measurement system used, since high quality data are necessary if meaningful comparisons of the equivalent fluxes for different surfaces are to be made.

Objective 2: Evaluation of Net Radiation Estimation Models. To establish an operationally useful, surface-sensitive method of estimating net radiation. The models investigated are those discussed in sections 2.1, 2.2 and 2.5. The following subsidiary objectives may be identified.

Objective 2.1: To evaluate the usefulness of (2.8) and (2.10) as surface-sensitive net radiation models for both clear and cloudy conditions. This is equivalent to an investigation of the degree to which β and λ are surface-sensitive parameters, by comparing the magnitudes of the outgoing and incoming longwave parameters.

Objective 2.2: To evaluate the usefulness of (2.14) and (2.15) as surface-sensitive net radiation models for both clear and cloudy conditions. This is equivalent to an investigation of the seasonal behaviour and a priori predictability of the input parameters to these models, as follows.

Objective 2.2.1: To determine the most desirable method of calculating daily α from intra-diurnal data, to minimise statistical and measurement error.

Objective 2.2.2: To establish the nature of the seasonal regime of α for each surface and to investigate the degree to which it is predictable from readily available surface and environmental variables.

Objective 2.2.3: To establish the nature of the seasonal regime of $\beta_{\uparrow}$ and $\lambda_{\uparrow}$ for each surface and to investigate the degree to which they are predictable from variables chosen as surrogates for the theoretically relevant factors identified in the previous section.

Objective 2.2.4: For the soil plot only, to compare measured values of the outgoing longwave parameters with those predicted by the theoretical equations (2.22) and (2.23), and to evaluate the relative significance of the radiation efficiency, substrate thermal property, surface temperature and energy input factors in determining the seasonal regime of $\beta_{\uparrow}$ and $\lambda_{\uparrow}$.

Objective 2.2.5: To establish the nature of the seasonal regime of $\beta_{\downarrow}$ and $\lambda_{\downarrow}$ and to investigate the degree to which they are predictable from readily available surrogates for atmospheric radiative properties.

Objective 2.2.6: To establish the nature of the seasonal regime of L_o and to investigate the degree to which it is predictable from readily available surface and/or atmospheric variables. Such an analysis will reveal whether it is necessary to recognise the surface dependence of this term.

Objective 2.3: To compare the accuracy of the net radiation

estimates generated by simple regression-type equations, (2.8), (2.14) and (2.15). In particular, to establish the following.

Objective 2.3.1: To determine whether the characteristics of the β- and λ-derived parameters are such that one model may be selected as preferable, on the basis of estimation error.

Objective 2.3.2: To determine whether the seasonal fluctuations in the defined parameters are sufficiently marked to necessitate their daily estimation ("variable parameter" models), or whether average values may be used for each surface type ("fixed parameter" models).

Objective 2.3.3: To determine whether equations derived from data aggregated from all surfaces result in significantly poorer estimates than those derived for each surface, i.e. to evaluate the significance of assuming surface controls on net radiation to be negligible.

CHAPTER 3

DATA ACQUISITION AND ANALYSIS

3.1: Site and Surface Description.

The measurement site (Fig. 3.1, Plate 1) was situated on the South Farm of the Experiment Station, on a gentle, south-facing slope of approximately one degree. The entire site area was occupied by sandy loam soils of the Caledon and Fox series (Anon., 1967) and at no radiometer location was a significant proportion of the sky hemisphere obstructed.

The grass plot was seeded in the spring of 1968 and, by the beginning of the 1969 experimental season, had attained an estimated ground coverage of 95%. Though initially fresh and green in appearance, throughout the months of August and September the vegetation became increasingly dessicated and yellowed, as available soil moisture decreased. The plot was mown periodically, the height of the plants never exceeding 70 mm during a measurement period (hereinafter termed a "run"). The characteristics of the grass plot over the period of measurement are illustrated in Fig. 3.2(a).

The corn (Zea mays, var. Seneca Chief) was planted at 0.3 m intervals, in rows 0.9 m apart, giving an average plant density of 3.7 plants m^{-2}. As row orientation was NW-SE, the sun was

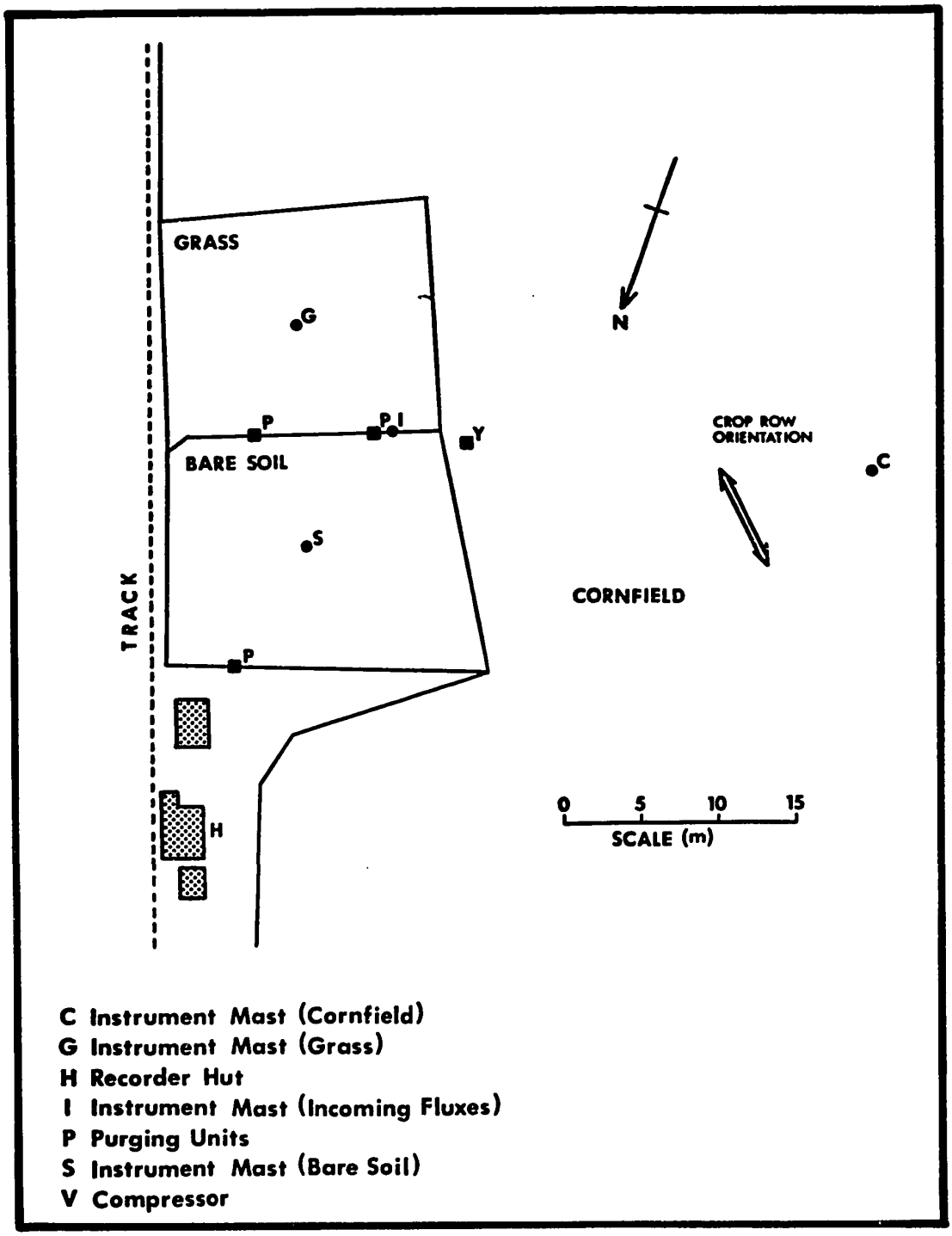

Figure 3.1: Measurement site.

Plate 1: Measurement site.

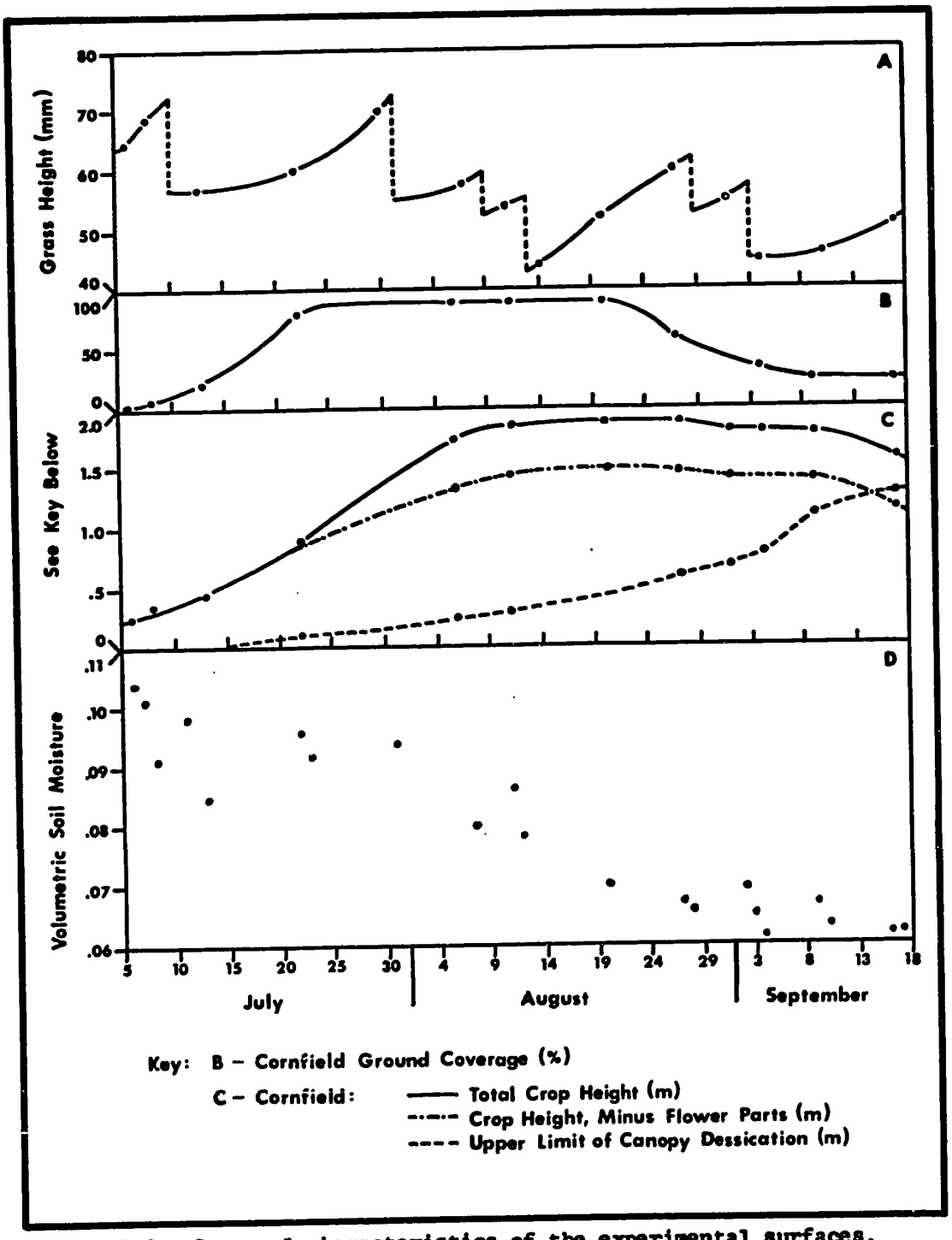

Figure 3.2: Seasonal characteristics of the experimental surfaces.

shining down the rows at 0900 LAT and across them at 1500 LAT. Fig. 3.2 (b and c) illustrates the characteristics of the corn canopy over the measurement period.

The soil plot consisted of Fox sandy loam, compacted at the surface by pre-season rolling. In the top 50 mm, dry bulk density was 1500 kg m^{-3} and dry soil porosity was 0.438. The same layer yielded an organic fraction of only 0.011 by volume, the remaining mineral component being derived from outwash sand parent material. The high sand content gave the dry soil a very light appearance. Colonising vegetation was removed by hand at frequent intervals, care being taken to avoid disturbing more soil than was necessary. The seasonal trend in the moisture content of the upper 50 mm of the soil is depicted in Fig. 3.2(d). Since both soil thermal conductivity and heat capacity are proportional to the volume fraction of soil moisture, Fig. 3.2(d) implies a trend toward lower values of these properties as the observation period progressed.

3.2: Radiometer Characteristics.

The Swissteco SW1 radiometer was used for all radiation flux measurements. Essentially, this instrument is of the Funk (1959) type, but two important modifications should be noted.

(i) The polyethylene hemispheres of the prototype may be removed and replaced by glass hemispheres or a black body cavity. By use of appropriate combinations of

cavity and/or dome types, measurements of fluxes other than R_n may be made.

(ii) Dew deposition on the hemispheres is prevented by the provision of a "ventilation ring", which directs numerous streams of air over the hemisphere surface. This feature replaces the "heating ring" of the original Funk model.

As no information was available, either from the manufacturer or in the radiation measurement literature, on the characteristics of the ventilation feature, laboratory tests were conducted by the National Atmospheric Radiation Centre (Scarborough) to establish the degree to which instrumental output was influenced by variations in the flow rate through the ventilation system. A small but noticable dependence of signal magnitude and stability was detected for small flow rates, though no further change was apparent after 8×10^{-5} m^3 s^{-1}. Accordingly, a rate of 11×10^{-5} m^3 s^{-1} was selected for use in all subsequent laboratory calibration experiments, field calibration checks and routine measurement.

The instrument configurations used in this investigation are presented in Table 3.1. The use of Swissteco radiometers as net and unidirectional pyranometers ensures that the response times of the components of the measurement system are similar. The lag coefficient of the Swissteco pyrradiometer is 40 s, compared with that of 4 s for the Eppley model 8-48 pyranometer.

TABLE 3.1

SWISSTECO RADIOMETER CONFIGURATIONS

Instrument	Upper Hemisphere	Lower Hemisphere	Flux Measured
Pyrradiometer	Polyethylene	Cavity	$(Q_{\downarrow} + L_{\downarrow})^{*}$
Pyranometer	Glass	Cavity	$Q_{\downarrow}$
Net pyrradiometer	Polyethylene	Polyethylene	R_n^{**}
Net pyranometer	Glass	Glass	Q_n^{**}

Notes:

* The pyrradiometer measures total incoming radiation only when an appropriate allowance is made for cavity temperature.

** These instruments were replicated for each surface, as the fluxes measured are surface-dependent.

Substitution of more conventional pyranometric instruments, therefore, would have generated considerable random error in the residual terms (L_n and $L_{\downarrow}$), the derived $L_{\uparrow}$ flux and all parameters subsequently computed from them, particularly on "cloudy-bright" days, when rapid changes in the magnitude of the measured fluxes takes place. In view of the importance of both the longwave terms and of non-clear conditions in the scope of this investigation, such an additional source of error was deemed undesirable.

However, the lack of experimental data on the performance of these instruments in the pyranometer mode necessitated special care in their calibration, and a number of additional field calibration tests were performed.

3.3: Radiometer Calibration.

The techniques employed to calibrate the instruments used in this study are outlined in Table 3.2.

The laboratory shortwave calibrations made use of the National Atmospheric Radiation Centre's secondary standard instruments. Optical bench determinations were performed with the instrument in net pyranometer mode, while the integrating sphere method necessitated the pyranometer configuration. No significant difference could be found between the results of the two methods (Fig. 3.3A).

The shortwave (optical bench) and longwave (black body cavity) calibrations were performed both prior to and after the

TABLE 3.2

TECHNIQUES EMPLOYED IN THE CALIBRATION OF SWISSTECO RADIOMETERS

I. Shortwave calibration

(i) Laboratory*

(a) Optical bench, vs. secondary standard**

(b) Integrating sphere, vs. secondary standard

(ii) Field calibration checks

(a) Occulting technique (pyranometer and net pyranometers only)

(b) Comparison technique (pyranometer only)

II. Longwave calibration

Laboratory* only - black body calibration (absolute)**

Notes: * National Atmospheric Radiation Centre.

** Calibration performed both prior to and after field season.

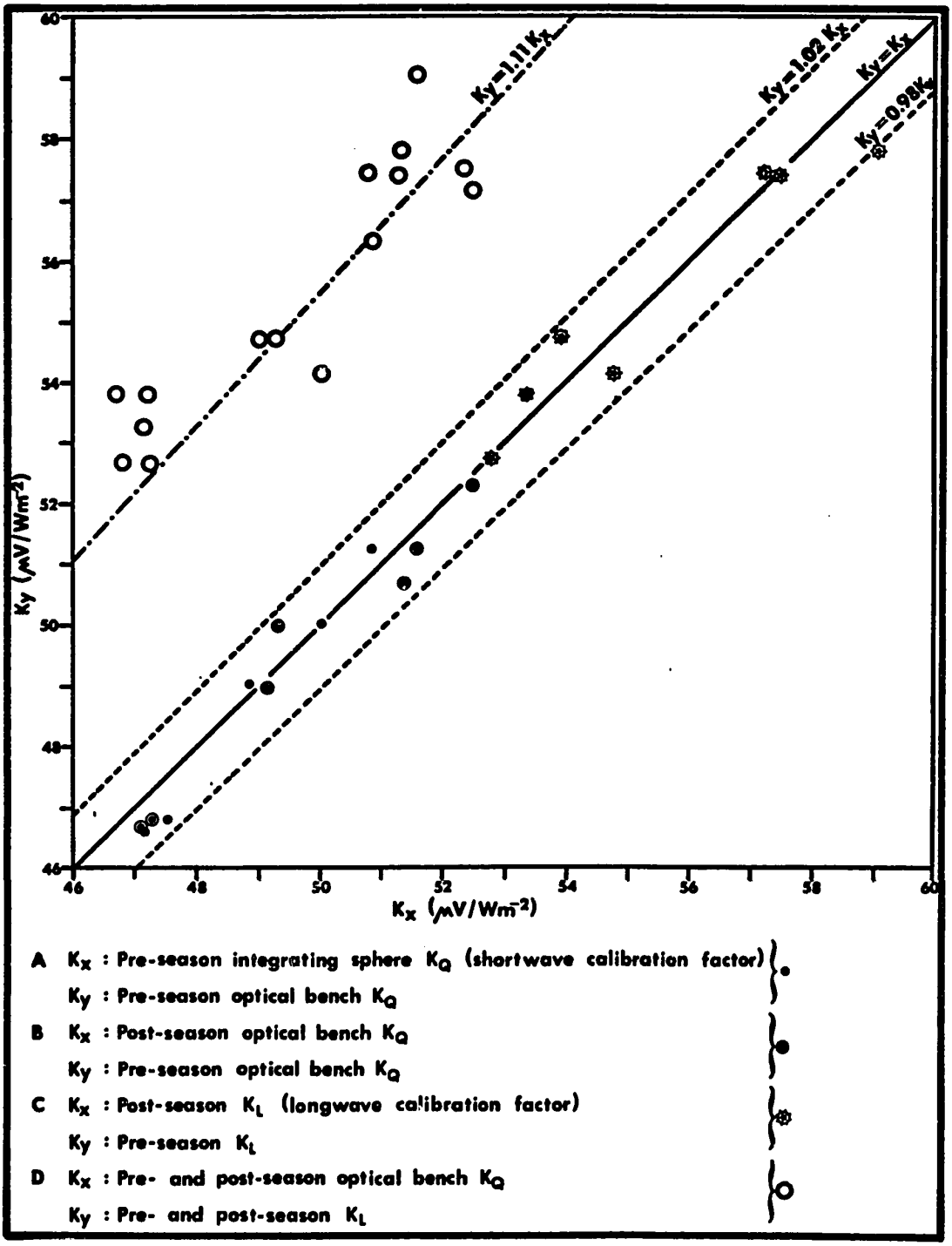

Figure 3.3: Comparison of laboratory derived calibration coefficients.

field season. In neither case was a significant difference found between the derived calibration factors (Figs. 3.3B and 3.3C). However, at both times, the longwave factors exceeded the shortwave ones by approximately 11% (Fig. 3.3D). No explanation could be found for this phenomenon, which necessitated unconventional procedures in flux computation (see section 3.5).

The standard temperature for the optical bench calibration was 26.7C, but the small temperature coefficient of the Swissteco instrument (V. Marsh, personal commmunication) rendered compensation unnecessary over the range of ambient temperatures encountered in the field. Instrument symmetry was excellent, the "top/bottom ratio" of the eight instruments used in this study averaging 1.009.

Field verification of the laboratory-derived calibration factors was sought for the pyranometer and the three net pyranometers. All four instruments were subjected to an occulting calibration in May, 1969. Unfortunately, owing to the 40 s lag coefficient of the Swissteco, it was necessary to allow a considerable period of time to elapse before the instrument under test reached equilibrium (generally over 720 s). As most of the days on which the determinations were made were not completely clear, the theoretical requirement of a constant diffuse to total ratio in the global radiation was probably not met in many cases, resulting in a larger scatter of determinations than was obtained under the more controlled laboratory conditions.

A comparison of the laboratory and field evaluations is presented in Table 3.3. The computed t statistics indicate a very low probability that the two determinations differ significantly for instruments 6630 and 6632. For instrument 6631 the probability is acceptable (around 85%), but the usefulness of the comparison is impaired by the less than ideal weather conditions which pertained during the field calibration and which may conceivably have biased the mean. However, further evidence in favour of the equality of the calibration factors is presented below. For instrument 6637, no useful comparison may be made, in view of possible non-random error introduced into the determination by poor atmospheric conditions on the day of calibration, though, from a purely statistical viewpoint, a significant difference in the coefficients is indicated by the computed t value.

A major source of difficulty with the occulting technique lies in obtaining an adequate number of observations in view of the time consuming nature of the calibration procedure. The data sets used in the previous analysis contained only 18-20 determinations. However, a field comparison between the Swissteco pyranometer (no. 6631) and a Kipp and Zonen pyranometer during clear periods on two days in August, 1968, yielded the 54 data points which are plotted in Fig. 3.4. The linear response of the Swissteco pyranometer, with no necessity for a cavity temperature correction, is clearly indicated. Also included are four data points computed from the unshaded data of the previously

TABLE 3.3

COMPARISON OF FIELD AND LABORATORY SHORTWAVE CALIBRATION COEFFICIENTS

Instrument	Calibration Coefficient ($\mu V/W\ m^{-2}$)				Degrees of Freedom	t	Weather
	Laboratory Mean	Laboratory Standard Deviation	Field Mean	Field Standard Deviation			
6630	51.25	0.38	51.36	1.52	21	0.138	Almost completely clear
6631	50.97	0.38	52.54	1.28	22	2.385	Ci and Cu, with clear periods
6632	52.36	0.14	52.58	0.86	22	0.491	Clear
6637	47.13	0.35	48.78	1.10	20	2.914	Cu, Ac and Ci, with clear periods.

Note: All field calibrations were conducted when the sun was apparently unobscured by cloud. During the tests performed on instruments 6631 and 6637, however, cloud passed close to the solar disk during the lengthy shading periods necessary to achieve equilibrium.

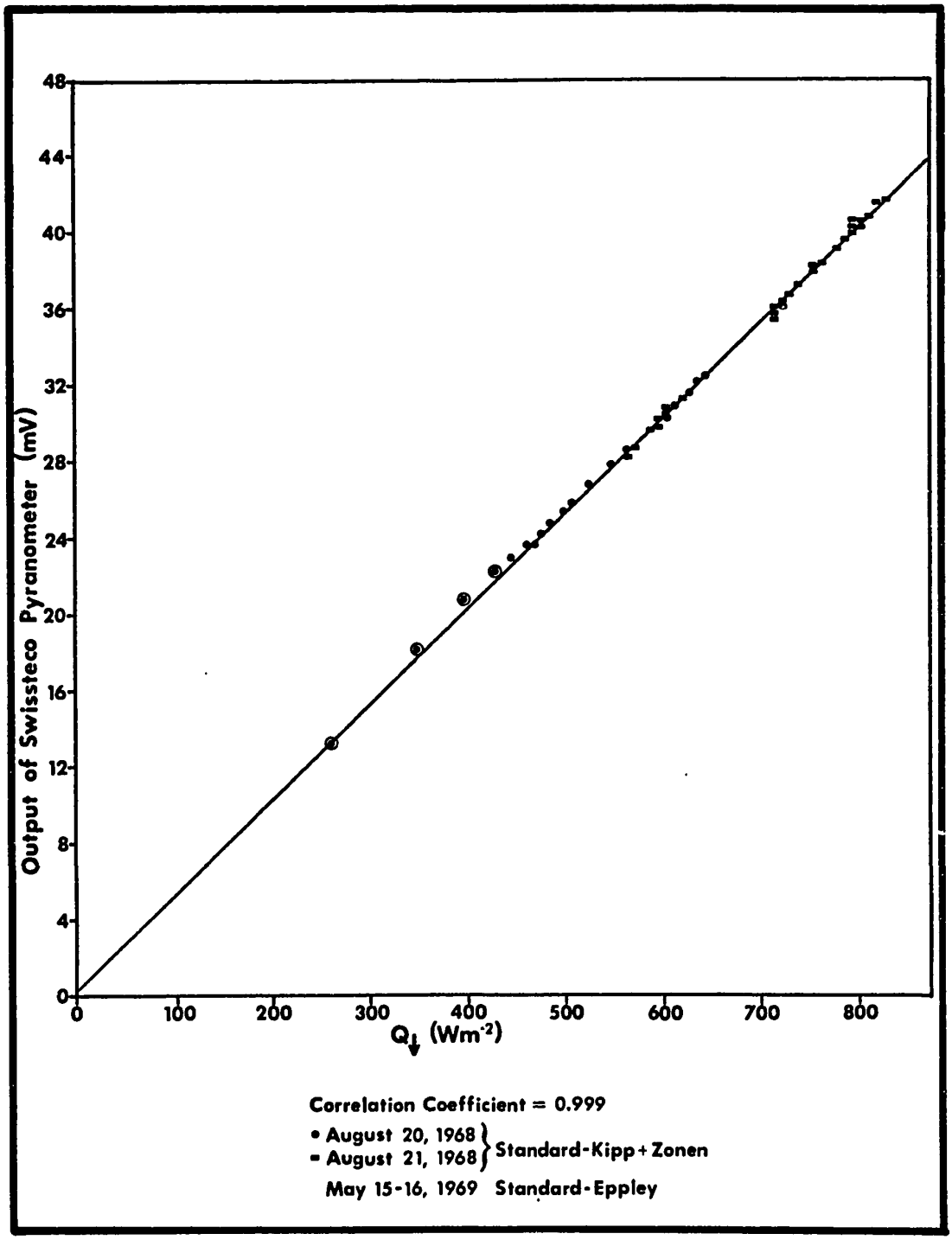

Figure 3.4: Comparison calibration for Swissteco pyranometer.

discussed occulting calibration, which used an Eppley 8-48 pyranometer as standard. These additional data suggest that the linearity of the relationship is preserved at least down to $Q_{\downarrow}$ = 250 W m^{-2}. The mean ratio of the Swissteco output to that of the Kipp and Zonen instrument was 4.015, which yields a shortwave calibration for the former instrument of 50.57 μV/W m^{-2}. This determination compares favourably with the laboratory-derived mean of 51.10 μV/W m^{-2}.

All calibration, both in the laboratory and in the field, was performed using the same techniques as were employed in measurement, particularly with regard to ventilation and purging flow rates. Instruments equipped with glass domes were calibrated with the same domes used for routine observations throughout the season, with the exception of instrument number 6637, the lower glass hemisphere of which had to be replaced following breakage in late August.

Table 3.4 presents, for each instrument, a summary of the factors derived from each of the previously mentioned calibration procedures, along with the values actually used for data reduction (see section 3.5). The small scatter of the determinations within each spectral region (with the exception of some occulting calibration values) is noteworthy. Owing to calibration equipment modifications, the laboratory determinations obtained after the measurement period are considered to be more reliable than those derived before the season (V. Marsh, personal

TABLE 3.4

SWISSTECO RADIOMETER CALIBRATION SUMMARY

Instrument		Shortwave Calibration					Longwave Calibration		Calibration Factors used for Data Processing	
Number	Use	a	b	c	d	e	f	g	h	i
6630	Net Pyranometer (soil)	51.29	51.58	50.86	51.36	-	57.81	59.03	51.58	-
6631	Pyranometer	50.72	51.29	51.29	52.54	50.57	57.45	57.45	51.29	-
6632	Net Pyranometer (grass)	52.29	52.44	52.44	52.58	-	57.52	57.16	52.44	-
6634	Net Pyrradiometer (corn)	-	50.86	-	-	-	-	56.30	50.86	56.30
6635	Net Pyrradiometer (grass)	46.70	47.13	47.13	-	-	53.80	53.30	47.13	53.30
6636	Pyrradiometer	49.00	49.14	48.85	-	-	54.73	53.87	49.14	53.87

(continued overleaf)

TABLE 3.4 (continued)

6637	Net Pyranometer (corn)	46.85	47.28	47.56	48.78	-	52.72	52.72	47.28	-
6639	Net Pyrradiometer (soil)	50.00	49.28	50.00	-	-	54.15	54.73	49.28	54.73
Temperature of Calibration			26.7C		13C	29C				

All calibrations expressed in $\mu V/W\ m^{-2}$

Key to calibrations:

a - Laboratory pre-season optical bench
b - Laboratory post-season optical bench
c - Laboratory pre-season integrating sphere
d - Field pre-season occulting method
e - Field pre-season comparison method
f - Laboratory pre-season black body
g - Laboratory post-season black body
h - Shortwave
i - Longwave

communication). Since no significant deviation from the pre-season calibrations could be demonstrated, therefore, these values were selected for routine data reduction.

3.4: Radiation Flux Measurement in the Field.

The locations of the masts upon which the radiometers were mounted are illustrated in Fig. 3.1. At each location, two instruments, oriented in a southerly direction, were attached by laboratory-type clamps at each end of a 1 m long cross-arm. At points G, S and C, the surface dependent fluxes were measured by net pyrradiometers and net pyranometers (Plate 2), while at I a pyrradiometer and a pyranometer were used to measure the incoming terms (Plate 3). The instruments were levelled at the beginning of each run of observations and were checked at frequent intervals during such periods, particularly in windy conditions.

Instrument height was 0.75 m above the grass and soil plots for the whole measurement period. Over the cornfield, a height of 1 m was maintained between the radiometers and the highest parts of the growing crop.

The view factors (i) for the three surfaces, (ii) for the instrument mast and (iii) for various objects on the periphery of the plots are listed in Table 3.5. Actually, those tabulated in section (i) must be considered underestimates, since they are computed for the largest circle, centered at the instrument mast, which is inscribed within the limits of each plot. As is apparent

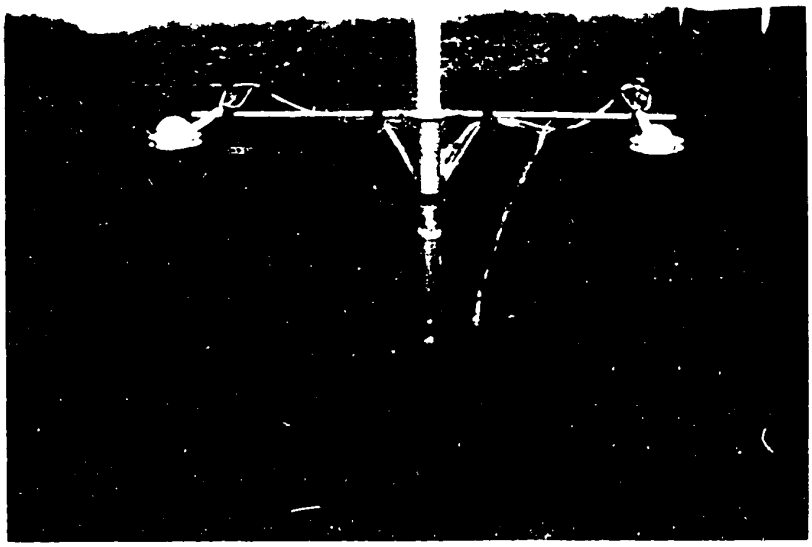

Plate 2: Net pyranometer (left) and net pyrradiometer.

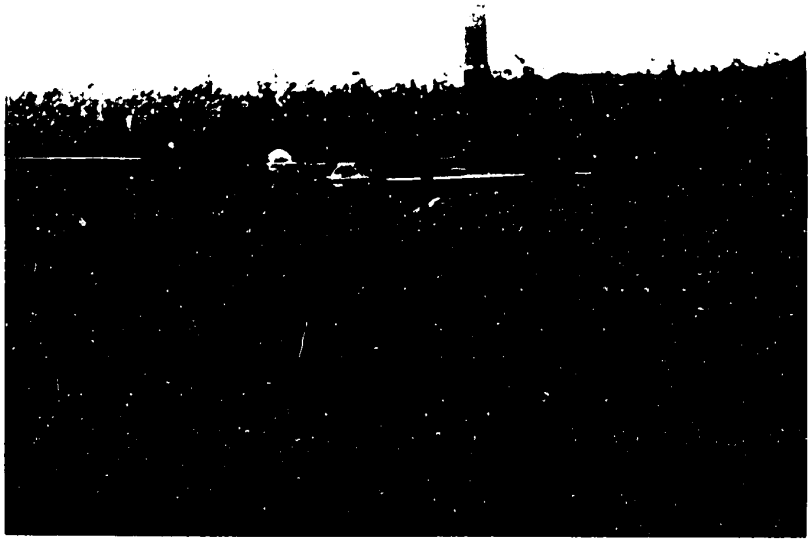

Plate 3: Pyranometer (rear) and pyrradiometer.

TABLE 3.5

VIEW FACTORS

(i) View factors for the three surfaces.

(a)	Grass	0.990
(b)	Soil	0.990
(c)	Cornfield	0.999

(ii) View factor for the instrument mast.

All surfaces	0.007

(iii) View factors for various objects on the periphery of the plots.

(a)	Edge of corn canopy (maximum height) for grass plot instruments	0.002
(b)	Edge of corn canopy (maximum height) for soil plot instruments	0.001
(c)	Instrument huts for soil instruments	0.000

from these data, no significant contribution of radiation may be expected from surfaces and objects outside the surface under consideration, and at no time were major shadows cast on the surfaces below the instruments, with the exception of those times, when the corn canopy was mature and when evening solar zenith angles exceeded about 86 degrees, when complete shading of the soil and grass plots occurred.

Initially, nitrogen was used for radiometer purging but this was replaced in the later part of the measurement period by dry air, delivered by small aquarium pumps and passed through silica gel dessication tubes. The purging units were located at points P in Fig. 3.1. The exit flow from each instrument passed through a water bottle at the mast, where the flow rate could be monitored by a bubble count.

Radiometer ventilation was provided by a self-regulating compressor unit, located at V in Fig. 3.1. Since the pyrradiometer and pyranometer required only one half of the flow fed to the net instruments (having only one hemisphere and ventilation ring), the excess flow to mast I was diverted to a flow meter, where ventilation rate could be monitored.

Pyrradiometer cavity temperature was monitored by a 24 gauge copper-constantan thermocouple, mounted in thermal contact with the radiating surface. This sensor had been previously calibrated against a standard (Rosemount) resistance thermometer and a second order polynomial was employed for data processing

purposes (correlation coefficient = 1.000, standard error of the estimate = 0.021C). The reference junction was inserted to a depth of 1.9 m in the soil, below the limit of influence of the diurnal temperature fluctuation. Reference temperature was monitored once daily by an auxiliary thermocouple system, employing a crushed ice reference.

Recording equipment was housed in a controlled environment hut (marked H in Fig. 3.1). The signals from the radiometers were recorded on an eight channel, Esterline-Angus E1124E multipoint recorder, having an operating range from -10 mV to 50 mV (approximately equivalent to a radiation flux range of -190 to 950 W m^{-2}). A chart speed of 406 mm hr^{-1} was employed and a scanning rate of 768 points hr^{-1} provided 96 samples per channel per hour, or one sample per radiometer each 37.5 s. Recorder accuracy and resolution errors, even if considered additive, amounted to approximately 4.6 W m^{-2}.

In the early part of the measurement period, pyrradiometer cavity temperature was recorded as digital output on a teleprinter, interfaced with a Solartron data logging system, at one minute intervals. On August 7, this system was replaced by a Honeywell Elektronic-194 strip-chart recorder. In the computation of the longwave flux emitted by the inner surface of the pyrradiometer cavity, recorder-induced errors in temperature measurement are of neglible importance.

3.5: Data Reduction and Analysis.

Measured radiation flux and pyrradiometer cavity temperature data were extracted from the record at two minute intervals, the unmeasured fluxes then being computed for each such instant. Owing to the previously mentioned inequality of the shortwave and longwave calibration factors, it was necessary, in effect, to calculate the proportion of the output of each pyrradiometric instrument which was attributable to each spectral component of the measured flux, and to apply the two calibration factors separately. Pyranometer and net pyranometer data were treated in the conventional manner; that is, the output of each instrument was divided by the appropriate calibration factor.

The following expressions were then used to obtain the longwave fluxes.

$$L_{\downarrow} = \frac{R^{*}_{\downarrow} - Q_{\downarrow}K_{Q}}{K_{L}} + \sigma T_{c}^{4} ,$$

where $R^{*}_{\downarrow}$ is the output of the pyrradiometer,

T_{c} is cavity temperature,

K_{L} is the longwave calibration factor for the instrument and

K_{Q} is the appropriate shortwave calibration.

For each surface

$$L_{n} = (R^{*}_{n} - Q_{n}K_{Q})/K_{L} ,$$

where R_n^* is the output of the net pyrradiometer.

Then, again for each surface,

$$R_n = Q_n + L_n ,$$

$$L_{\uparrow} = L_{\downarrow} - L_n ,$$

$$Q_{\uparrow} = Q_{\downarrow} - Q_n$$

and

$$\alpha = 1 - (Q_n/Q_{\downarrow}) .$$

Standard procedures (List, 1966) were used to convert all observation times to Local Apparent Time (LAT) and to compute solar azimuth and zenith angle. All times reported in this study are expressed as LAT.

The radiation fluxes were numerically integrated, by Simpson's Rule, and a characteristic reflection coefficient computed, for individual hours and for the whole daylight period. In addition, integration was performed over the total run length. The following reflection coefficient statistics were evaluated for each analysis period:

(i) The arithmetic mean, and standard deviation of each instantaneous α.

(ii) The mean α value, weighted by incoming solar radiation intensity.

(iii) The ratio of the reflected shortwave radiation, integrated over the period, to the integrated incoming flux.

(iv) The slope of the regression of $Q_{\uparrow}$ on $Q_{\downarrow}$, a procedure, suggested by Stanhill et al (1966), to weight the computed α value in favour of high solar radiation intensities.

An analysis of the influence of the method of computation on the reflection coefficient estimate is presented in Chapter 5.

Linear regression was used to calculate the longwave parameters defined in Chapter 2. Table 3.6 summarises the analyses performed, which utilised all appropriate instantaneous flux data for the daylight period.

3.6: Supplementary Field Observations.

SOIL ANALYSIS. Soil dry bulk density (ρ_d) was calculated from 14 samples extracted from the soil plot in the vicinity of the instrument mast, after the end of the measurement season. Only the upper 50 mm of soil were sampled, to correspond to the layer for which soil moisture determinations were made and the depth at which soil heat flux plates were located. A mean value of 1500 kg m^{-3}, with a standard deviation of 88 kg m^{-3}, was obtained.

A dry soil organic fraction of 0.011 (standard deviation 0.0016; 41 samples) was obtained by a loss-on-ignition analysis. Volume fractions of the soil constituents were then computed by

TABLE 3.6

METHODS OF CALCULATION OF THE LONGWAVE PARAMETERS

Parameter	Method(s) of Calculation
b	Regression (R_n on $Q_\downarrow$)*
β'	$\beta' = (1 - b)/b$
β	Regression (L_n on R_n)
λ	$\lambda = b - 1$ or regression (L_n on Q_n)
$\beta_\uparrow$	Regression ($L_\uparrow$ on R_n)
$\beta_\downarrow$	$\beta_\downarrow = \beta_\uparrow - \beta$ or regression ($L_\downarrow$ on R_n)
$\lambda_\uparrow$	Regression ($L_\uparrow$ on Q_n)
$\lambda_\downarrow$	$\lambda_\downarrow = \lambda - \lambda_\uparrow$ or regression ($L_\downarrow$ on Q_n).

Note: * also yields L_o

$$x_o = 0.011 \rho_d / \rho_o = 0.012 ,$$

$$x_m = (1 - 0.011) \rho_d / \rho_m = 0.550 ,$$

$$x_w = M \rho_d / \rho_w = 1.5M$$

and $$x_a = 1 - (x_o + x_m + x_w) = 0.438 - 1.5M ,$$

where x_o is the volume fraction of soil organic material,

ρ_o is the mean density of soil organic material, given as 1300 kg m^{-3} by de Vries (1963),

x_m is the volume fraction of soil mineral material,

ρ_m is the mean density of soil mineral material given as as 2700 kg m^{-3} by de Vries,

x_w is the volume fraction of soil water,

ρ_w is the density of water (1000 kg m^{-3}),

M is the soil moisture, by weight, and

x_a is the volume fraction of soil air (or soil porosity, when M = 0).

SOIL MOISTURE. Determinations of M were made once, twice or three times daily. Each determination was the mean of 10 samples, extracted from the upper 50 mm of soil and dried for a minimum of 24 hours, at 105C.

SOIL HEAT CAPACITY. The heat capacity of the upper 50 mm of the

soil plot (C) was calculated from

$$C = x_o C_o + x_m C_m + x_w C_w + x_a C_a ,$$

where the subscripted C terms denote the average heat capacities of the soil constituents. Since $C_o = 2.511 \times 10^6$ J m^{-3} K^{-1}, $C_m = 1.925$ J m^{-3} K^{-1}, $C_a = 100$ J m^{-3} K^{-1} (de Vries, 1963) and $C_w = 4.186 \times 10^6$ J m^{-3} K^{-1},

$$C = (1.088 + 6.278M) \times 10^6 \quad \text{J m}^{-3}\ \text{K}^{-1} .$$

SOIL TEMPERATURE. Three-junction 24 gauge copper-constantan thermopiles provided a spatially-integrated estimate of soil temperature at 5, 10, 20, 30 and 50 mm in the soil plot, within 0.5 m of the radiometer mast. A soil reference system and calibration procedure similar to that described for the pyrradiometer cavity temperature sensor were employed. Measurements were made at 0.5, 1.0 or 1.5 hour intervals, with a potentiometer or Solartron digital voltmeter.

SOIL HEAT FLUX. Two Middleton plates, wired in series, were used to provide a spatially-integrated measurement of the soil heat flux at 50 mm in the soil (G_{50}), in the vicinity of the soil plot radiometer mast. They were monitored at the same times, and by the same means, as the soil temperature sensors.

Surface soil heat flux was then computed by accounting

for the vertical divergence of the flux,

$$G_o = \bar{G}_{50} + 0.05\frac{\Delta\bar{T}}{\Delta t}C \ ,$$

where the bar over G_{50} denotes the mean value of the flux during a time period and $\Delta\bar{T}/\Delta t$ represents the average time rate of change of the depth-weighted mean soil temperature, $\bar{T}$, over the period.

SOIL THERMAL CONDUCTIVITY. Since no reliable estimate of the temperature gradient at the soil surface could be made, thermal conductivity determinations were made for the 50 mm depth and assumed to be applicable to the soil layer above. Use was made of the relationship

$$k = -\frac{G_{50}}{dT/dz}$$

where dT/dz was an estimate of the slope of the temperature profile at 50 mm. Mean values were assumed to characterise a daily period, although k values calculated when G_{50} was between 14 and -14 W m^{-2} were rejected, owing to the sensitivity of the above relationship to error in the flux or the gradient at these times.

METEOROLOGICAL STATION DATA. Standard meteorological network

data were obtained at an Atmospheric Environment Service station located on the Experiment Station, some 270 m from the measurement site. The variables used in this study were:

(i) screen temperature

(ii) screen vapour pressure

(iii) wind speed and

(iv) cloud type and amount.

3.7: Measurement Programme.

Not all of the supplementary observations described in the previous section were made on every day for which radiation data are available, and not all records of radiation data are suitable for all the forms of analysis employed in this investigation. Table 3.7 presents a summary of the details of each measurement period. Longer runs have been subdivided to include only one daylight period, and are designated "A" and "B".

3.8: Error Analysis for Radiation Budget Components.

Little information is available on the absolute accuracy of net radiometers, primarily because of the lack of any generally accepted standard with which individual instruments may be compared. Error estimates for net pyrradiometers range between 3 and 10%. In this analysis, values of 3, 6½ and 10% are assumed for the radiometers measuring R_n, Q_n and $Q_{\downarrow}$. The pyrradiometer measurements are less reliable, since additional error is associated with the calculation of the longwave flux from the cavity.

TABLE 3.7

MEASUREMENT PROGRAMME

Run	Date	Run Starts (LAT)	Run Ends (LAT)	Data Used for Model Parameter Computation	Soil Moisture	Soil Heat Flux and Temperature	Met. Station Data	Infrared Thermometer Data
1	July	6 0850	2114	*	-	*	*	-
2		7 0824	1840	*	-	*	*	-
3		8 2234+	2234	*	*	*	*	-
4		11 0534	1648	*	*	*	*	-
5A		13 0650	1932	*	*	0	*	-
5B		14 0424	1140	-	*	0	*	-
6		22 0428	1946	*	*	*	*	*
7		23 0502	1300	-	*	0	*	*
8		30 0640	1000	-	-	-	*	-
9		31 0652	0932	-	-	-	*	-
10	August	7 0542	1532	*	*	*	*	-
11		11 0502	1948	*	*	*	*	-
12A		12 0504	0000	*	*	0	*	-
12B		13 0000	0924	-	-	0	*	-
13		14 1134	1544	-	-	-	*	-

(continued overleaf)

TABLE 3.7 (continued)

14 August	27	0516	1936	*	*	*	*	-
15A	28	0504	0000	*	*	0	*	-
15B	29	0000	1856	*	-	*	*	-
16 September	1	0552	1900	*	-	-	*	-
17	2	0528	1932	*	*	*	*	-
18	3	0600	1940	*	*	*	*	-
19	4	0546	1914	*	*	*	*	-
20	9	0600	1346	*	*	*	*	-
21	10	1842+	1942	*	*	*	*	-

Key: * Useful quantity of data available

0 Data incomplete

+ Time refers to previous day.

Recorder error is assumed to be 1%, while that in the measurement of the radiative temperature of the inner surface of the pyrradiometer cavity is taken as 1, 3 and 5K, equivalent to 1.4, 4.1 and 6.8% errors in the computed flux at 293K.

Since these sources of inaccuracy, with the exception of the small recorder term, are independent, a root-sum-square analysis of error propagation is appropriate. The resulting estimates, for each combination of radiometer and cavity temperature errors, are given in Table 3.8.

The $L\uparrow$ flux is of major importance in this investigation, yet it is necessarily the least reliable of the radiation balance components. With 10% instrumental error in the initial flux measurements, estimated error in $L\uparrow$ could exceed 20% (Table 3.8). Accordingly, an attempt was made to check this term against completely independent measurements.

Subsurface temperature profiles in the soil (section 3.6) were extrapolated to the surface and the resulting temperature estimate, $\hat{T}_s$, was used to obtain the longwave flux radiated by the soil:

$$\hat{L}_r = \epsilon\sigma\hat{T}_s^4 .$$

Radiation balance data for the same time were also used to compute the radiated portion of $L\uparrow$ as

TABLE 3.8

ESTIMATED ERROR IN MEASURED AND COMPUTED RADIATIVE FLUXES

Instrumental Error = 3%

T_c Error	R_n	Q_n	$Q_\downarrow$	$Q_\uparrow(\&\,\alpha)$	L_n	$L_\downarrow$	$L_\uparrow$
1K	3.2	3.2	3.2	4.5	4.5	4.7	6.5
3K	3.2	3.2	3.2	4.5	4.5	6.1	7.5
5K	3.2	3.2	3.2	4.5	4.5	8.2	9.3

Instrumental Error = 6½%

T_c Error	R_n	Q_n	$Q_\downarrow$	$Q_\uparrow(\&\,\alpha)$	L_n	$L_\downarrow$	$L_\uparrow$
1K	6.6	6.6	6.6	9.3	9.3	9.4	13.2
3K	6.6	6.6	6.6	9.3	9.3	10.2	13.8
5K	6.6	6.6	6.6	9.3	9.3	11.5	14.8

Instrumental Error = 10%

T_c Error	R_n	Q_n	$Q_\downarrow$	$Q_\uparrow(\&\,\alpha)$	L_n	$L_\downarrow$	$L_\uparrow$
1K	10.0	10.0	10.0	14.2	14.2	14.3	20.1
3K	10.0	10.0	10.0	14.2	14.2	14.8	20.5
5K	10.0	10.0	10.0	14.2	14.2	15.8	21.2

$$L_r = L_{\uparrow} - (1 - \epsilon)L_{\downarrow} ,$$

and the percentage difference between these two estimates was given by $100(\hat{L}_r - L_r)/\hat{L}_r$. Values of this term, for assumed ϵ values between 0.8 and 1.0, are plotted in Fig. 3.5. For ϵ typical of sandy soils ($0.85 \leq \epsilon \leq 0.95$; Sellers, 1965), the frequency of occurrence of differences greater than 15% is small (3.3 - 7.4%). The skewed distributions indicate a tendency toward consistent underestimation by the radiation balance method. A comparison of Fig. 3.5 and Table 3.8 suggests that error in the initial radiation flux measurements is probably in the vicinity of 6½%.

An infrared radiation thermometer (Barnes Engineering Co., model PRT 5), available for two days during the measurement season (July 22 and 23), was used to measure the radiative surface temperature of each plot. The fluxes computed from these data were compared with those obtained by the radiation balance technique (Fig. 3.6). For each surface, the latter method gave results within 8% of the infrared thermometer estimate, though the absolute magnitude of the difference was not random, but increased with increasing $L_{\uparrow}$. Fig. 3.6 suggests that the radiation balance method consistently underestimates $L_{\uparrow}$ for grass and soil but overestimates for the cornfield. This is presumably related to the magnitude and direction of the errors exhibited by the individual instruments used in the evaluation of the components

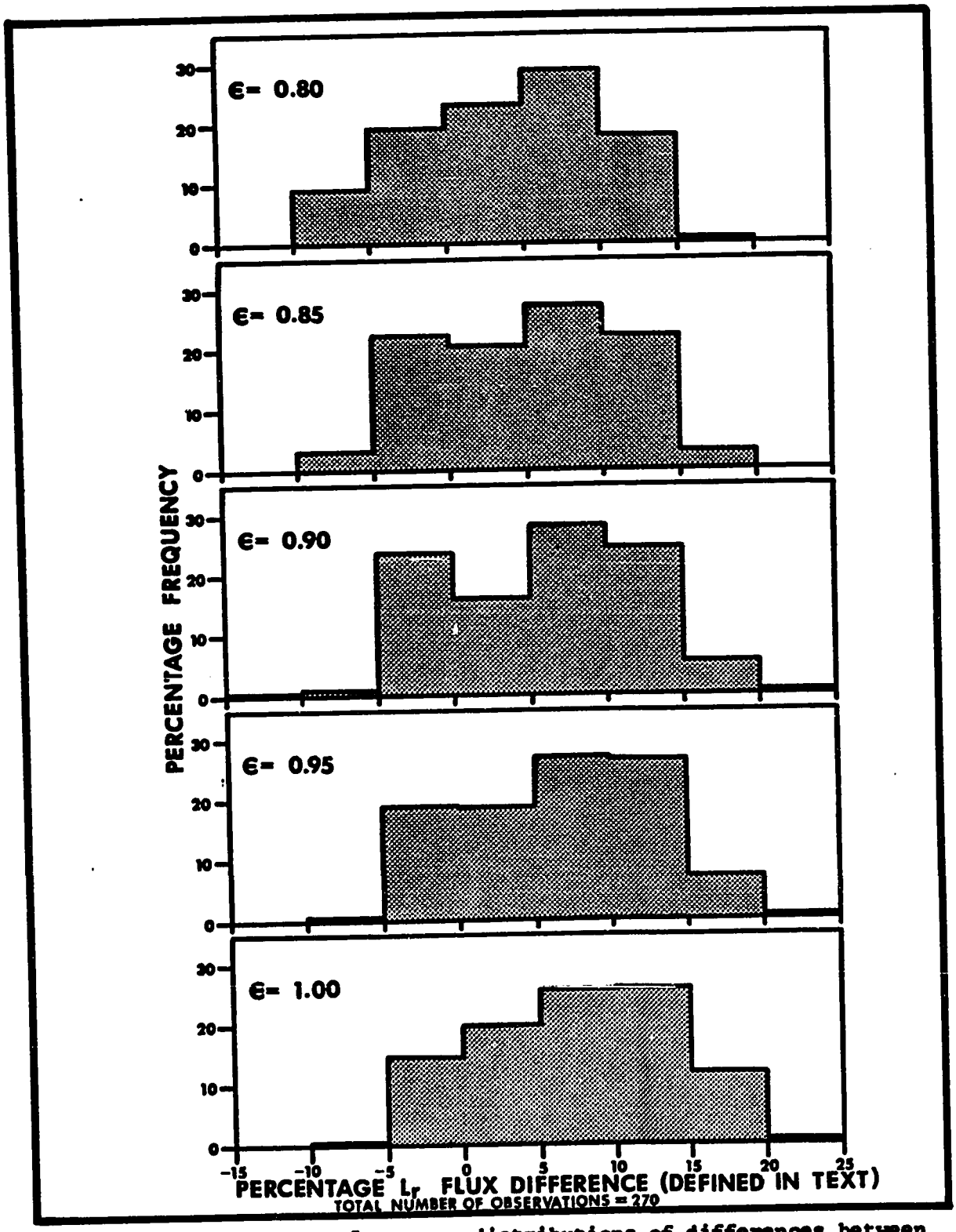

Figure 3.5: Percentage frequency distributions of differences between radiation balance and estimated surface temperature methods of L_r calculation.

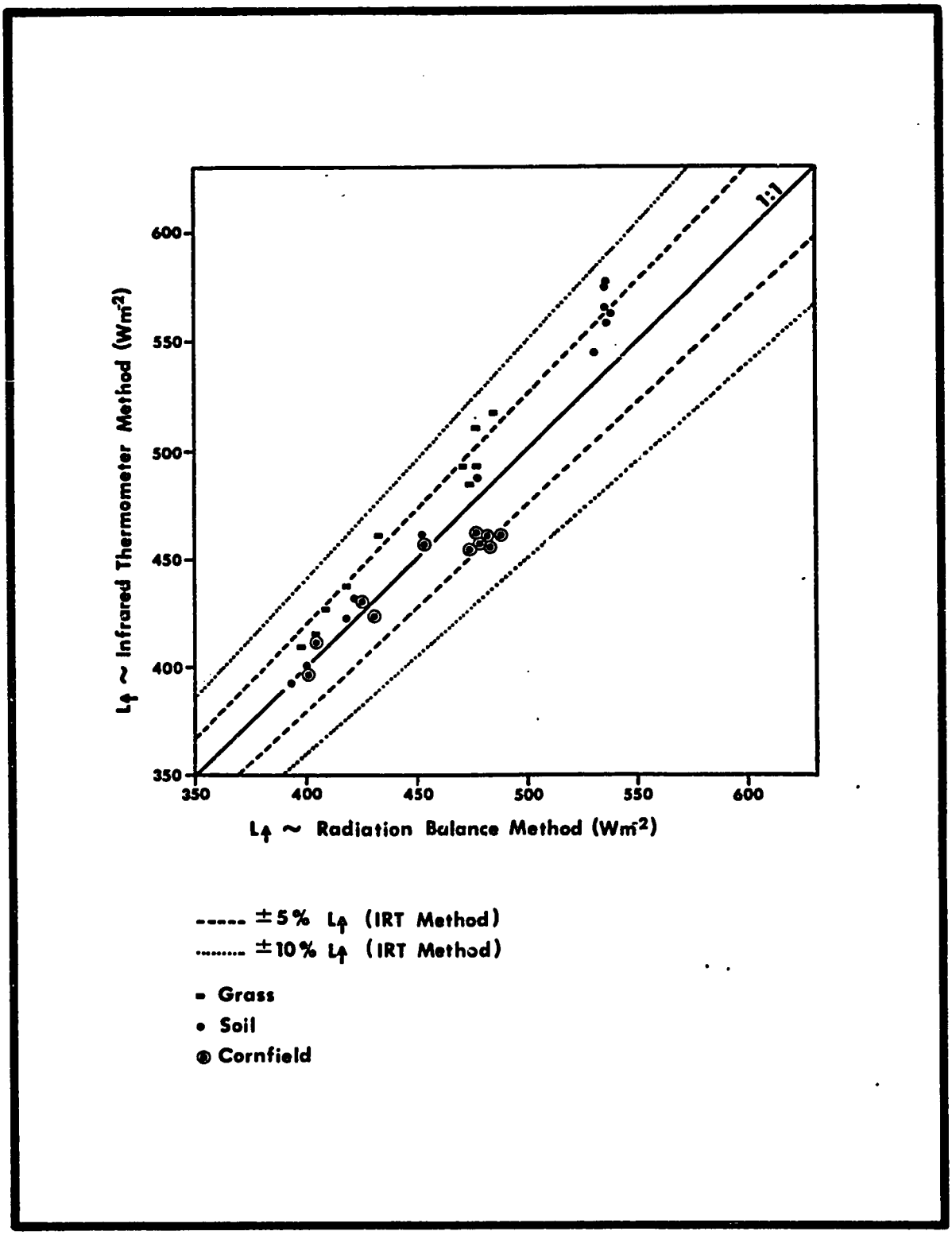

Figure 3.6: Comparison of surface radiative temperature and radiation balance methods of $L_{\uparrow}$ flux computation.

of the radiation balance of each surface.

Reviewing the evidence, it would appear that $L_{\uparrow}$ can be evaluated with the instrumental system described, to within 8 - 15%, a level of accuracy deemed adequate for the purposes of this investigation. It should be noted that, in comparing the outgoing longwave fluxes, or the derived parameters $\beta_{\uparrow}$ and $\lambda_{\uparrow}$, for the three surfaces, smaller differences than those implied by the above error statistics will be significant, as each will be biased in the same direction by errors in the pyrradiometer, pyranometer and cavity temperature measurements. Furthermore, many of the potential sources of inaccuracy in the measurements of net shortwave radiation and net radiation (e.g. ambient temperature dependence, imperfect cosine response) will also tend to produce errors of the same sign in the computed $L_{\uparrow}$ flux for each surface.

CHAPTER 4

THE DIURNAL RADIATION BUDGET

The purpose of the following account (section 4.1) is to compare the diurnal regimes of the radiation budget components of the surfaces used in this investigation and to identify the surface and atmospheric controls on net radiation which the parameters defined in Chapter 2 are intended to represent. Only days selected to illustrate particular features will be considered. Mean hourly fluxes for all runs are tabulated in Appendix 2. The diurnal behaviour of the reflection coefficient is more appropriately treated in the following chapter, in conjunction with an analysis of the problem of computing a representative daily value of this parameter. Section 4.2 deals more generally with the ratio of net to incoming shortwave radiation and compares values obtained in this study to those found previously.

4.1: Diurnal Regimes of the Radiation Budget Components. July 22 (Fig. 4.1).

This day is typical of the early season, when soil moisture content was high beneath both plots, the grass was fresh and green and was transpiring efficiently. Cloud cover was changeable, with heavy (0.5 - 0.6) Cu development between 1200 and 1400 and extensive (0.8) Ci layers after 1700, leading to

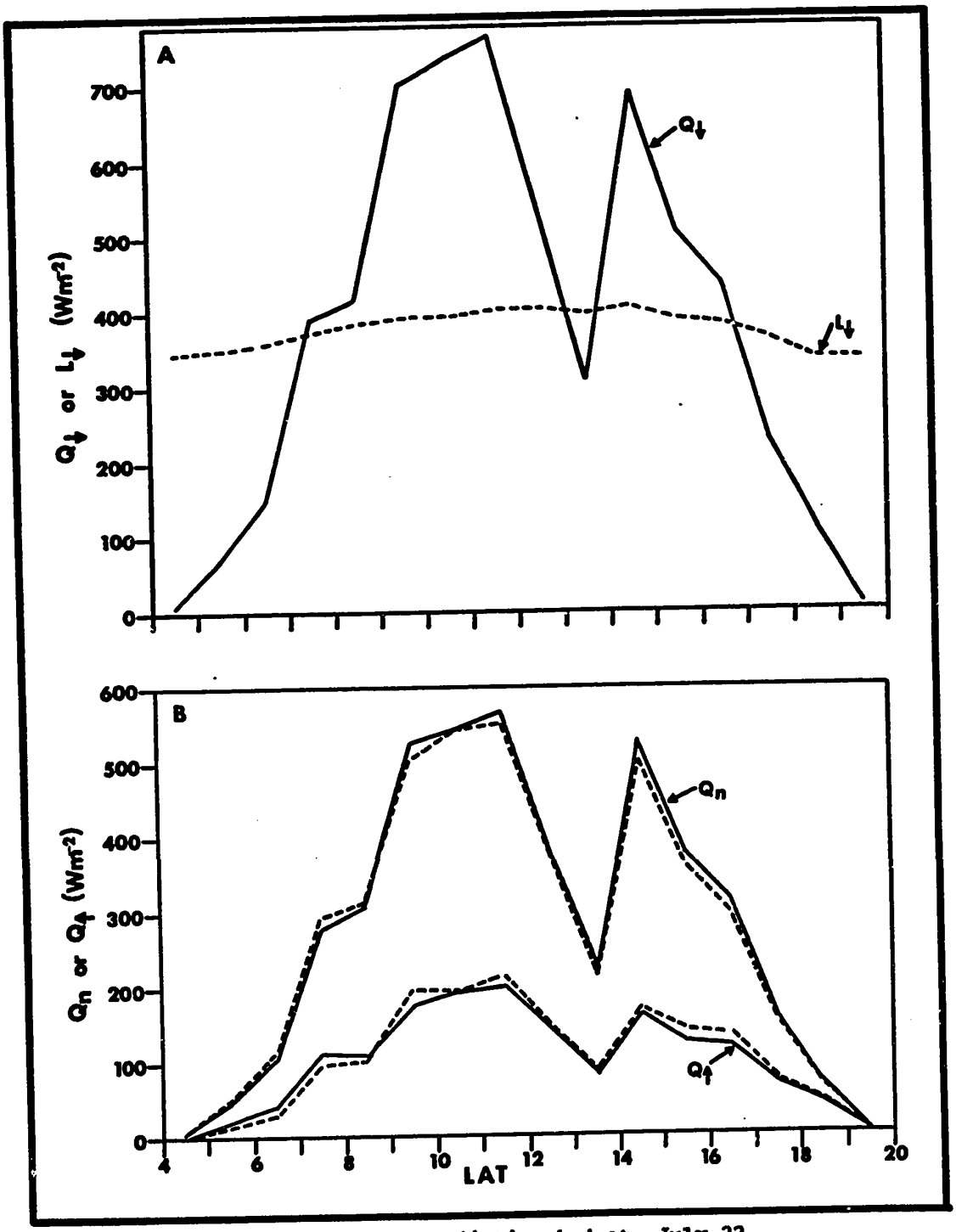

Figure 4.1: Components of the radiation budget, July 22.
(Continuation of diagram and key overleaf)

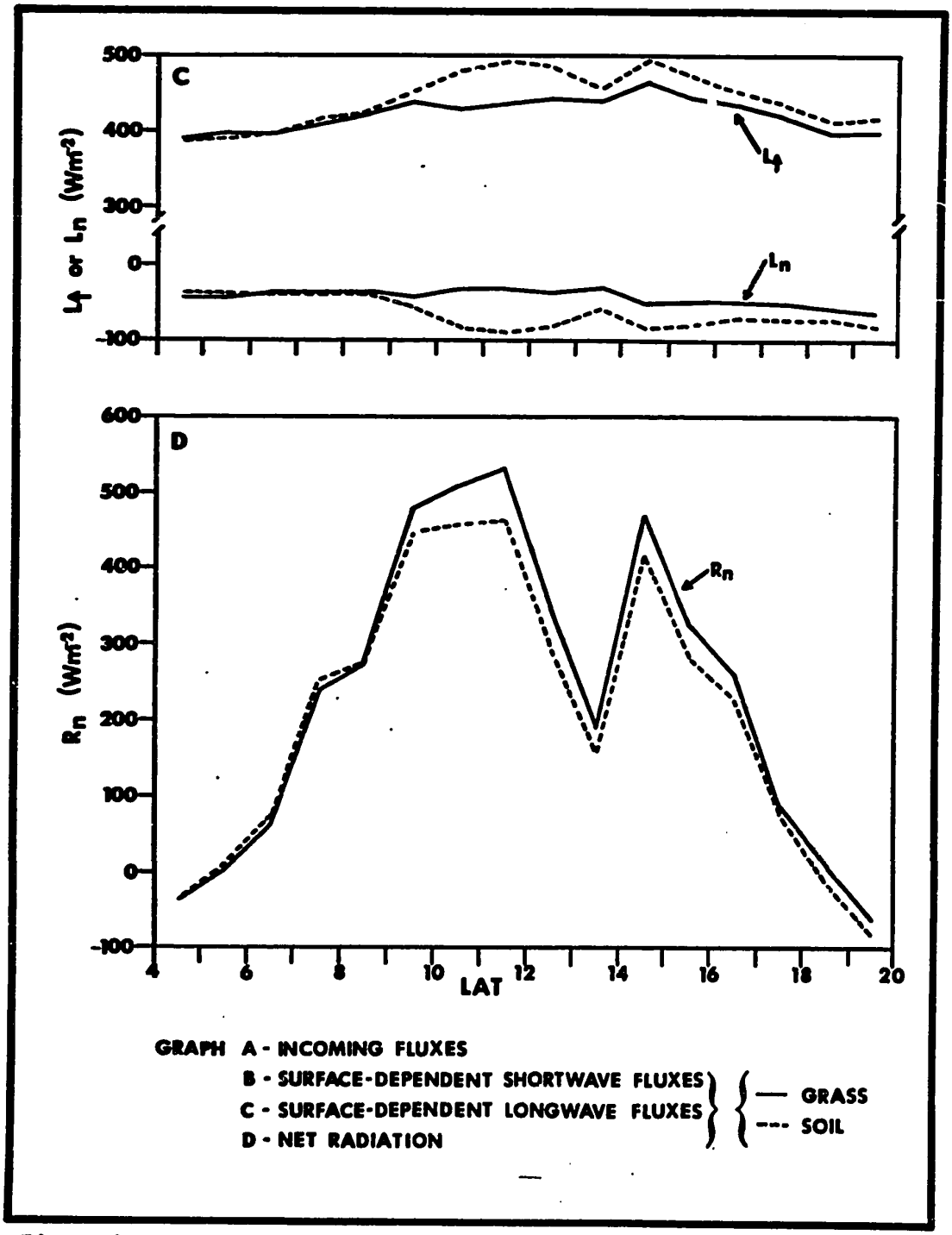

Figure 4.1; continued.

marked fluctuations in the shortwave fluxes.

The thermal response of the soil was more extreme than that of the grass, a phenomenon which might be expected from the likely magnitudes of the evaporative losses from each. The surface radiative temperature of the two plots also showed a response to the early afternoon cloudy spell, the temperature reduction being more marked for soil than for grass. The incoming longwave flux exhibited a slight (70 W m^{-2}) diurnal fluctuation.

Absorbed shortwave radiation was only slightly smaller for soil than for grass. It will be shown in the following chapter that the reflection coefficients of these two surfaces were similar during most of July, when soil moisture was high in the soil plot. (On this day, grass α = 0.268, soil α = 0.281.) The inequality of the net radiation totals of these surfaces, therefore, was mainly a function of longwave, rather than shortwave, differences.

August 11 (Fig. 4.2).

The sky was virtually clear until about 0830 (< 0.1 Sc or Ac), after which larger quantities of broken low-level cloud formed, and persisted for the remainder of the day (0.5 - 0.7 Cu and Sc), thus accounting for the fluctuations in the $Q_{\downarrow}$ curve after the late morning. The $L_{\downarrow}$ flux exhibits a marked change over the diurnal period.

By the second week in August, soil reflection coefficient had increased and was greater than that of the grass. Hence the

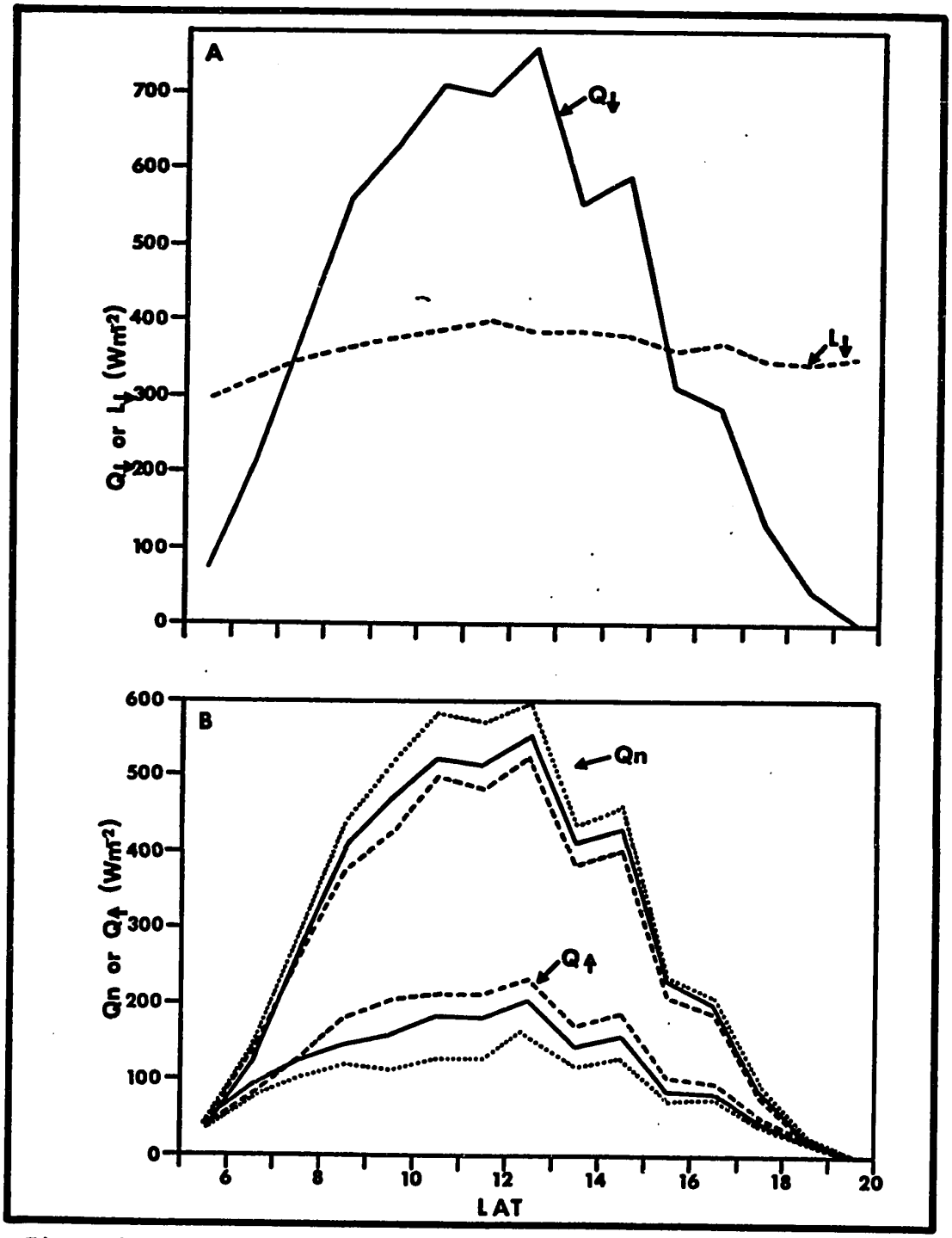

Figure 4.2: Components of the radiation budget, August 11.
(Continuation of diagram and key overleaf)

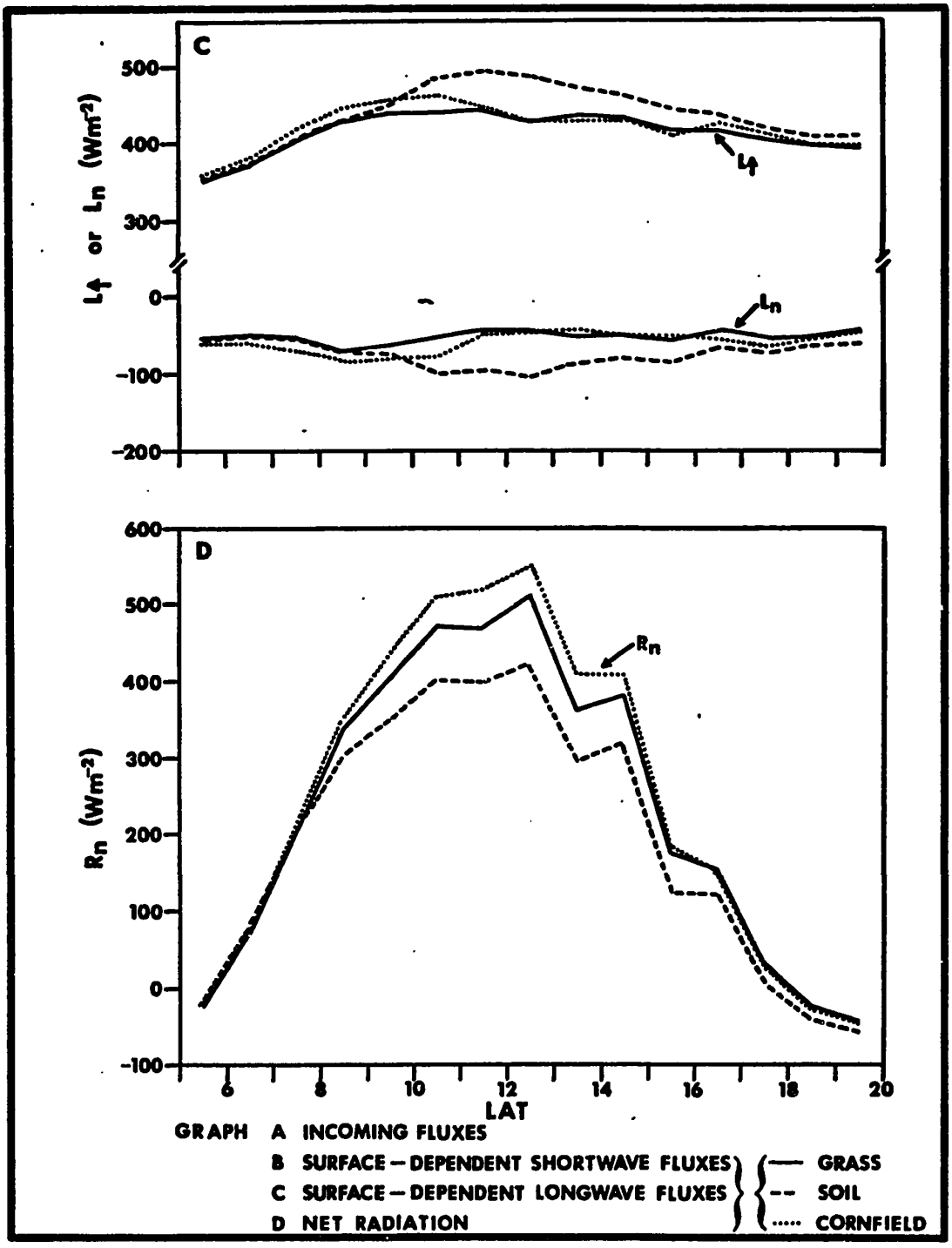

Figure 4.2; continued.

latter surface absorbed 6% more solar radiation. Nevertheless, for most of the day (0800 onwards), the soil surface was warmer than the grass. During the daylight period, some 2211.6 x 10^4 J m^{-2} were lost from the soil by radiated and reflected longwave radiation, in contrast to 2098.6 x 10^4 J m^{-2} from the grass. The early morning similarity in the $L\uparrow$ fluxes from these surfaces may be related to the moist condition of the surface soil layers at this time and the consequent retardation of soil heating by evaporative energy loss. The soil moisture in the upper 2 mm of the soil plot declined from over 3% by weight at dawn to around ½% by 1000. The heavier cloud development of the afternoon hours gave rise to a pre-noon maximum in $L\uparrow$ for both the soil and grass plots.

The cornfield absorbed 15% more solar radiation than the soil, but exhibited a diurnal mean radiative temperature 2.6C lower. The use of such a mean value, however, conceals the unusual diurnal pattern in the $L\uparrow$ flux from the cornfield. Before 1000, cornfield $L\uparrow$ exceeded the soil flux, while in the afternoon it was similar in magnitude to grass $L\uparrow$. Although it could be argued that the corn canopy might be more nearly "black" than either of the other surfaces, a difference in ϵ of 0.03 could change the radiated flux by only 14 W m^{-2} at most. The effect on $L\uparrow$ would be smaller still and, moreover, ought to be present all day, unless a mechanism of diurnal ϵ change is postulated.

Inspection of the $Q\downarrow$ and Q_n curves of Fig. 4.2 reveals

that a larger proportion of incoming solar radiation is absorbed during the morning than in the afternoon. In Chapter 5, an attempt is made to link this phenomenon to changes in canopy transmission with solar azimuth, induced by the row orientation of the crop. However, while the canopy as a whole was absorbing a larger proportion of incident radiant energy in the morning, it might be supposed that the heating resulting from this process would be distributed throughout a deeper canopy layer and might not be apparent in the outgoing longwave flux emerging from its upper surface. In contrast, more effective penetration of the canopy would result in more marked heating of the underlying soil surface. Only the development of a fairly sophisticated model of the processes of shortwave absorption and longwave exchange within the canopy will provide an adequate solution to this problem. However, it is noteworthy that Kalma and Stanhill (1969) report unusual diurnal regimes of $L_{\uparrow}$ for an orange orchard, which they link to daily changes in the location, within the canopy, of the zone of maximum solar radiation absorption.

Differences in net radiation retention between the surfaces originated in disparities in longwave and shortwave losses, both of which, on a diurnal basis, were least for the cornfield and greatest for the soil.

August 27 (Fig. 4.3).

This day was relatively free of low and middle layer cloud. Only 0.1 - 0.2 Ac was recorded prior to 0700, and 0.1

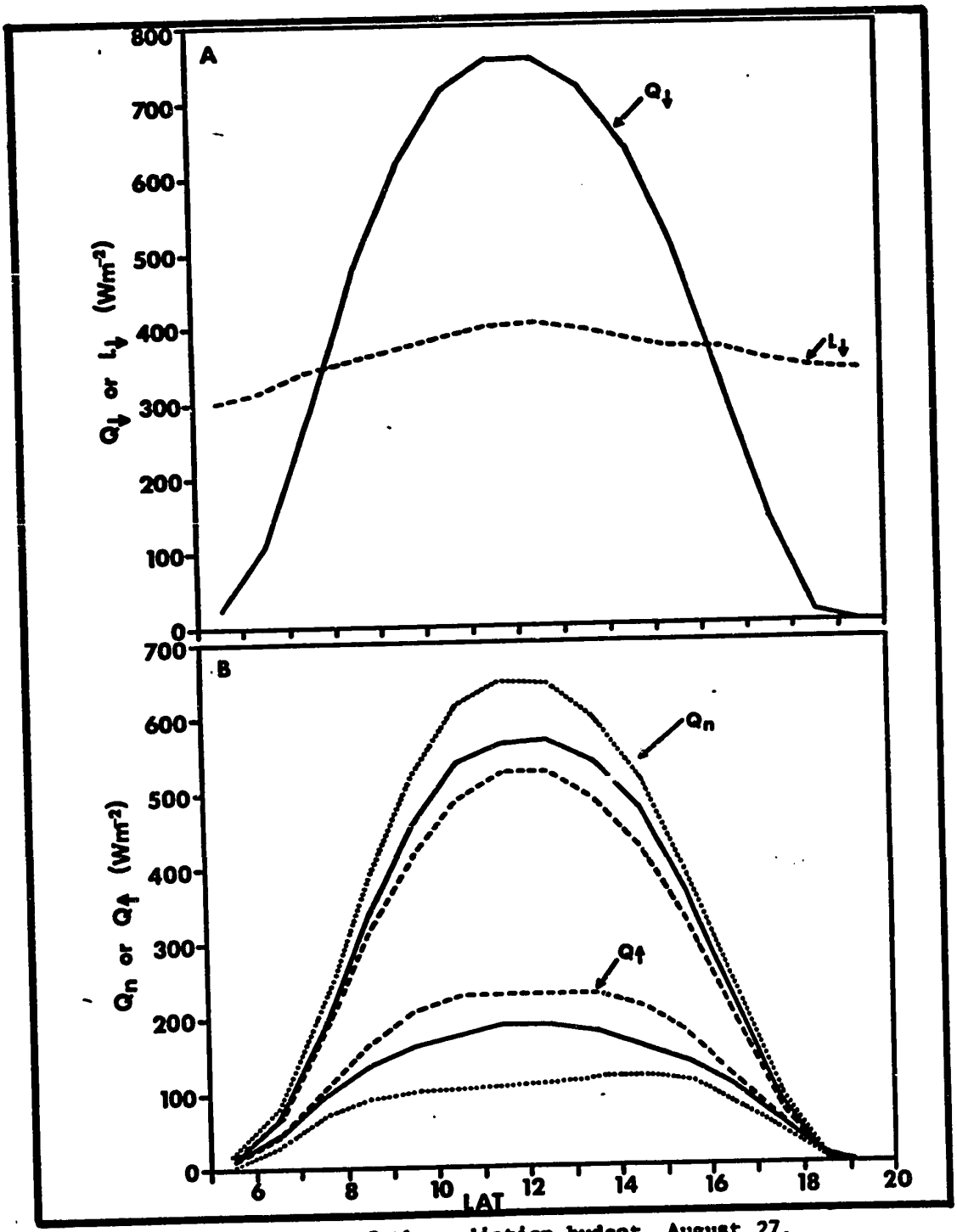

Figure 4.3: Components of the radiation budget, August 27.
(Continuation of diagram and key overleaf)

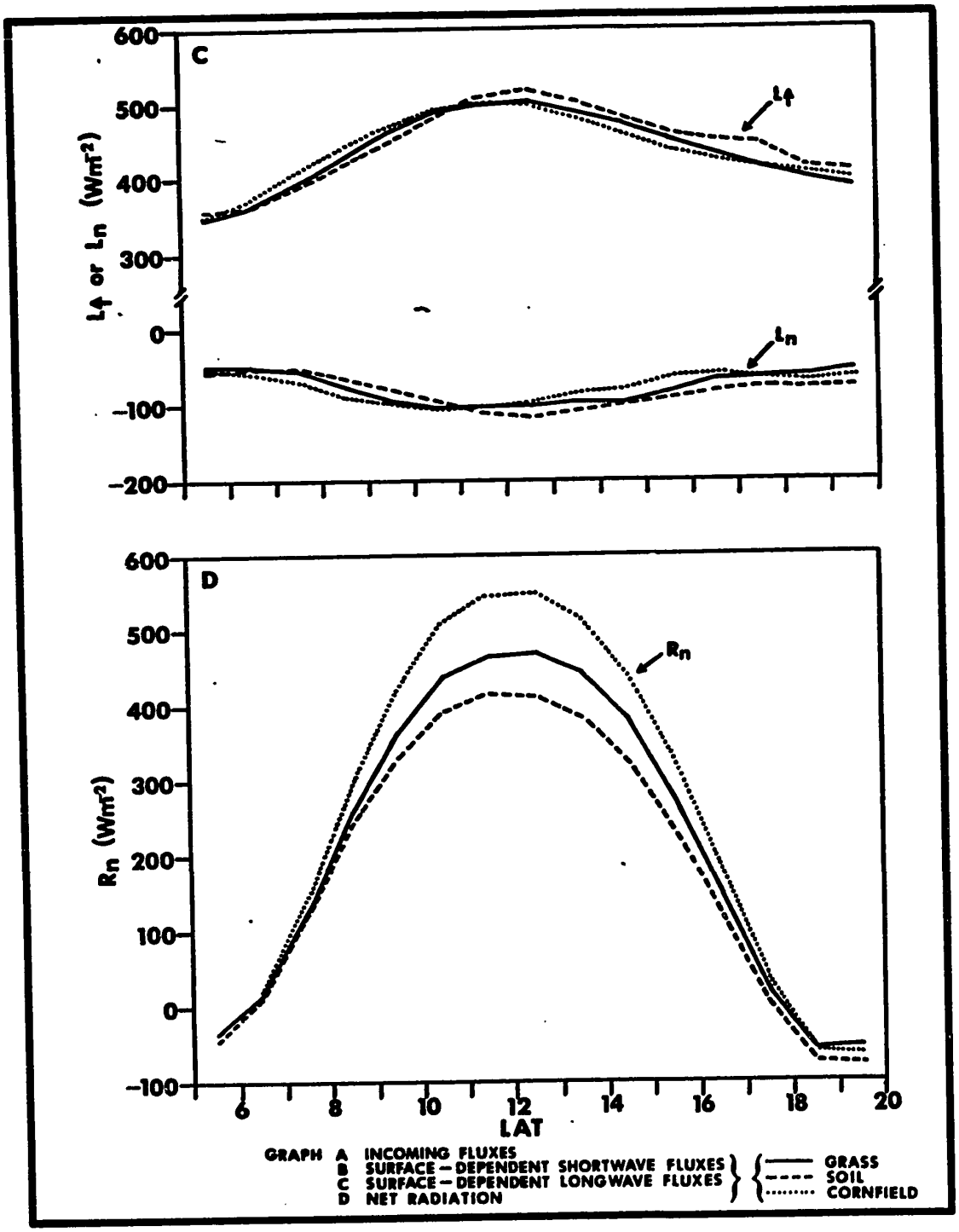

Figure 4.3; continued.

Cu at 1030. Extensive layers of Ci (0.8 - 0.9), observed at sunrise, were no longer present by 1200 and the afternoon was completely clear. Nevertheless, $L_{\downarrow}$ had undergone a decrease of 62.8 W m^{-2} by sunset, casting some doubt on the validity of the Monteith and Szeicz assumption of $L_{\downarrow}$ constancy during cloudless periods.

Shortwave absorption varied considerably between surfaces, but differences between the $L_{\uparrow}$ fluxes were smaller than those encountered on August 11. Total longwave loss from the soil during the daylight period was only about 25.1 x 10^4 J m^{-2} greater than that from the other surfaces, which exhibited virtually identical integrated $L_{\uparrow}$ totals. Hence, net radiation differences were largely determined by shortwave factors.

For grass and soil, the phase lag between surface heating and $Q_{\downarrow}$ is clearly discernible. Moreover, $L_{\uparrow}$ was generally larger in the afternoon, at a given value of R_n (or Q_n), than in the morning. For corn, the phase lag effect is not apparent and maximum radiative temperature was attained prior to solar noon.

Soil $L_{\uparrow}$ did not exceed that of grass until approximately 1100. While a more rapid response of soil temperature to radiant energy input might be expected, Idso et al (1969) have published a similar diurnal regime for a bare soil and a grass sod, measured directly, using an infrared thermometer.

Differences between the surface heating rates exhibited by the grass and soil surfaces were generally small. Though this

is in part attributable to the dessicated state of the grass plot in late August, it should also be noted that the reflection coefficient of the soil (seasonal mean, 0.311) is much higher than the majority of other soil types with a higher organic content and moisture retention capacity (see Table 2.2). Most soils will show larger shortwave radiation absorption than grass, which would tend to give rise to more marked surface heating, a tendency which is enhanced further by the smaller evaporative heat loss from dry soils. Only the lower emissivity of dry sandy soil (Sellers, 1965) will tend towards a reduction in longwave emission relative to that of a vegetated surface.

The differences encountered between the outgoing longwave fluxes from the three surfaces were generally of similar magnitude to those depicted in Fig. 4.3 until the end of the measurement season. However, daily reflection coefficient differences continued to increase (Chapter 5), leading to further disparity in absorbed solar radiation totals. Net radiation differences between the surfaces, in late August and September, were thus largely determined by the shortwave factor.

September 2 (Fig. 4.4).

The greatest similarity in longwave loss from the three surfaces occurred on September 2, a day characterised by heavy cloud cover (mean 0.95). Maximum $Q_{\downarrow}$ (491.4 W m^{-2}) was attained in the hour 1300-1400, during a clearer spell. The diurnal regime of Q_n for each surface was markedly depressed, but

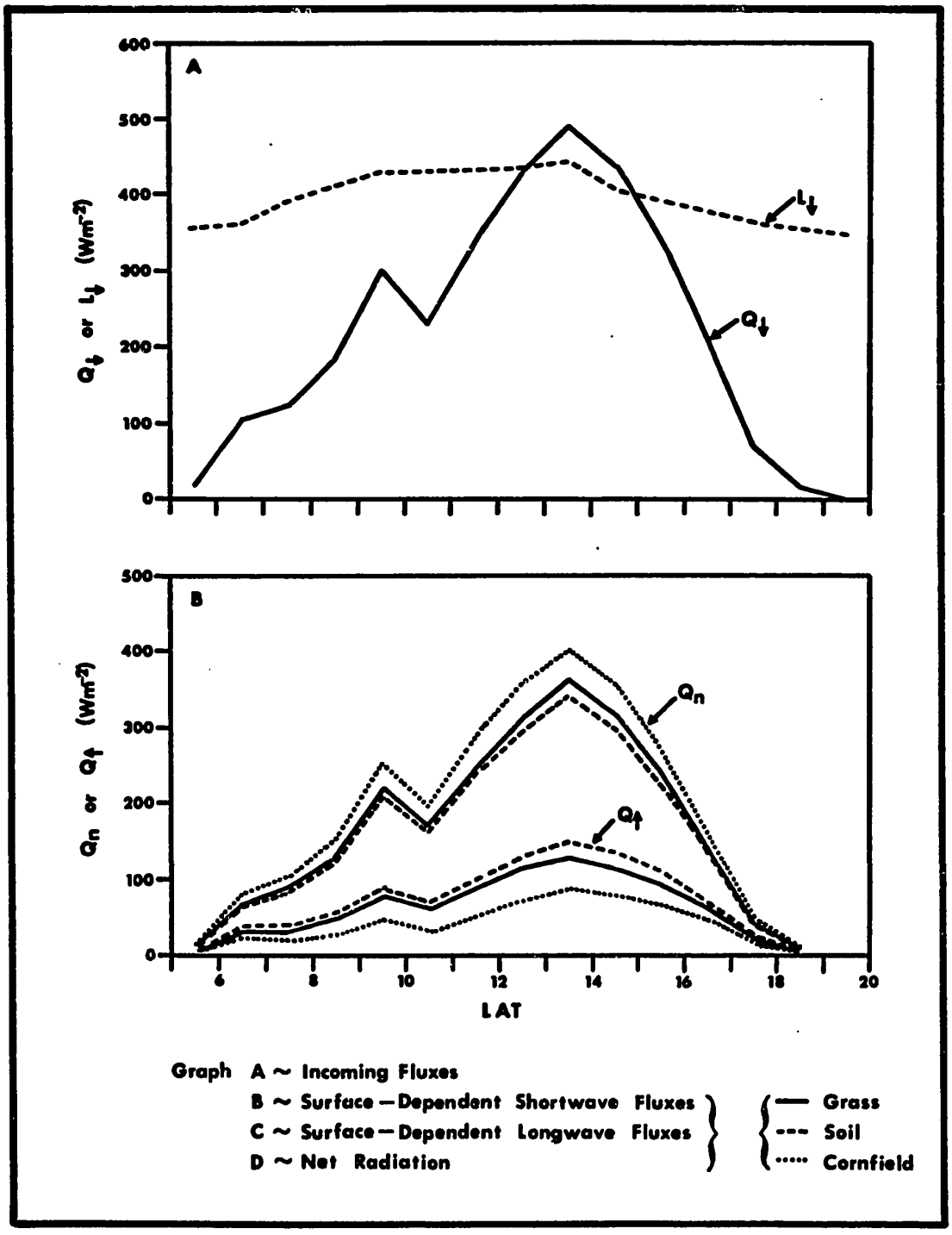

Figure 4.4: Components of the radiation budget, September 2.
(Continued overleaf)

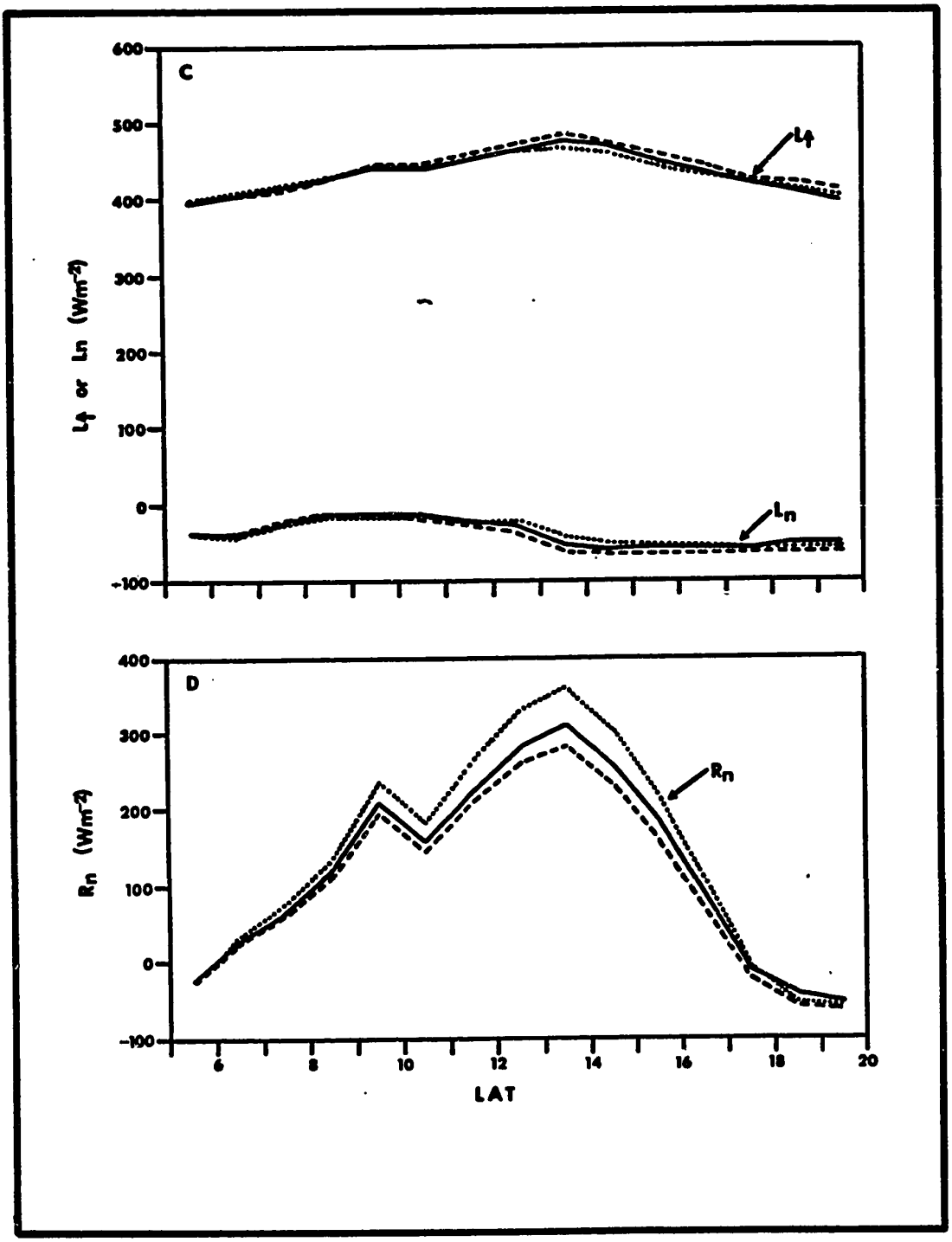

Figure 4.4; continued.

significant differences were still apparent. Under these conditions, surface heating is much reduced. The range of the soil $L_{\downarrow}$ flux on September 2 was only 87.2 W m^{-2} (equivalent to 14.7C), in contrast to the 161.2 W m^{-2} (27.4C) range encountered on August 27. Maximum temperatures for all plots were reached in the hour 1300-1400, during the clearer period. Differences in the $L_{\downarrow}$ flux between surfaces were small, but maximum loss was experienced by the soil and least by the corn.

Although total cover remained high, the mean height of the cloud increased after 1300 and less dense forms predominated. This change was accompanied by a reduction in $L_{\downarrow}$ which, in association with the increase in $L_{\uparrow}$ in the early afternoon, led to a marked increase in net longwave loss.

4.2: The Ratio of Net to Incoming Solar Radiation.

Table 4.1 lists values of the ratio of daily total net radiation to total incoming solar radiation for each surface. Values of this ratio have been published in a number of previous investigations, for several surfaces, including grass and corn. Most of the determinations for grass (Table 4.2) are smaller than those listed in Table 4.1. However, since they were mainly obtained under clear sky conditions and since longwave loss decreases more rapidly than solar radiation income in the presence of clouds (Monteith and Szeicz, 1962), higher values might be expected for the cloudy conditions encountered in this study.

Nevertheless, the mean value of 0.64 for the cornfield

TABLE 4.1

THE RATIO OF TOTAL NET TO TOTAL INCOMING SOLAR RADIATION

Date		Grass	Soil	Cornfield
July	6	0.65	0.60	0.65
	7	0.64	0.56	0.61
	8	0.61	0.52	0.58
	11	0.65	0.57	0.63
	13	0.64	0.53	0.62
	22	0.63	0.56	0.65
August	7	0.68	0.58	0.69
	11	0.59	0.50	0.64
	12	0.60	0.51	0.65
	27	0.55	0.48	0.65
	28	0.56	0.50	0.64
	29	0.56	0.50	0.65
September	1	0.58	0.53	0.66
	2	0.58	0.52	0.67
	3	0.55	0.50	0.64
	4	0.59	0.54	0.68
	9	0.57	0.53	0.64
	10	0.52	0.46	0.61
MEAN		0.60	0.53	0.64

TABLE 4.2

PUBLISHED VALUES OF THE RATIO $[R_n]/[Q_s]$ FOR GRASS

Source	Ratio
Aslyng and Nielsen (1960)	0.51
Brooks (1963)	0.50
Fritschen and Van Bavel (1964)	0.52
McIlroy and Angus (1964)	0.44
Monteith and Szeicz (1962)	0.41
Pruitt and Angus (1961)	0.56
Scholte-Ubing (1959)	0.56
Tanner and Lemon (1962)	0.55

compares well with the determinations of Decker (1964; ratio = 0.67) and Kyle (1971; ratio = 0.63). The value for soil was lower than those of the vegetated surfaces, since shortwave reflection and longwave emission from this surface were generally greatest.

4.3: Significance of Results.

To the author's knowledge, the data presented in this chapter and in Appendix 2 are the first simultaneous evaluations of the components of the radiation budget for more than one surface, over a growing season. Nevertheless, they show several points of similarity with previously published incomplete budgets and complete budgets for single surfaces, suggesting that these data are not atypical and that conclusions drawn regarding the relationships between the individual fluxes are likely to be of general validity.

On only one day was there any semblance of a constant atmospheric emission, and that day was not cloud-free. The qualitative conclusion must be that β and λ cannot be treated solely as surface parameters and that their use in net radiation estimation models is invalid. The quantitative effect of atmospheric emission on the magnitude of the net longwave coefficients is considered in Chapter 6.

Significant differences exist in the net radiant energy input to the three surfaces for a given incoming shortwave

radiation flux. Seasonal average R_n was smallest for the soil; grass and cornfield totals were respectively 12% and 23% larger. Both longwave and shortwave factors are equally significant in determining variations in available radiant energy, not only between surfaces but also for one surface at different times during the season. This conclusion is in conflict with the view of Stanhill et al (1966) that the reflection coefficient is the most important discriminant in determining net radiation totals. It is to be expected that the effects of these surface differences and seasonal changes will be reflected in the behaviour of the surface parameters α, $\beta_\uparrow$ and $\lambda_\uparrow$.

CHAPTER 5

THE REFLECTION COEFFICIENT

The need for diurnally applicable values of the model parameters has been stressed in Chapters 1 and 2. The derivation of appropriate values of the reflection coefficient for the three surfaces used in this investigation is the subject of sections 5.3 - 5.6. Nevertheless, it is not inappropriate to consider first the behaviour of this parameter within the diurnal period. Such a consideration is relevant to the prime objectives of this study for two major reasons. Firstly, the statistical validity of the various methods of computing daily α is dependent upon the nature of any intra-diurnal variation. Secondly, the physical validity of any daily value must depend on the degree to which any such variation is a function of instrumental inadequacy, rather than a real aspect of surface behaviour.

5.1: Influence of Computation Method on Hourly α Values.

Fig. 5.1 presents hourly values of the reflection coefficient for grass on August 12, a predominantly clear day with a maximum cloud cover of 0.2 (Cu, Ac and Ci). There are pronounced deviations between the hourly α values calculated by the four techniques listed in section 3.5. Generally, the arithmetic mean, weighted mean and integrated flux methods will give identical

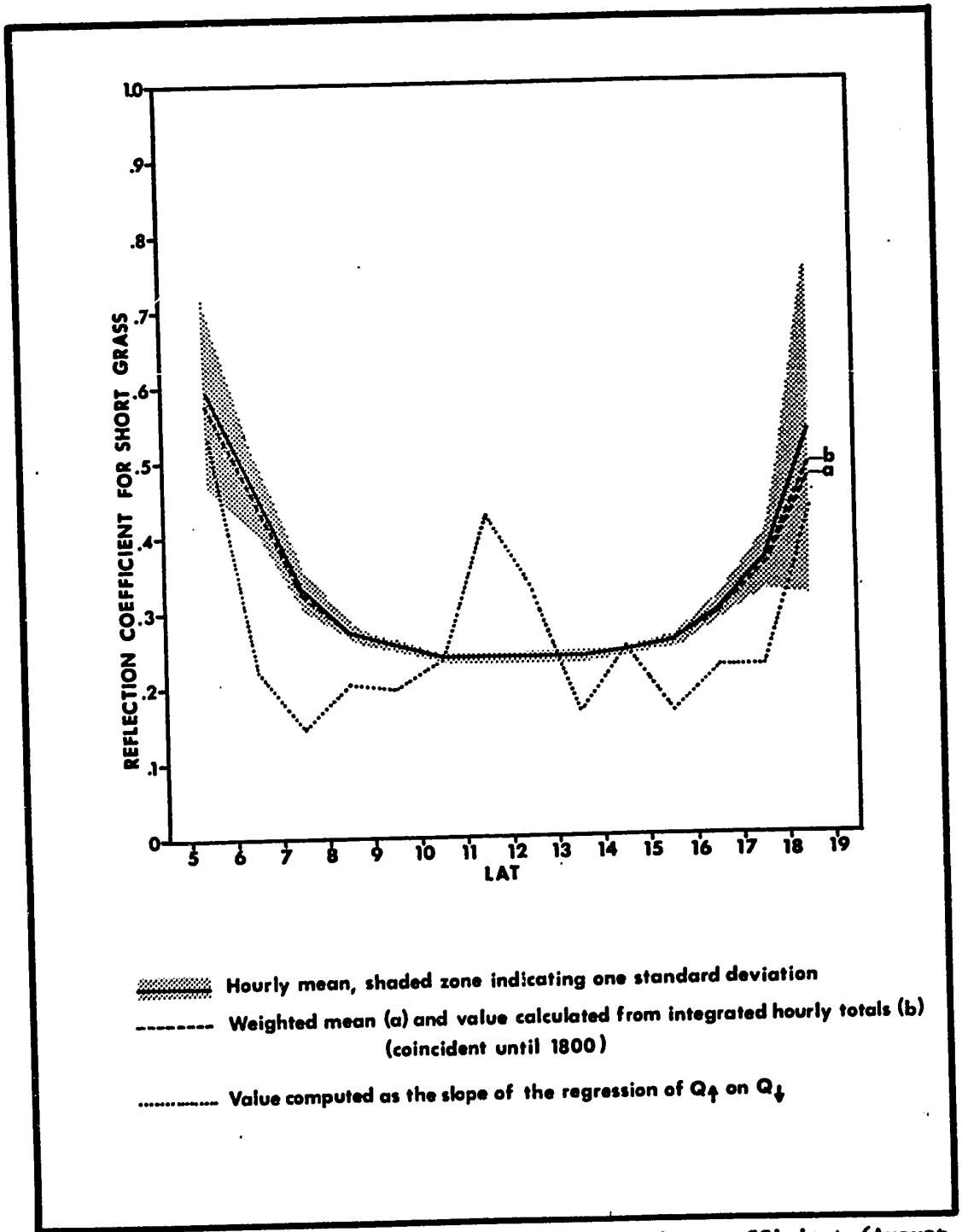

Figure 5.1: Diurnal behaviour of grass reflection coefficient (August 12), calculated by different methods.

results in the middle part of a clear day, when large fluctuations of $Q_{\downarrow}$ do not occur and the weighting procedure is redundant. In the early morning and late afternoon hours, however, the rapid changes which take place in the intensity of incoming solar radiation produce small differences between the results of method (i) and methods (ii) and (iii). The dependence of the intensity weighted estimates on solar zenith angle is thus less than that of the conventional mean. Occasionally, differences such as those indicated before 0900 and after 1500 will occur in the middle part of the day, when broken cloud results in large fluctuations of $Q_{\downarrow}$.

The standard deviation range around the arithmetic mean hourly α values is typical of a clear or slightly cloudy day. The increase in this statistic at large zenith angles results from the rapid changes in measured α which occur at these times. Standard deviation increases also occur during "cloudy-bright" periods, when data acquisition and analysis procedures are less reliable and greater (random) error is inherent in instantaneous determinations and/or when variations in the quality of $Q_{\downarrow}$ (spectral distribution or diffuse proportion) may result in real α instability.

The weighted mean and integrated flux methods will necessarily give similar results for most hours. Since the weighted mean reflection coefficient α_w is given by

$$\alpha_w = \frac{\sum \alpha Q_\uparrow}{\sum Q_\uparrow} = \frac{\sum Q_\downarrow}{\sum Q_\downarrow} ,$$

it is equivalent to an integrated flux method using the Rectangular, rather than Simpson's, Rule. Since these numerical integration procedures will give similar results when the change in the shortwave fluxes within the analysis period is virtually linear, derived α values must be similar too. Only within one or two hours of sunset and sunrise, or during marked "cloudy-bright" periods, will the results of these methods differ, and then only in the third decimal place. For all practical purposes, therefore, they may be regarded as identical.

The regression method performs poorly on an hourly basis. Within one hour of sunset and sunrise, when the shortwave fluxes are near-zero and are changing rapidly, α estimates approximate those given by the other methods. In the middle section of the day, however, little change in either $Q_\uparrow$ or $Q_\downarrow$ occurs, the points on a plot of one flux vs. the other are clustered, and the correlations are not significant. During these periods, the slope of the regression line is a poor estimate of α, values >1 and <0 being not uncommon. The use of this method for periods of less than one day is not to be recommended, therefore, and no further data of this type are presented.

5.2: Diurnal Behaviour of the Reflection Coefficient.

Selected examples of the diurnal behaviour of α,

computed by the integrated flux method, are presented in Fig. 5.2. In all cases, a marked diurnal change is indicated, the magnitude of which varies both with surface type and between days. As suggested in the previous section, it is also dependent upon the method used to calculate α.

All complete hourly reflection coefficient values and all values for 66%—complete sunrise and sunset hours are plotted against solar zenith angle in Fig. 5.3. The integrated flux method was used in this analysis, though use of the arithmetic or weighted mean would not alter the general form of the observed relationship. For all surfaces, a positive dependence of reflection coefficient on solar zenith angle is indicated, though considerable scatter exists, particularly at high angles. Midday scatter is smaller for grass than for soil or corn, a result of the seasonally more stable surface properties of this plot.

The degree to which the observed dependence of α on solar zenith angle (Z) is a function of computation method, surface type and cloud cover may be analysed if the data plotted in Fig. 5.3 are linearised by an appropriate transformation of Z. A function of the form

$$\alpha = c + d \cos Z \qquad (5.1)$$

was found to yield correlation coefficients significantly greater than those resulting from the use of an untransformed independent

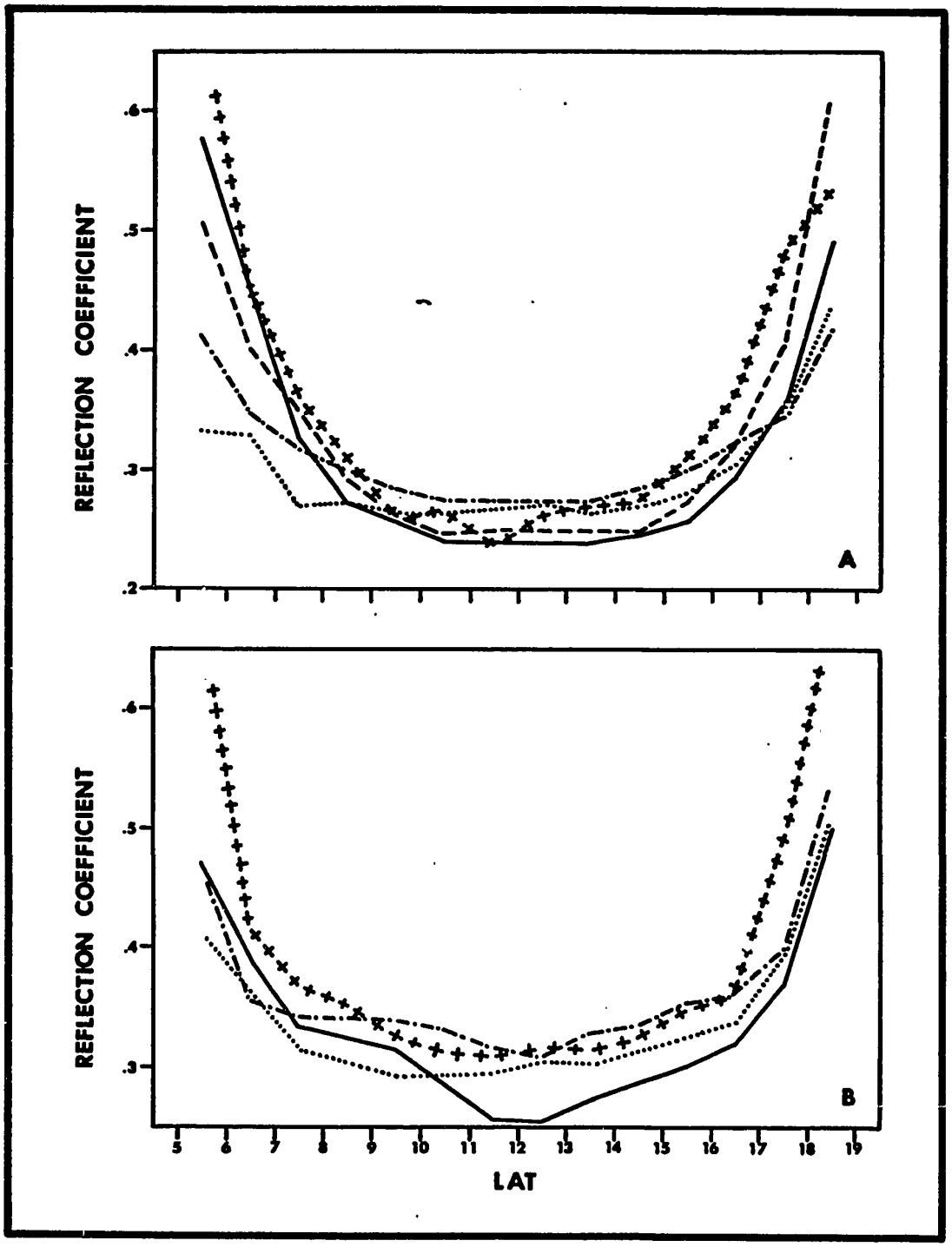

Figure 5.2: Selected examples of the diurnal behaviour of the reflection coefficient.
(Continuation of diagram and key overleaf)

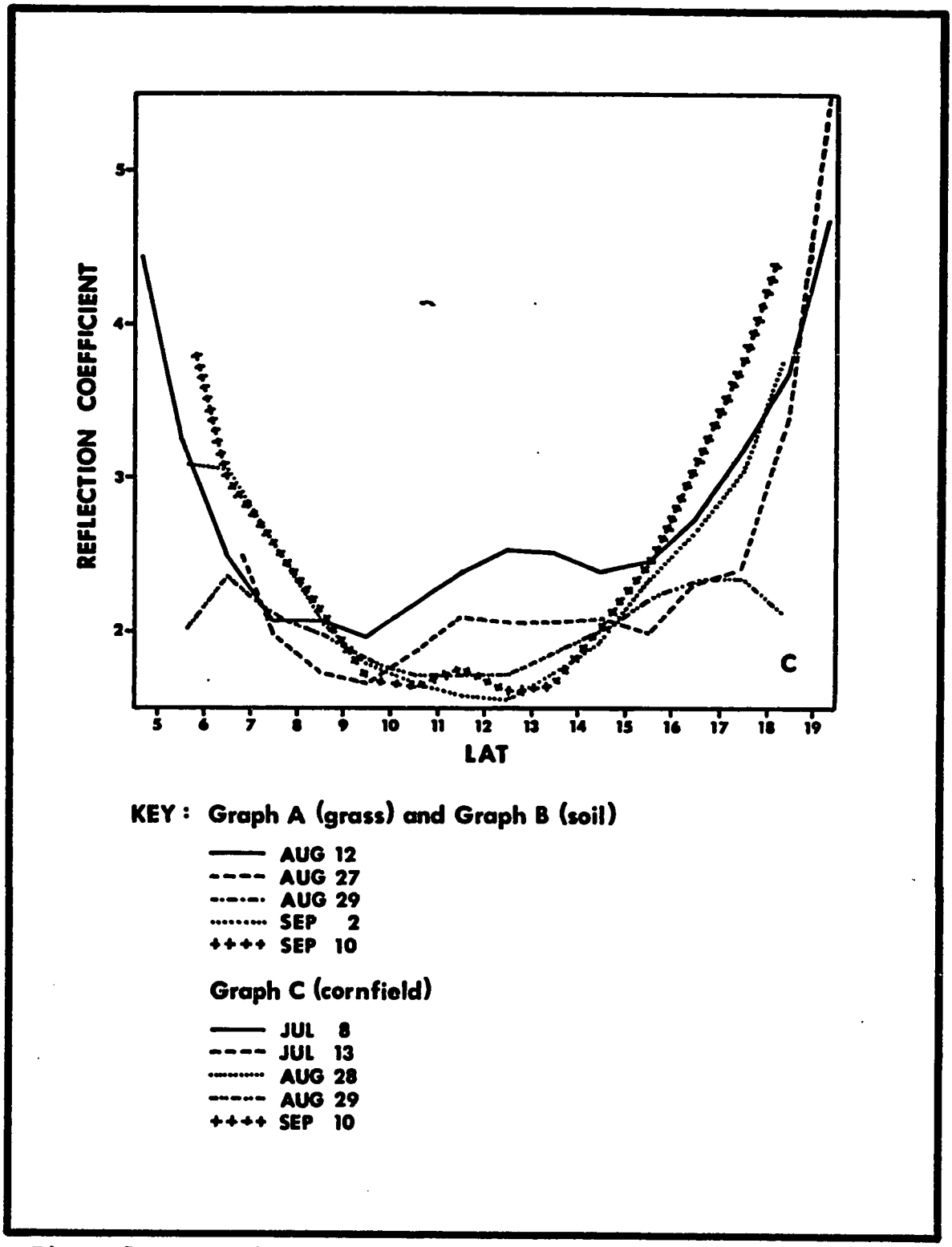

Figure 5.2; continued.

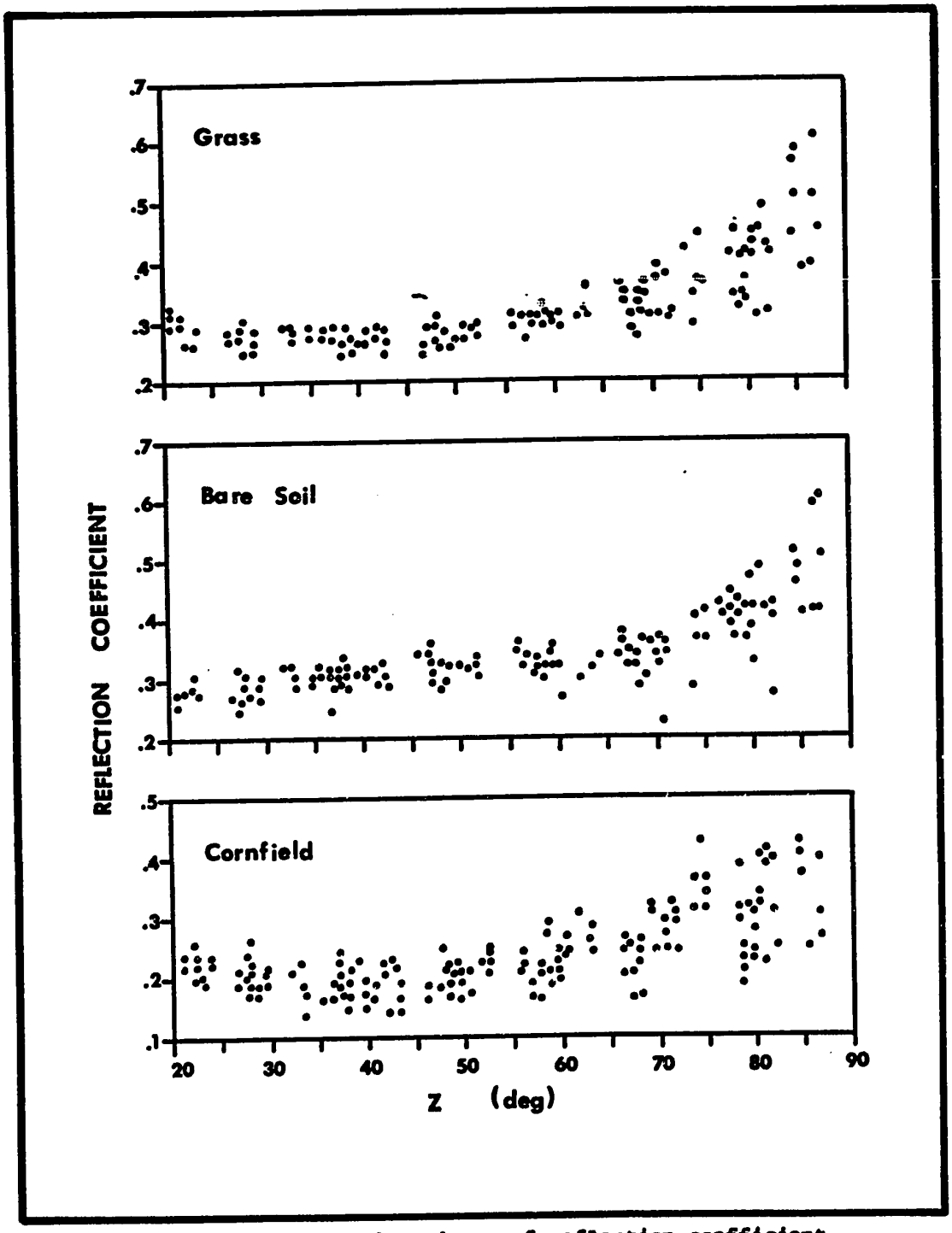

Figure 5.3: Zenith angle dependence of reflection coefficient.

variable. The coefficients of this relationship, as well as the correlation coefficient (r), were calculated for each combination of computational method and cloud cover category and are listed in Table 5.1. The regression coefficient d may be interpreted as a measure of the intensity of the zenith angle dependence of α.

The intensity-weighted α calculations for grass and soil show a slightly weaker relationship with Z than the arithmetic mean, as might be expected. For corn, the opposite is the case, though no explanation can be suggested for this. Of the weighted mean and integrated flux methods, the latter shows a stronger relationship with zenith angle in all cases, suggesting that the nature of the deviation between these two methods observed for August 12 (Fig. 5.1) is a regular occurrence. The differences are, however, very small. Correlations are generally better for the intensity-weighted methods because the cosine transformation was not always completely successful in linearising the relationship when the arithmetic mean method was used.

The influence of surface type and the effect of cloud cover are, however, independent of the method of calculation. Consideration will thus be given solely to the statistics derived from the analysis of the integrated flux method α determinations.

For all cloud cover categories, a stronger dependence is exhibited by grass α than soil α, a result which might have been expected if variations in the efficiency of a multiple reflection process at the surface of a rough landscape element are

TABLE 5.1

REGRESSION AND CORRELATION STATISTICS OF (5.1).

Method of Computation	Cloud	Grass			Bare Soil			Cornfield		
		c	d	r	c	d	r	c	d	r
(i) Arithmetic mean	A	0.426	-0.205	-0.703	0.438	-0.181	-0.668	0.308	-0.148	-0.631
	B	0.463	-0.284	-0.816	0.427	-0.148	-0.833	0.359	-0.242	-0.916
	C	0.451	-0.235	-0.748	0.458	-0.210	-0.765	0.319	-0.157	-0.676
	D	0.387	-0.151	-0.612	0.415	-0.152	-0.534	0.277	-0.112	-0.488
(ii) Weighted mean	A	0.414	-0.190	-0.761	0.417	-0.152	-0.721	0.314	-0.156	-0.669
	B	0.468	-0.295	-0.884	0.431	-0.154	-0.852	0.367	-0.256	-0.919
	C	0.439	-0.220	-0.815	0.434	-0.177	-0.838	0.328	-0.169	-0.716
	D	0.368	-0.127	-0.666	0.388	-0.116	-0.550	0.280	-0.114	-0.528

(continued overleaf)

TABLE 5.1 (continued)

(iii)	Integrated flux value	A	0.415	-0.192	-0.761	0.419	-0.155	-0.722	0.315 -0.158 -0.669
		B	0.471	-0.299	-0.888	0.433	-0.157	-0.858	0.369 -0.259 -0.921
		C	0.441	-0.223	-0.812	0.435	-0.178	-0.831	0.329 -0.171 -0.716
		D	0.369	-0.128	-0.668	0.391	-0.120	-0.557	0.280 -0.114 -0.526

Fractional cloud cover categories:

A	0.0 - 1.0	234	observations
B	0.0 only	32	"
C	0.1 - 0.5	106	"
D	0.6 - 1.0	96	"

postulated as the cause of such phenomena. However, the dependence of corn α on zenith angle is similar to that for soil when all data are included in the regression computation, and is more marked than for soil only under clear skies. A relative measure of the change in α per unit change in $\cos Z$ may be obtained if d is expressed as a proportion of mean surface reflection. For soil, grass and corn respectively, the resulting ratios are -0.498, -0.686 and -0.782 (cloud category A), indicating that percentage change in α is positively related to surface roughness.

The regression lines represented by coefficients c and d, derived from the integrated flux data, for cloud categories B, C and D (Table 5.1), are plotted in Fig. 5.4. For the vegetated surfaces, a marked decline in the strength of the dependence of α on Z occurs as cloud cover increases. This suggests that diurnal reflection coefficient change is related to variations in canopy interception with solar elevation, since cloud cover would tend to increase the diffuse component of $Q_{\downarrow}$, which is more nearly isotropic than direct beam radiation. Such an effect has been noted by Graham and King (1961), Impens and Lemeur (1969) and Kyle (1971).

The results for these surfaces show a tendency for cloud cover to increase the minimum daily reflection coefficient, a phenomenon reported by Angström (1925), Kalitin (1930), Rijks (1967), Grulois (1968), Impens and Lemeur (1969) and Kalma and

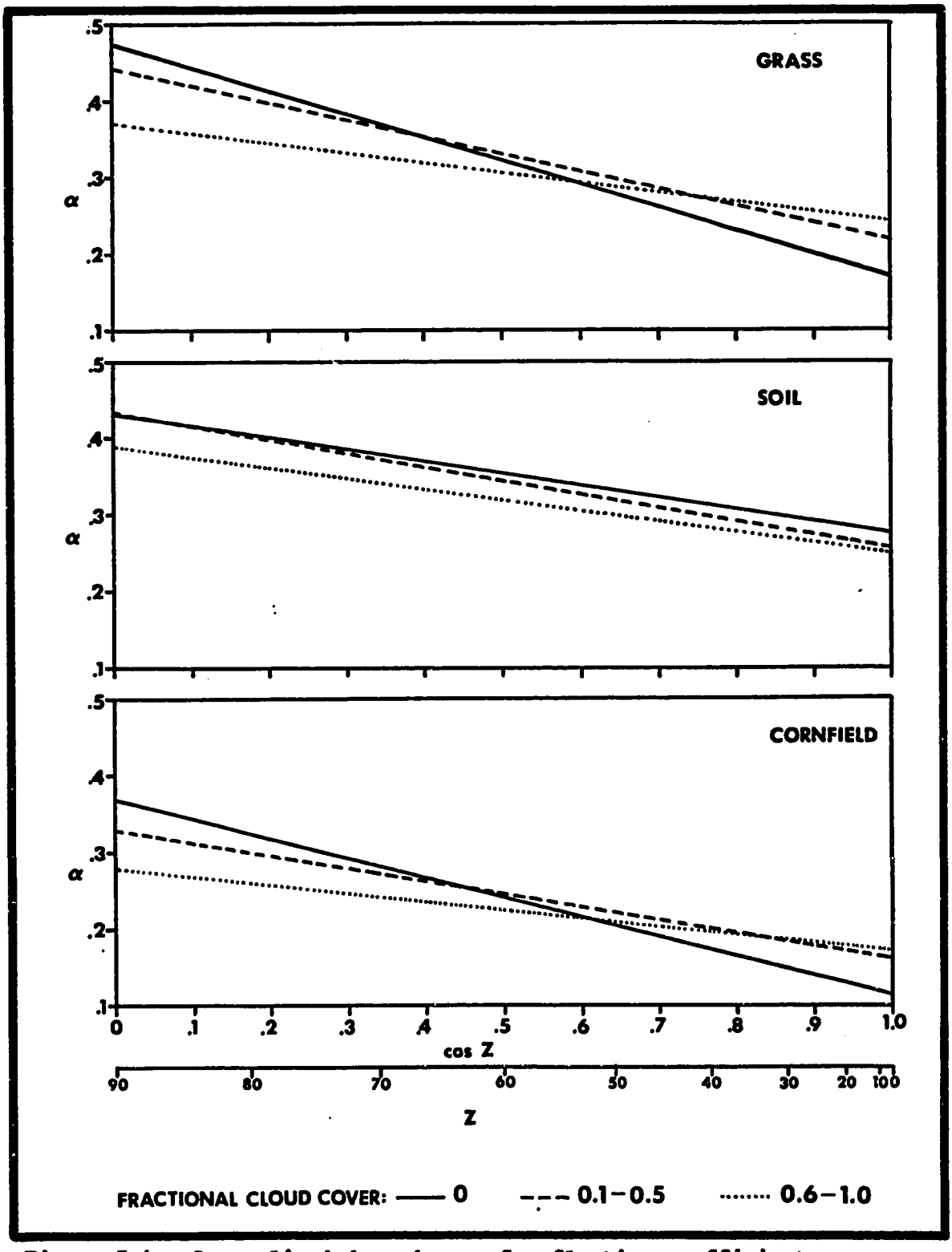

Figure 5.4: Generalised dependence of reflection coefficient on solar zenith angle (Z).

Stanhill (1969). However, since a cloud cover present all day will also tend to reduce the higher α values measured at large zenith angles, the effect on the daily mean may not be marked. This might explain the difficulty encountered by Stanhill et al (1966) and Stanhill and Fuchs (1968) in detecting any clear relationship between daily α and cloud amount.

For soil, no clear trend of increasing cloud cover on either d or minimum α may be detected. This may be related to the smoothness of the surface, relative to the vegetated plots, and a consequent near independence of changes in the diffuse to direct ratio in $Q_{\downarrow}$.

Many of the diurnal curves of cornfield α display marked asymmetry, afternoon values exceeding morning ones at the same zenith angle (Fig. 5.2). This phenomenon, which is most clearly apparent in the early part of the measurement season, is interpreted as a result of a distinct diurnal pattern in shortwave absorption within the corn canopy. The pre-noon minimum is associated with an efficient multiple reflection process which can take place when the solar beam is parallel to the crop rows and can readily penetrate to depth. In the afternoon, when the sun is shining across the rows, shortwave radiation penetration is more restricted and reflection is enhanced. As the canopy matures, this effect might be expected to become less pronounced.

In Fig. 5.5, plotted for each day's data over the season is $\Delta\alpha$, the difference between α for the hour during which

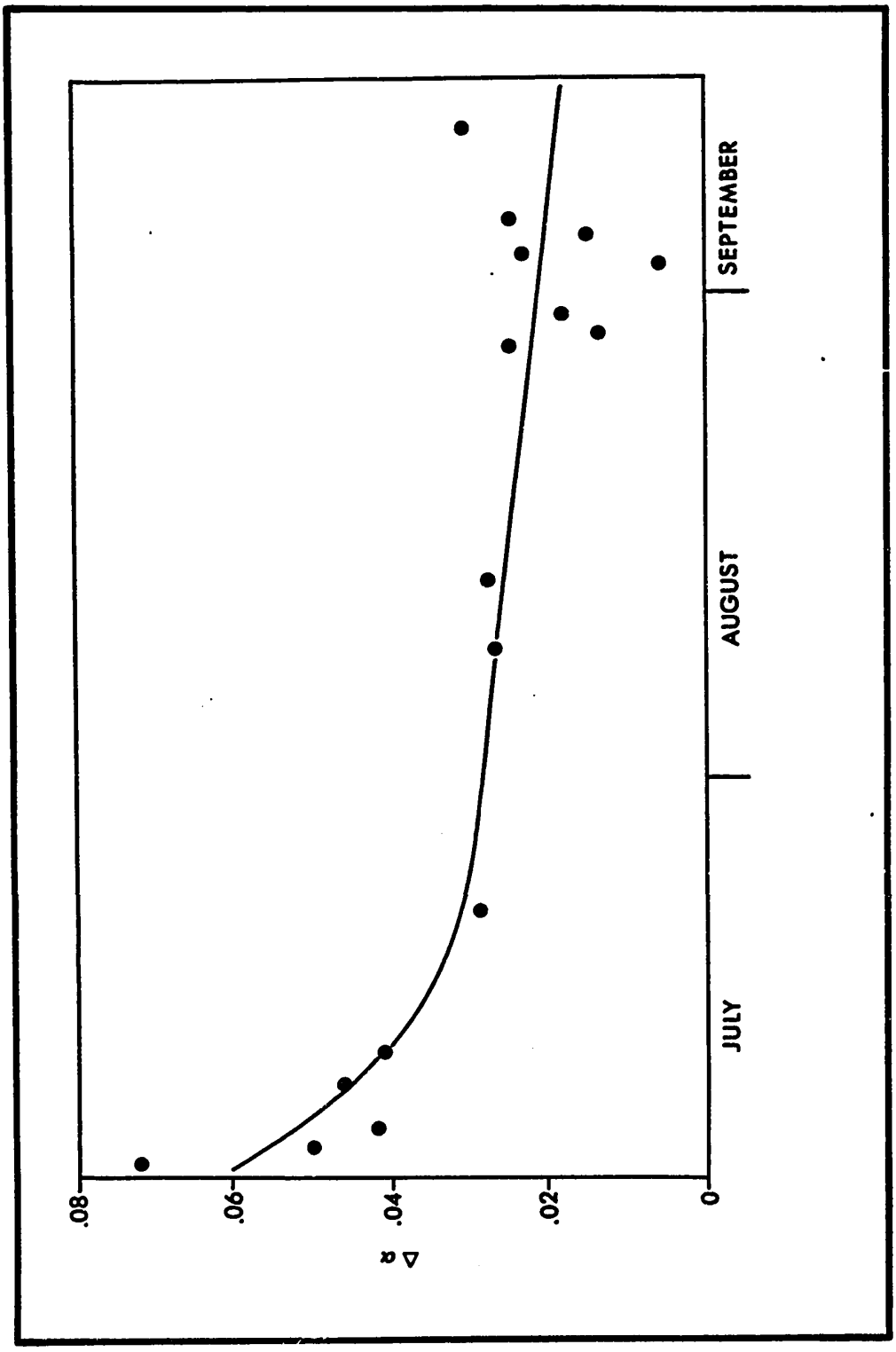

Figure 5.5: Seasonal behaviour of $\Delta\alpha$ (defined in text) for cornfield.

solar azimuth was 45° west of S and that when solar azimuth was 45° east of S. The decrease in $\Delta\alpha$ from early June to September follows the attainment of canopy maturity. It is noteworthy that the most rapid change in $\Delta\alpha$ takes place at the time when ground coverage and crop height were increasing most rapidly (c.f. Fig. 3.2).

Nevertheless, it is significant that positive values of $\Delta\alpha$ were noted on every day for which data are available, suggesting that the row effect was always operative to some extent, even with full canopy development, or that the leaf moisture content or wilting effects, invoked by Stanhill et al (1968) and Impens and Lemeur (1969) for corn, and Kalma and Stanhill (1969) and Kondrat'yev (1969) for other canopy types, may be significant.

5.3: Significance of Instrumental Error in Daily Reflection Coefficient Evaluation.

The reality of the previously discussed systematic diurnal reflection coefficient fluctuations has been questioned by Fritschen (1967) and Brown et al (1970). They postulate that, at high zenith angles, a portion of the incoming solar radiation flux may be intercepted by the glass hemisphere covering the downfacing element and be reflected and/or refracted to the thermopile surface, resulting in spuriously high reflection coefficient determinations. While the general validity of their argument is not assessed in this investigation, an attempt is made to estimate

the degree to which any such potential error could bias the daily reflection coefficients evaluated for use in net radiation estimation models.

From the configuration of the Swissteco net pyranometer used in this study, the critical zenith angle (Z_c) at which the lower hemisphere of the instrument became entirely shaded in the morning and unshaded in the afternoon, was calculated. Since the collar around the thermopile unit is of variable width, Z_c is a function of solar azimuth angle (Fig. 5.6B). When $Z<Z_c$, the type of error hypothesised by Fritschen and Brown et al may be discounted. Fig. 5.6A indicates the extent of such periods over the measurement season. An inspection of Fig. 5.2 reveals that, even during this portion of the day, α exhibits a dependence on zenith angle. When $Z_c<Z<90^o$, the possibility of such an error cannot be rejected, but significant effects of the type postulated are unlikely to occur while the angle of incidence of the solar beam on the lower glass dome is small.

During the measurement season, the average incoming solar radiation receipt during the period when $Z<Z_c$ exceeded 80% of the daily total. An intensity-weighted method of daily reflection coefficient calculation will be also, therefore, strongly weighted in favour of that part of the day when refraction/reflection error can be discounted. Furthermore, the fact that the degree of dependence of α on Z varies between surfaces on the same day suggests that at least part of the change in reflection coefficient

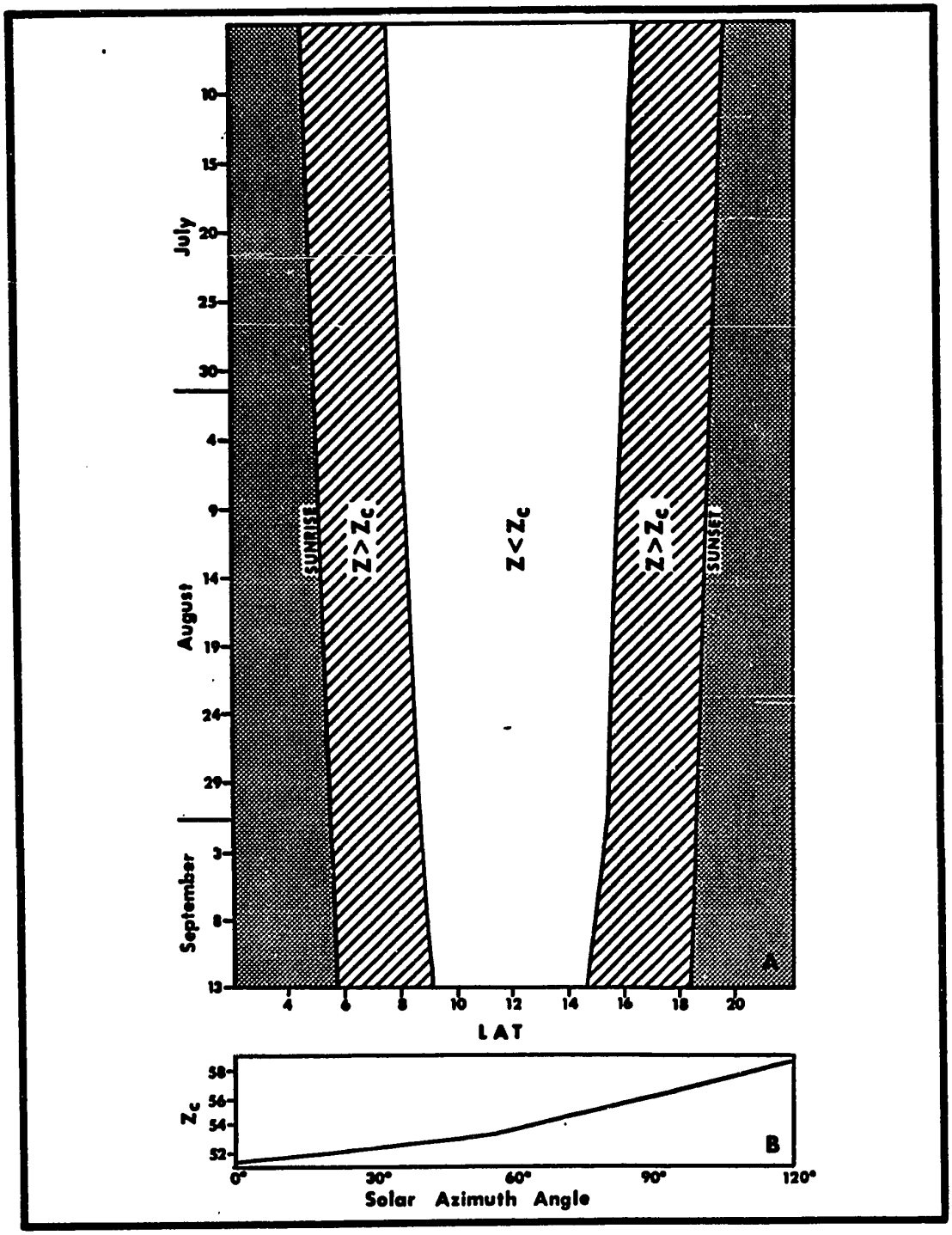

Figure 5.6: Occurrence of potential net pyranometer error.

during times when $Z>Z_c$ is a real aspect of the radiative behaviour of vegetation and soil surfaces.

However, considerable caution should be exercised in the interpretation of the arithmetic mean daily α value, since this method assigns equal weight to all data, irrespective of prevailing zenith angle.

Future studies should guard against the possibility of errors of this type by the use of suitable shading rings around the sensor measuring the surface-dependent shortwave flux (either Q_n or $Q_\uparrow$). Such configurations will possess large Z_c values, which can be exceeded only at large solar zenith angles. Nevertheless, care should be taken to ensure that such modifications do not cause undue interference with the underlying surface, by casting shadows within the significant sampling area of the instrument.

5.4: Influence of Computation Method on Daily α Values.

Table 5.2 presents, for each surface and method of calculation, seasonal mean values, standard deviations and coefficients of variation of the daily reflection coefficients. The dependence on method of calculation, present in the mean values, was found also for all individual days and is identical for each of the three surfaces. The weighted mean and integrated flux values never differed by more than 0.001, while the arithmetic mean exceeded the integrated value by an average of 10% for the vegetated surfaces and 8% for the soil. Conversely, the

TABLE 5.2

SEASONAL MEAN REFLECTION COEFFICIENTS AND RELATED STATISTICS

Surface and Method of Calculation		Mean	Standard Deviation	Coefficient of Variation $x10^2$
Grass:	arithmetic mean	0.308	0.018	5.8
	weighted mean	0.280	0.009	3.3
	integrated flux value	0.280	0.009	3.3
	regression value	0.247	0.020	8.1
Soil:	arithmetic mean	0.335	0.028	8.3
	weighted mean	0.311	0.020	6.5
	integrated flux value	0.311	0.020	6.6
	regression value	0.289	0.024	8.4
Corn:	arithmetic mean	0.222	0.028	12.8
	weighted mean	0.202	0.021	10.4
	integrated flux value	0.202	0.021	10.5
	regression value	0.175	0.023	13.2

regression calculation is lower than the integrated value, by 12% for grass, 7% for soil and 13% for corn. Correlations between $Q_{\uparrow}$ and $Q_{\downarrow}$ were high, generally exceeding 0.95 for all surfaces, although slightly lower values (0.85 -0.90) were noted for corn in July, due to diurnal asymmetry in the shortwave reflection properties of the canopy. The smaller α values yielded by this method, which have been described also by Davies and Buttimor (1969), appear to be a result of the previously noted diurnal fluctuation in reflection coefficient. Only when the $Q_{\uparrow}/Q_{\downarrow}$ ratio is virtually constant over a daily period will the linear regression line fitted to the data pass through the origin, and the slope of the line approximate the instantaneous values of the ratio. If α increases at high zenith angles, data points near the origin will lie above the best-fit line characteristic of midday data, will yield a positive intercept on the $Q_{\uparrow}$ axis and will tend to lower the slope of the line. Intercept values between 7 and 35 W m^{-2} were noted in this investigation. While this constitutes a form of weighting in favour of high intensity $Q_{\downarrow}$ fluxes, resulting daily α values are frequently lower than the minimum hourly value encountered during that day, a phenomenon also noted by Idso et al (1969). Moreover, since the same data may be used to compute simply an exact $Q_{\downarrow}$ intensity weighted α value, the use of this technique is to be discouraged.

Despite the influence of the method of computation on the daily α value, however, the selection of the appropriate value

for use in a net radiation model is not an arbitrary one. An essential prerequisite for the estimation of R_n is the calculation of the net shortwave radiation, a fact implied in (2.8), (2.10), (2.14) and (2.15) by the inclusion of the terms $(1 - \alpha)[Q_\downarrow]$. Since the net radiation estimate sought is an integrated daily total, and since the $Q_\downarrow$ data input to the model will be in this form, only the α value calculated by the integrated flux method will yield an appropriate Q_n total. (These remarks apply equally to daily means derived from daily totals.) The use of any other method of α calculation is strictly invalid for this purpose. However, since the weighted mean technique has been shown to yield essentially identical estimates, the use of this simpler method is permissible, if sufficient data are available.

In the following analysis, only integrated flux determinations will be used.

5.5: Seasonal Behaviour of the Reflection Coefficient.

Table 5.2 reveals that, both on an absolute (standard deviation) and percentage basis, grass α exhibits the greatest seasonal stability. Though the standard deviations of the daily means for corn and soil are similar, the smaller reflection coefficient for the vegetated surface results in a larger percentage deviation from the seasonal mean. The stability of the surface properties of each plot is reflected in the relative magnitudes of the coefficients of variation. Little change occurred in the

appearance of the grass plot throughout the season, but soil colour varied considerably with fluctuations in soil moisture content. Very large seasonal changes in crop ground cover, plant height and canopy appearance may be considered responsible for the large value of the coefficient of variation for corn.

Mean reflection coefficients for the vegetated surfaces compare well with previously published values (Table 2.2), although the grass α of 0.280 is slightly larger than the value of 0.26 hypothesised by Monteith (1959) to be typical of short crops, completely covering the soil. This may be a result of the incomplete ground cover (95%) and the high reflection coefficient of the underlying soil. The bare soil α value is high relative to the published data in Table 2.2, and this is attributed to the low organic content of the Fox sandy loam, of which the soil plot was composed. Soil reflection coefficients derived in this investigation are similar to published values for sand (e.g. Budyko, 1956; Sellers, 1965; Kondrat'yev, 1969).

Table 5.3 lists values of the reflection coefficient for each of the three surfaces, over the measurement period. While soil α exhibits an increasing trend throughout the season, the grass coefficient appears to fluctuate randomly around the seasonal mean value. The regime for corn is complex, showing relatively high values (mean = 0.218) until the second week in August, followed by a period of low values (mean = 0.186). The seasonal behaviour of corn α during late July, August and September is similar to

TABLE 5.3

DAILY MEAN REFLECTION COEFFICIENT VALUES

Date		Grass α	Soil α	Corn α
July	6	0.273	0.263	0.209
	7	0.304	0.298	0.237
	8	0.291	0.303	0.242
	11	0.283	0.292	0.197
	13	0.271	0.301	0.201
	22	0.267	0.261	0.224
August	7	0.278	0.318	0.228
	11	0.282	0.323	0.223
	12	0.269	0.299	0.205
	27	0.272	0.333	0.181
	28	0.281	0.342	0.195
	29	0.288	0.335	0.191
September	1	0.274	0.306	0.169
	2	0.276	0.314	0.180
	3	0.282	0.321	0.193
	4	0.274	0.320	0.181
	9	0.284	0.315	0.181
	10	0.291	0.336	0.201

that reported by Stanhill et al (1968). Their data showed a maximum in early August, followed by a progressive decline. The high values of early July are absent from the Israeli data, however, possibly as a result of the much lower soil reflection coefficients (0.10 - 0.11) reported for that location. It is noteworthy that on July 6, 7 and 8, when corn ground coverage was less than 10%, measured α for the cornfield is less than that for the bare soil plot. This suggests greater multiple reflection at the former surface, due to the immature corn plants which were 0.25 - 0.35 m high, and/or the greater roughness of the soil surface, associated with the furrowing which accompanied seeding operations (Skvortzov, 1928).

The suggestion of a seasonal trend in the soil and corn data is borne out by an analysis of the sequence of α determinations above and below the surface median (Siegel, 1956). At the 0.05 level, the hypothesis that the observed sequence is attributable to chance may be rejected for soil and corn, but not for the grass plot. Further evidence for the lack of any significant seasonal trend in the grass data is presented in the following section.

5.6: Estimation of the Reflection Coefficient.

Table 5.4 presents simple correlations between measured reflection coefficient values and a number of readily available surface and environmental variables whose relationship to α has

TABLE 5.4

CORRELATION AND STANDARD ERROR OF ESTIMATE STATISTICS FOR α ESTIMATION

Independent Variable	r	s	r_p
(A) Grass:-			
(i) Daily mean soil moisture	0.014	0.010	-0.016
(ii) Daily median zenith angle	0.046	0.010	0.192
(iii) Daily mean cloud cover	-0.093	0.010	-0.070
(iv) Grass height	0.145	0.010	0.222
(B) Bare soil:-			
(i) Daily mean soil moisture	-0.804*	0.013	-0.719*
(ii) Daily median zenith angle	0.422	0.019	-0.152
(iii) Daily mean cloud cover	-0.292	0.020	-0.117
(C) Cornfield:-			
(i) Daily mean soil moisture	0.740*	0.014	0.467
(ii) Daily median zenith angle	-0.638*	0.017	-0.330
(iii) Daily mean cloud cover	-0.134	0.022	0.249
(iv) Crop height	-0.558*	0.018	-0.197
(v) Percentage ground cover	0.062	0.022	0.152
(vi) Proportion of biomass dessicated	-0.700*	0.016	-0.333

(continued overleaf)

TABLE 5.4 (continued)

(D) Multiple correlation coefficients and standard errors of estimate:-

Surface	R	s	Order in which independent variables (above) entered analysis.
Grass	0.266	0.011	(iv), (ii), (iii), (i)
Bare soil	0.817*	0.013	(i), (ii), (iii)
Cornfield	0.806*	0.015	(i), (iii), (ii), (iv), (v), (vi)

*denotes correlation coefficients significant at 0.05 level.

been demonstrated or hypothesised. The variables used in this analysis for each surface are listed in the first column. Also tabulated are the standard error of the estimate for each associated linear regression relationship (s), the partial correlation coefficient, with all other variables held statistically constant, (r_p), the multiple correlation coefficient between α and all independent variables (R) and the standard error of the estimate for the related multiple regression equation.

No significant correlations could be demonstrated between grass α and the four independent variables use in the analysis, thus strengthening the hypothesis that the daily fluctuations in reflection coefficient exhibited in Table 5.3 are essentially random.

Only soil moisture was shown to be significantly correlated with soil α, the lower reflectivity of water than that of most solid soil constituents giving rise to an inverse relationship. Such a dependence, noted in several previous studies (Monteith, 1959; Fritschen, 1967; Ogunloyinbo, 1970; Idso, 1971), gives rise to the trend exhibited in Table 5.3, since soil moisture declined progressively over the measurement period (Fig. 3.2).

Four variables exhibit significant correlations with cornfield α. Though soil moisture explains most of the variance in reflection coefficient, the sense of the relationship is opposite to that for soil. Furthermore, the negative correlation with daily median zenith angle is quite unexpected. It is noteworthy

that significant relationships occur with variables which exhibit approximate monotonic trends over the season and it may be that α depends upon variables other than those considered here or (probably more likely) upon different factors at different stages in the development of the canopy. Unfortunately, an insufficient amount of data is available to adequately test this hypothesis. The large number of variables necessary to characterise the seasonal development of the cornfield surface reduces markedly the degrees of freedom for correlation analysis and, consequently, none of the partial correlation coefficients may be regarded as significant at the 0.05 level.

For no surface can significant dependencies on environmental variables be considered adequately demonstrated. Reflection coefficient shows no correlation with cloud cover, suggesting that the apparent effect of a high diffuse component of $Q_{\downarrow}$ on midday values, for the vegetated surfaces, is offset by the tendency for lower values at lower solar elevation. The only zenith angle dependency found is that for corn, and that is of opposite sense to that expected from hourly data. However, since daily median Z increases monotonically during the measurement season, the possibility of the previously-discussed spurious correlation cannot be rejected. It should not be overlooked that, over a longer time period, when zenith angle change is more pronounced, consideration of this variable may be necessary to adequately estimate α.

The use of a stepwise multiple regression analysis failed

to yield better predictive relationships than those implied in section A, B and C of Table 5.4. For grass, the standard error of the estimate of the relationship

$$\alpha = \bar{\alpha} = 0.280 \qquad (5.2)$$

was no larger (0.010) than that for all simple and multiple regression equations. No significant multiple correlation coefficients were found.

For soil, though all derived multiple correlation coefficients were significant at the 0.05 level, no further reduction in s occurred with the addition of second and third independent variables. The equation

$$\alpha = 0.402 - 1.139 x_w \qquad (5.3)$$

may thus be considered adequate for predictive purposes and has the additional virtue of using as the predictor a variable whose physical significance is readily intelligible.

Similarly, for cornfield data, the use of more than one independent variable failed to reduce s below 0.014, though multiple correlation coefficients increased as the degrees of freedom were reduced. The relationship

$$\alpha = 0.124 + 1.003 x_w \qquad (5.4)$$

will predict cornfield α with almost the same absolute error as that for soil, though percentage error will be greater for the vegetated surface. However, it must be borne in mind that the causal basis for (5.4) is obscure. Neither the existence of a significant positive correlation with x_w, nor, indeed, the seasonal pattern of α exhibited in Table 5.3, is readily explicable and considerable caution should attach to its use.

5.7: Significance of Results.

The estimation of net radiation, using (2.8), (2.10), (2.14) or (2.15), requires a representative and accurate value of the parameter α. The results described in this chapter are relevant to this objective in several ways.

Firstly, the data are an addition to the body of knowledge concerning the reflective properties of short grass, bare soil and corn. Though previous determinations of α for these surfaces are available, few studies have concerned themselves with the seasonal fluctuations of the parameter, or with the related problem of establishing relationships, ideally predictively useful relationships, with surface and environmental variables. The reflection coefficient is not necessarily a constant for a given surface type. Variance in this parameter will contribute to variance in R_n totals, not merely between surfaces but also for one surface at different times during the growing season.

Secondly, the α values found and the error associated

with their estimation are data required in the subsequent analysis (Chapter 7) of the sensitivity of net radiation estimates to inaccuracy in the model input parameters.

Finally, this study provides data on the diurnal variation of α, as it influences the method of computation and physical reality of the derived daily value, a topic which has received scant attention in previous work. Only the integrated flux and the $Q_{\downarrow}$ intensity weighted mean methods yield a daily value appropriate for use in the proposed net radiation equations. The arithmetic mean and regression technique should not be employed since they, respectively, overestimate and underestimate α. Though the diurnal fluctuation cannot be attributed solely to instrumental inadequacy, the recommended methods of calculating α have the additional advantage of rendering negligible the effect of potential error in Q_n or $Q_{\downarrow}$ measurements at large solar zenith angles.

CHAPTER 6

THE LONGWAVE PARAMETERS

6.1: Net Longwave Parameters.

Evaluations of the terms b, β', β and λ for each day of measurement are presented in Table 6.1. Statistical data for each defining relationship are tabulated in Appendix 3. Correlation coefficients and standard errors of the estimate for the R_n vs. Q_n relationship fall within the range of previously published values. The lowest determination of r was 0.976 (for soil), while the surface means all exceeded 0.99. In all cases, $\beta' > \beta$, the magnitude of the difference being variable, unpredictable and often large (Fig. 6.1).

In every case but one (soil on September 2), the net longwave coefficients derived from b in this investigation are included within the range of values previously reported for the three surfaces (Figs. 6.2 and 6.3). However, for soil and corn, the means of the two sets of evaluations differ considerably (Table 6.2), since present values all fall between the literature mean and zero, indicating a less pronounced dependence of L_n on R_n or Q_n. For grass, this phenomenon is less clearly marked and the β' and λ values of Table 6.1 resemble more closely the majority of previously published determinations (Table 6.2 and

TABLE 6.1

NET LONGWAVE COEFFICIENTS

Date	Grass				Bare Soil				Cornfield			
	b	β'	β	λ	b	β'	β	λ	b	β'	β	λ
Jul 6	1.024	-.023	-.026	.024	.963	.039	.031	-.037	.940	.064	.061	-.060
7	1.091	-.083	-.086	.091	.949	.054	.046	-.051	.924	.082	.078	-.076
8	1.014	-.014	-.016	.014	.911	.098	.086	-.089	.910	.099	.097	-.090
11	1.020	-.020	-.027	.020	.925	.081	.074	-.075	.903	.107	.098	-.097
13	1.007	-.007	-.011	.007	.942	.061	.049	-.058	.918	.089	.080	-.082
22	1.007	-.007	-.011	.007	.963	.039	.027	-.037	1.005	-.005	-.012	.005
Aug 7	1.039	-.037	-.041	.039	.943	.061	.054	-.057	.961	.041	.035	-.039
11	.994	.006	.003	-.006	.962	.040	.030	-.038	1.007	-.007	-.012	.007
12	.976	.025	.024	-.024	.885	.130	.121	-.115	.997	.024	.020	-.023
27	.909	.101	.099	-.091	.907	.102	.096	-.093	.933	.072	.071	-.068
28	.932	.073	.069	-.068	.929	.077	.071	-.071	.954	.048	.047	-.046

(continued overleaf)

TABLE 6.1 (continued)

Aug	29	.943	.060	.056	-.057	.946	.057	.050	-.054	.967	.034	.031	-.033
Sep	1	.920	.087	.084	-.080	.909	.100	.093	-.091	.939	.064	.062	-.061
	2	.985	.015	-.011	-.015	.985	.016	-.022	-.015	1.027	-.026	-.042	.027
	3	.942	.062	.053	-.058	.949	.053	.033	-.051	.993	.007	.004	-.007
	4	.897	.114	.092	-.103	.912	.096	.058	-.088	.930	.075	.058	-.070
	9	.917	.090	.073	-.083	.951	.051	.037	-.049	.921	.086	.059	-.079
	10	.919	.088	.077	-.081	.953	.050	.024	-.047	.977	.024	.014	-.023
Mean		.974	.029	.022	-.026	.938	.067	.053	-.062	.955	.049	.042	-.045
Standard Deviation		.053	.055	.053	.053	.025	.028	.032	.025	.036	.038	.039	.036
Coeff. of Variation		.054	1.863	2.367	-2.043	.026	.422	.608	-.399	.037	.787	.928	-.787

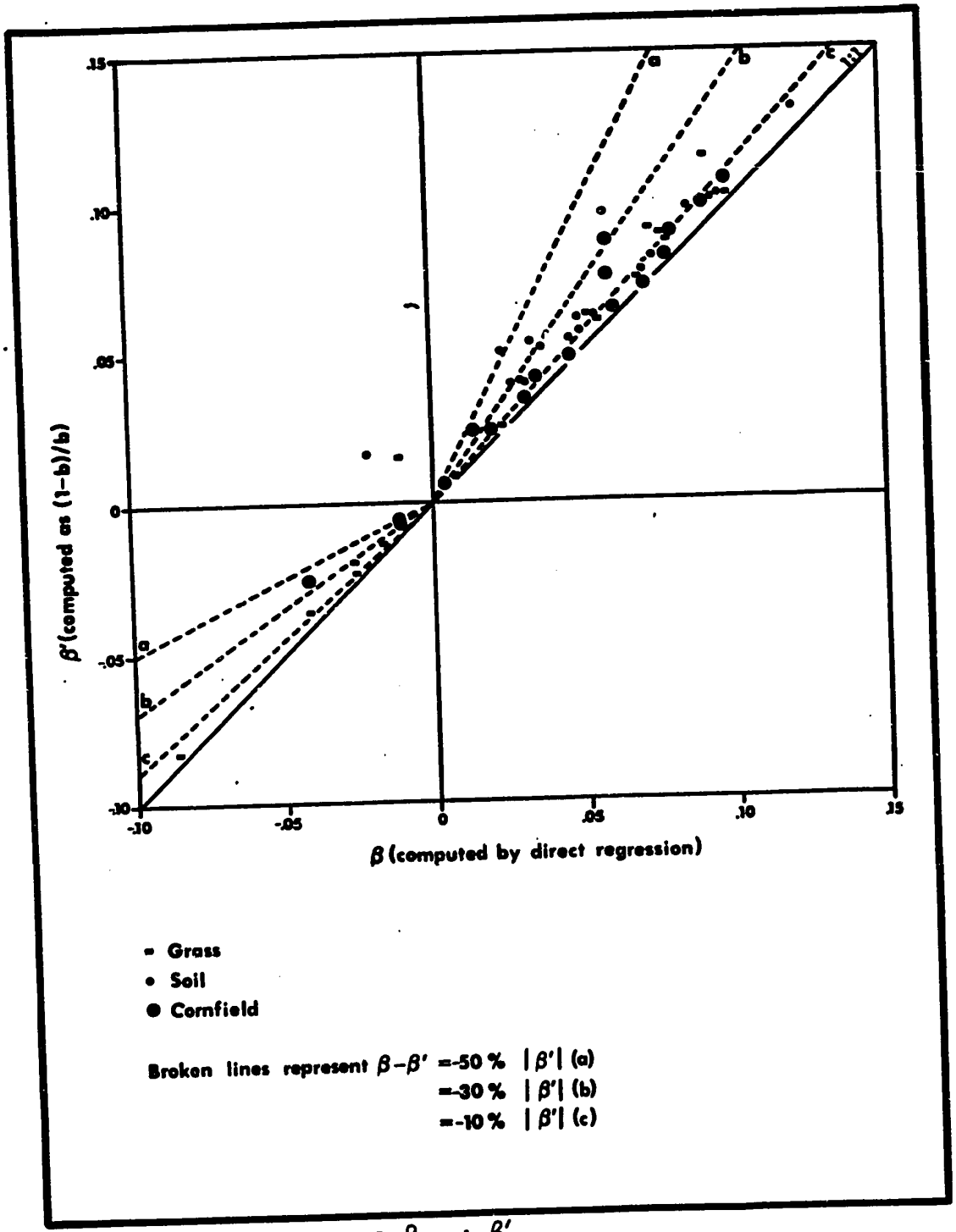

Figure 6.1: Comparison of β and β'.

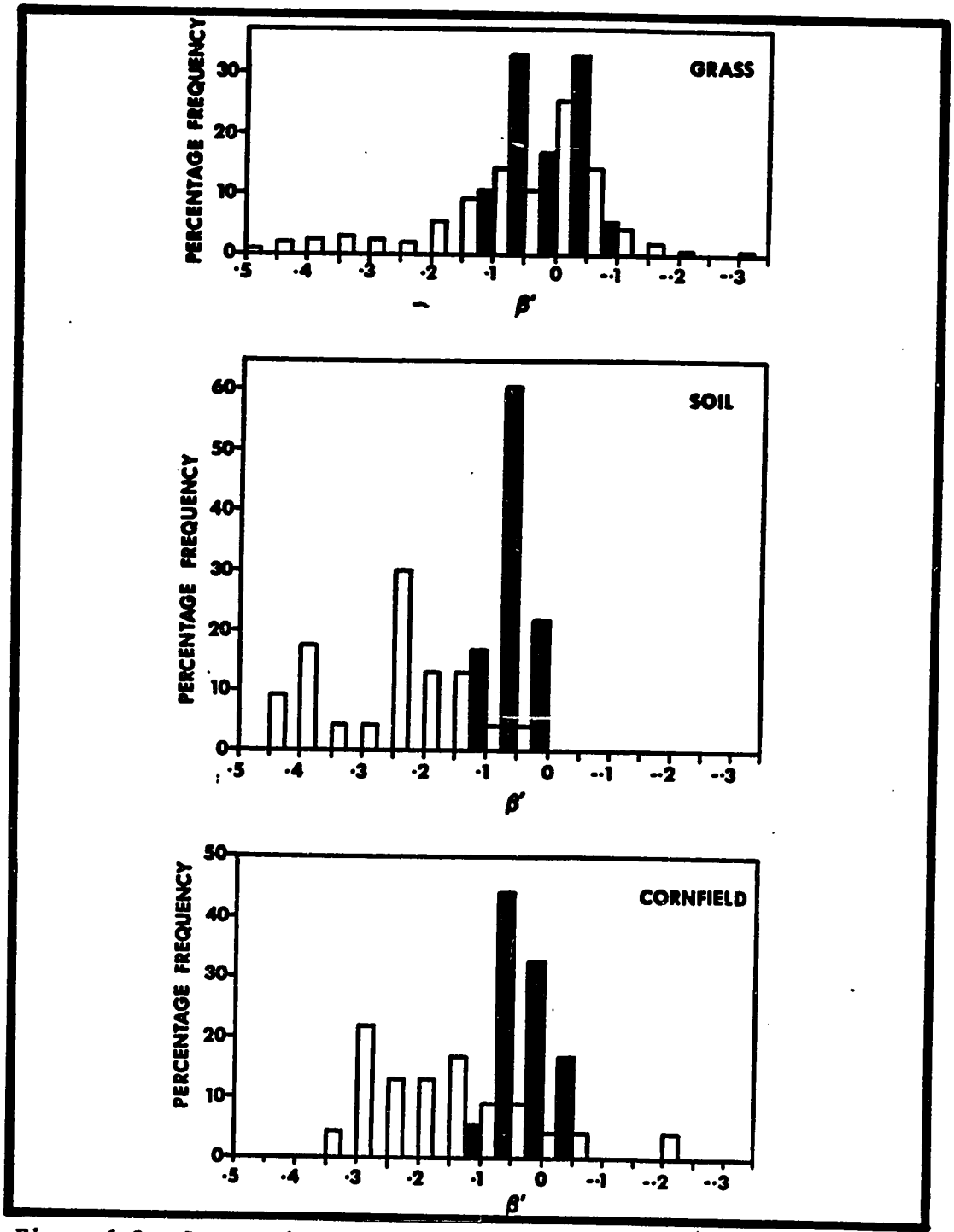

Figure 6.2: Comparative frequency distributions of β' values from the literature (open columns) and this investigation (shaded columns).

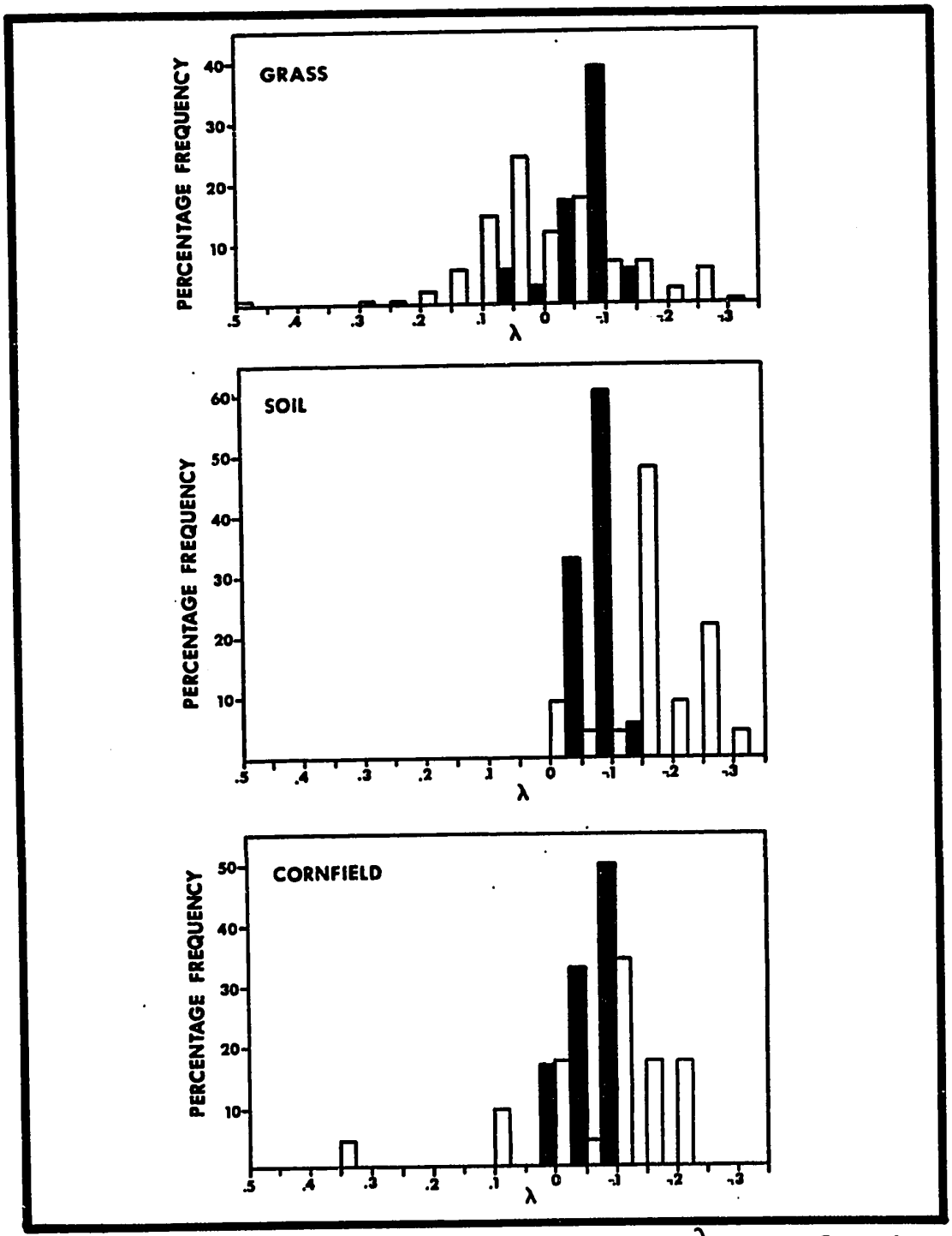

Figure 6.3: Comparative frequency distributions of λ values from the literature (open columns) and this investigation (shaded columns).

TABLE 6.2

MEAN VALUES OF β' AND λ

Surface	β'		λ	
	A	B	A	B
Grass	0.043	0.029	-0.025	-0.026
Soil	0.245	0.067	-0.191	-0.062
Cornfield	0.138	0.049	-0.099	-0.045

A - mean of previously reported values

B - mean from this investigation.

Figs. 6.2 and 6.3). In both the present and literature data, however, the relative ranking of the three surface means is the same, with soil showing the strongest and grass the weakest dependence of L_n on R_n or Q_n.

Positive associations between L_n and R_n or Q_n (i.e. $\beta < 0$, $\lambda > 0$) occur most frequently in the grass and least frequently in the soil data (Table 6.3). For all surfaces, the percentage frequency of such occurrences in this investigation is similar to that in all previously reported data.

Though the means of the net longwave parameters evaluated in this investigation do not differ by large amounts, this fact masks the very different seasonal behaviour of these terms between surfaces. Nevertheless, since it will be shown in the following sections that the variance in these parameters is not attributable solely to changes in the constitution and properties of the surfaces, but is equally a function of variations in the radiative behaviour of the atmosphere, a useful analysis of the seasonal regime is not appropriate at this point, but will be treated in subsequent consideration of the outgoing and incoming longwave parameters.

6.2: Seasonal Behaviour of the Outgoing Longwave Parameters.

The parameters $\beta_\uparrow$ and $\lambda_\uparrow$, for all surfaces, are listed in Table 6.4. Statistical data for the defining relationships are tabulated in Appendix 3.

TABLE 6.3

PERCENTAGE FREQUENCY OF NET LONGWAVE COEFFICIENTS INDICATING A POSITIVE RELATIONSHIP BETWEEN L_n AND R_n OR Q_n

Surface	Present data, β', λ	Present data, β	Literature
Grass	39	44	47
Soil	0	6	0
Cornfield	17	17	13

TABLE 6.4

OUTGOING LONGWAVE PARAMETERS

Date		Grass		Soil		Cornfield	
		$\beta_\uparrow$	$\lambda_\uparrow$	$\beta_\uparrow$	$\lambda_\uparrow$	$\beta_\uparrow$	$\lambda_\uparrow$
July	6	.006	.009	.066	.069	.093	.090
	7	.002	.006	.144	.142	.173	.164
	8	.058	.060	.170	.164	.174	.160
	11	.063	.067	.170	.164	.189	.176
	13	.076	.080	.144	.147	.168	.160
	22	.095	.099	.141	.147	.088	.094
August	7	.049	.053	.159	.155	.122	.120
	11	.129	.130	.166	.171	.102	.106
	12	.168	.165	.285	.265	.154	.152
	27	.240	.220	.249	.236	.194	.183
	28	.226	.214	.245	.234	.185	.178
	29	.236	.225	.241	.237	.187	.183
September	1	.215	.199	.225	.213	.175	.165
	2	.202	.207	.206	.221	.142	.150
	3	.253	.245	.243	.251	.174	.175
	4	.200	.190	.178	.183	.152	.148
	9	.205	.178	.169	.151	.185	.163
	10	.244	.231	.200	.213	.157	.158
Mean		.148	.143	.189	.187	.156	.151
Standard Dev.		.085	.078	.051	.049	.033	.029
Coeff. of Var.		.576	.547	.272	.260	.211	.189

The greatest seasonal stability in $\beta_\uparrow$ and $\lambda_\uparrow$ is exhibited by the cornfield, and the least by the grass plot. The large range in values for the latter surface is attributable to changes in the thermal properties of both the vegetation and the substrate which occurred between the early season period, when soil moisture content was high and the grass was freely transpiring, and the dry late season, when many plants were dead and the long-wave response of the grass closely resembled that of the soil. These two distinct regimes give rise to the bimodal frequency distribution for grass in Fig. 6.4. For the other two surfaces, the frequency distributions are unimodal but negatively skewed.

The soil data display a similar seasonal pattern to that for grass, attributable to soil moisture content (Fig. 3.2), but early season parameters are larger than grass values until August 27. By early September, however, they were slightly lower. The early season relationship between the two surfaces is expected from the known characteristics of the energy balances of bare soils and freely transpiring vegetation. The large magnitude of the change brought about by plant dessication and death, however, is rather unexpected. A more detailed analysis of the seasonal regime of the soil $L_\uparrow$ parameters is presented in the following section.

For the cornfield, no simple seasonal trend may be identified, although the following observations may be significant.

(i) In early July, when corn covered less than 15% of the

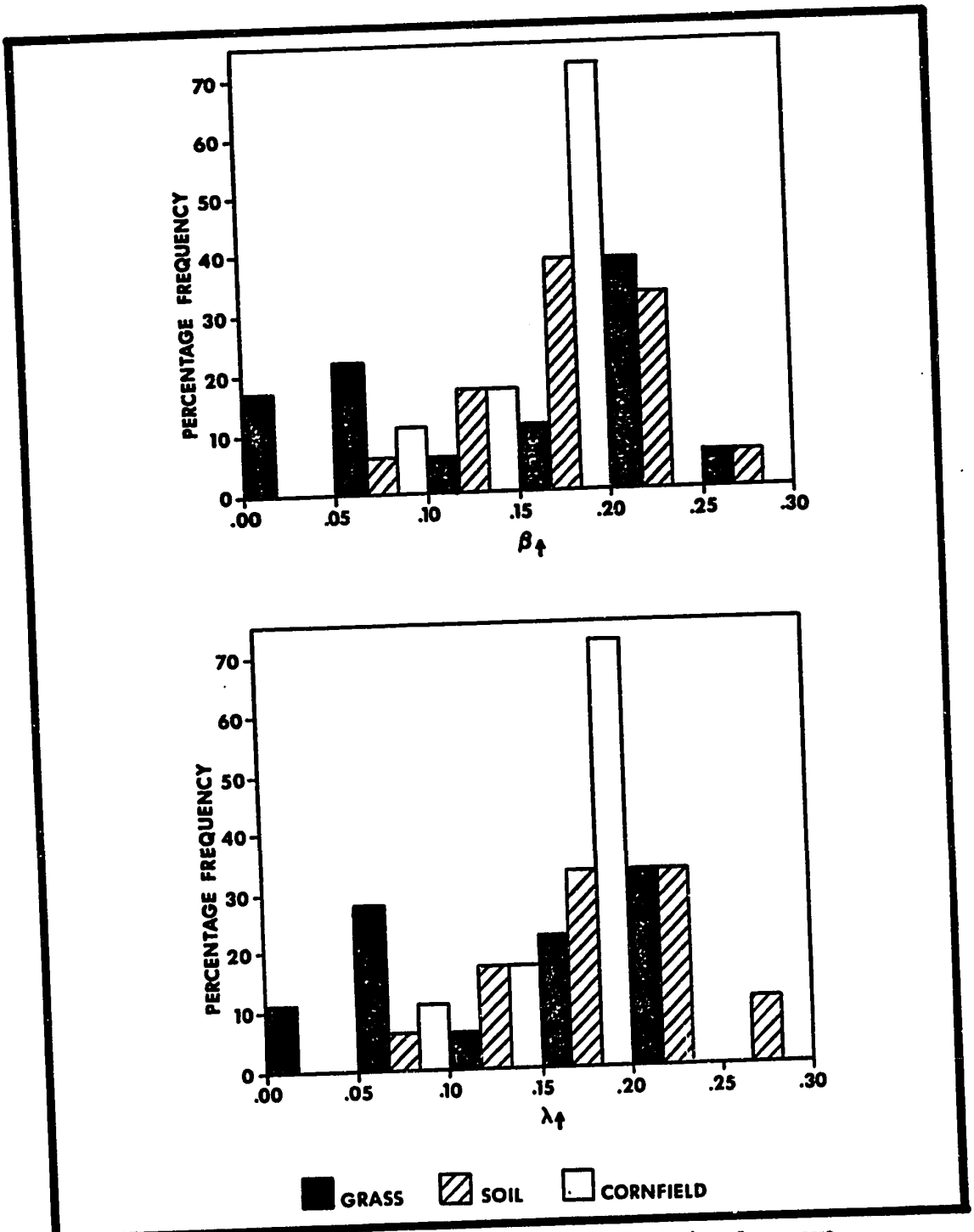

Figure 6.4: Frequency distributions of the outgoing longwave parameters for each surface.

ground, $\beta\uparrow$ and $\lambda\uparrow$ for this surface and the bare soil were similar.

(ii) Attainment of maximum ground cover corresponded to the minimum values of the $L\uparrow$ parameters (July 22).

At no time after canopy closure was complete did cornfield $L\uparrow$ parameters exceed those of the grass. This may be related to the greater rooting depth of the corn plants, which would provide a larger moisture reserve, and the rougher surface of the canopy, which might enhance atmospheric turbulence, both factors which would tend to reduce the surface temperature range of the plot. These factors, in addition to the observed inverse relationship between crop height and reflection coefficient, would explain the generally higher daily net radiation totals characteristic of taller vegetation (Decker, 1959).

No negative $L\uparrow$ parameters were found (i.e. surface temperature and R_n or Q_n were always positively related). However, on July 6 and 7, the grass coefficients were very small, indicating a near constant diurnal course of surface temperature. During the period of moderate grass temperature response (July and up until August 7), the $L\downarrow$ parameters exceeded the $L\uparrow$ ones and a positive relationship between L_n and R_n or Q_n resulted (i.e. $\beta < 0$, $\lambda > 0$). Such relationships also occurred on July 22 and August 11 for corn, during the period of maximum ground cover, when surface thermal response was moderate, and for all surfaces on September 2, when surface heating was marked but a large diurnal fluctuation

in atmospheric emission took place, associated with heavy convective cloud development.

An analysis of the sequence of values of $\beta_\uparrow$ and $\lambda_\uparrow$ above and below their medians indicates that, for grass and soil, the sequence may be regarded as significantly different from a random one at the 0.05 level, especially that of the grass plot, since all $L_\uparrow$ coefficients up to and including August 12 were below the median and all subsequent determinations were above. For the cornfield, however, the null hypothesis of a random distribution of parameters through time could not be rejected by this form of analysis. The magnitude of the thermal response of the cornfield is apparently determined by different variables at different times during the development of the crop canopy and this is regarded as contributory to the complex seasonal behaviour of the $L_\uparrow$ parameters.

6.3: Theoretical Estimation of Soil $L_\uparrow$ Parameters.

In section 6.4, the seasonal fluctuations in the $L_\uparrow$ parameters are related empirically to a number of readily available variables, to permit their a priori estimation. These variables are chosen as surrogates for the radiative and thermal properties which have been shown to determine the magnitude of $\beta_\uparrow$ and $\lambda_\uparrow$ for simple surfaces (section 2.6). For the soil plot, the assumptions necessitated in the analytical treatment are approximately valid, and a comparison may be made between the measured $L_\uparrow$ parameters and those predicted by the theoretical equation.

For convenience, this comparison is made only for $\beta\uparrow$. However, the stability of the relationship between R_n and Q_n ensures that the conclusions drawn from the analysis will apply equally to $\lambda\uparrow$.

The techniques employed in measuring the soil thermal properties are detailed in section 3.6. The dependence of C on the soil moisture volume fraction is illustrated in Fig. 6.5A. For a given soil type, thermal conductivity is also a function of x_w (de Vries, 1963); Fig. 6.5B presents this relationship for Fox sandy loam over the moisture range encountered. Fig. 6.5C illustrates the resulting generalised dependence of the soil thermal admittance on volumetric soil moisture. Soil moisture and, hence, $(Ck)^{\frac{1}{2}}$ showed a downward trend over the season, resulting in a tendency for an increase in the magnitude of $\beta\uparrow$.

Since the emissivity of water is in the vicinity of 0.97 (Davies et al, 1970) and that of quartz sand is near 0.90 (Falckenberg, 1928), ϵ for a natural mineral soil is affected significantly by surface moisture content. The data used in this analysis are those of Fuchs and Tanner (1968); Fig. 6.6A illustrates the relationship used. The tendency toward a decrease in $\beta\uparrow$ over the season, resulting from the seasonal trend in ϵ, is more than offset by the dependence of the coefficient on soil thermal property changes.

Daily mean surface temperature, evaluated from extrapolated soil temperature profiles, was available on four days only. The assumption was made that the mean daily (screen) air temperature

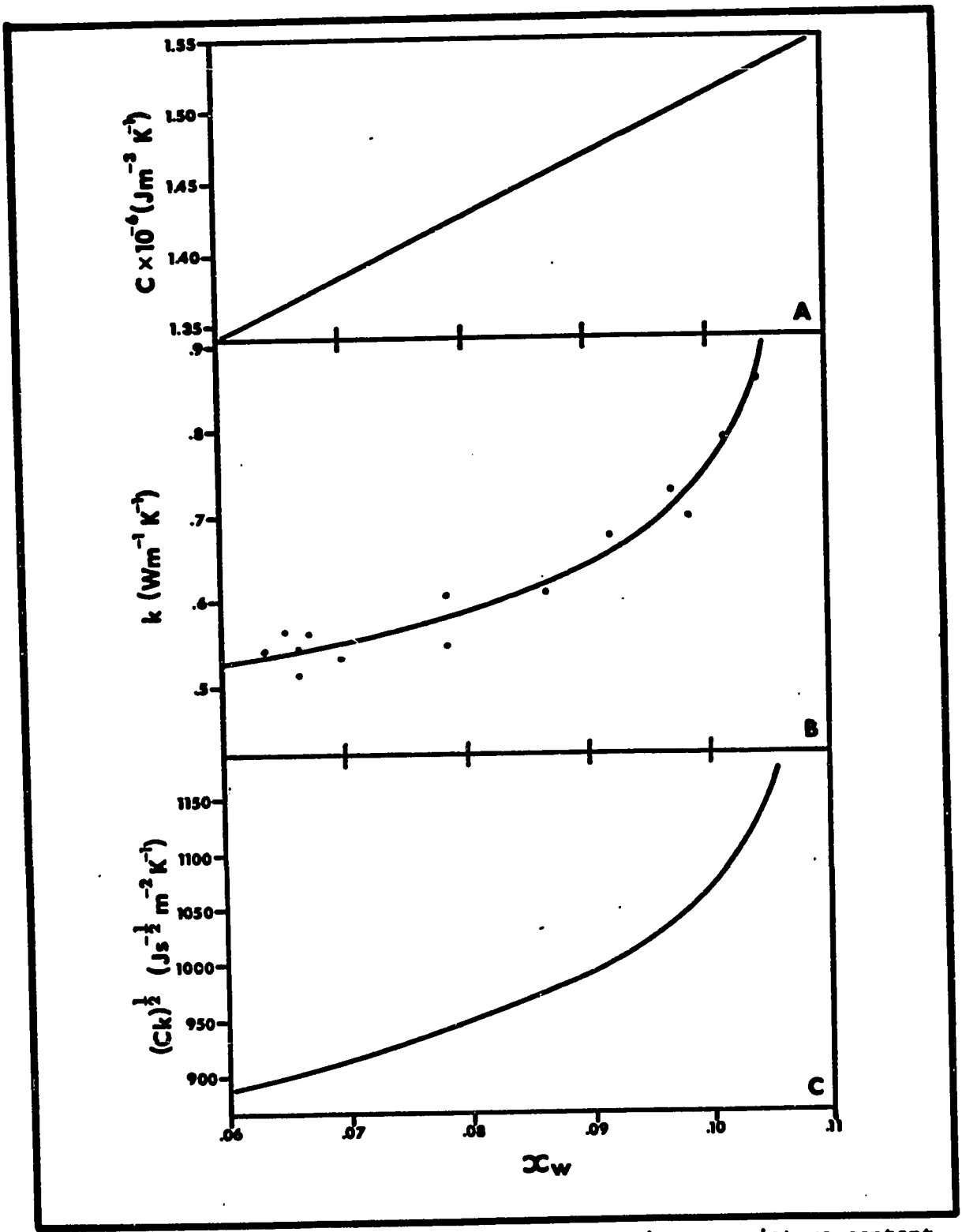

Figure 6.5: Dependence of soil thermal properties on moisture content.

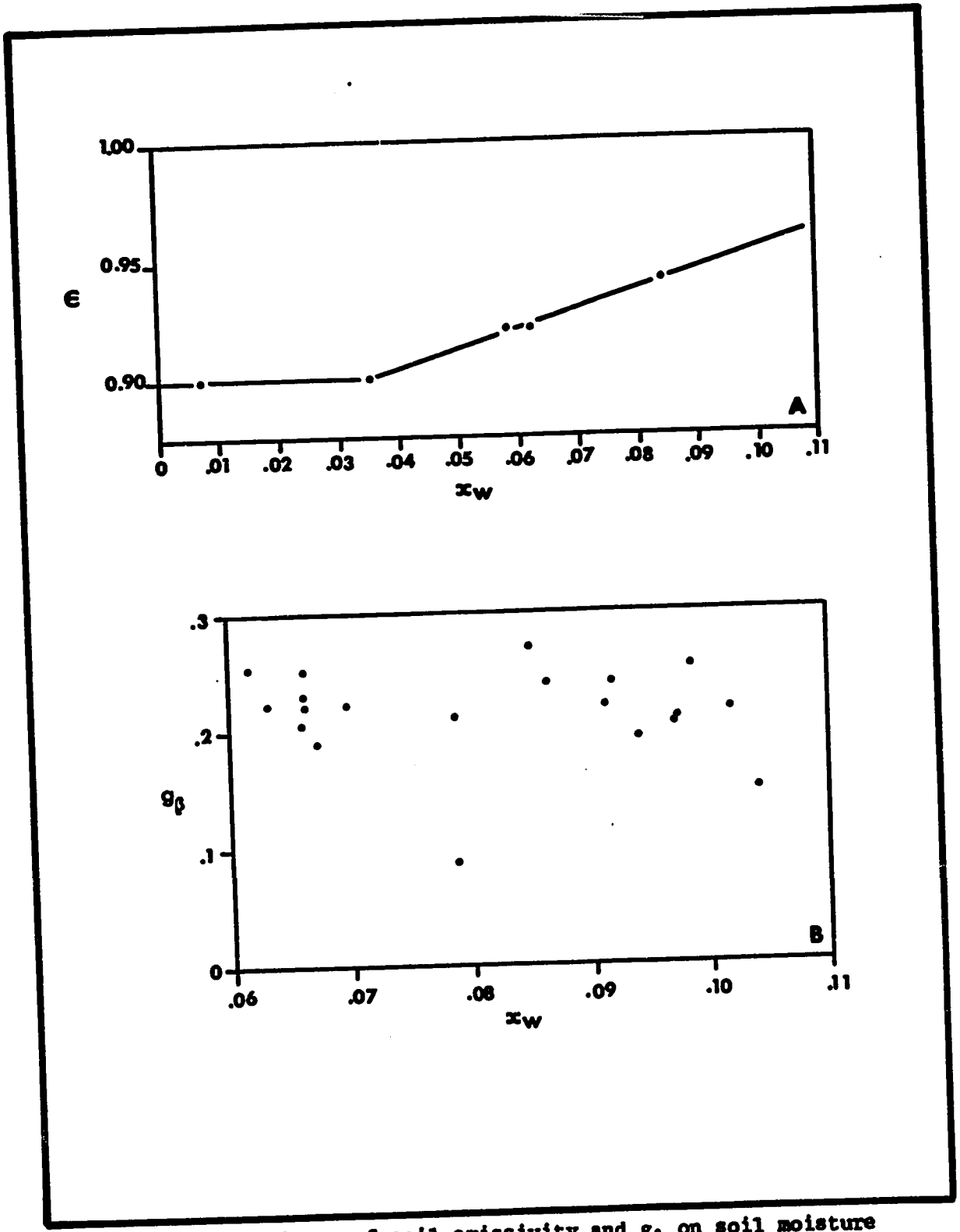

Figure 6.6: Dependence of soil emissivity and g_β on soil moisture content.

would approximate $\bar{T}_s$. For the data available, this approximation resulted in an underestimate of 2.8K on average, equivalent to a 3% underestimate of $(dL_r/dR_n)_d$. No simple trend was apparent in the seasonal pattern of mean air temperature.

The energy input term g_β was calculated by

$$g_\beta = \frac{\sum G_o}{\sum R_n},$$

where the summation extends over all available instantaneous G_o evaluations and simultaneous R_n measurements. Fig. 6.6B indicates that most of the values fall around $g_\beta \approx 0.22$, with no dependence on soil moisture content. The explanation for this stability may be that, as soil moisture decreases and evaporation is retarded, the increase in the proportion of R_n potentially available for the substrate heat flux is offset by an increase in the resistance of the soil to conductive heat transfer. No seasonal pattern is apparent in g_β.

Measured values of $\beta_\downarrow$ were used in the analysis. The significance of the second term on the right-hand side of (2.22) was slight, however, as $(1 - \epsilon)$ varied between 0.044 and 0.078. No clear seasonal trend in $(1 - \epsilon)\beta_\downarrow$ is apparent.

Fig. 6.7 shows the relationship between measured and estimated $\beta_\uparrow$. The standard error of the estimate is 0.048. In general, the equation shows a tendency to underestimate $\beta_\uparrow$

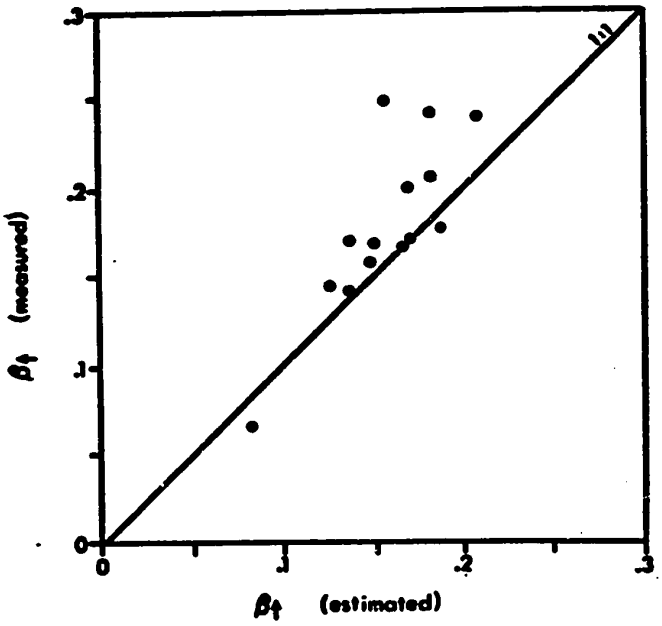

Figure 6.7: Comparison of measured and estimated β_f for soil.

(by 13% on average), the magnitude of the error increasing with increasing values of the parameter. For measured $\beta_\uparrow \leq 0.2$, the standard error is only 0.017. The deviation between the two methods may be due in part to the error in estimating $\overline{T}_s$, but is more likely to result from a systematic overestimate of thermal admittance at low soil moisture (i.e. high $\beta_\uparrow$). When the soil is moist, vertical gradients of water content are probably small and the determinations of C and k will approximate the surface values of these properties. However, soil drying will affect the surface layers initially, so that, as x_w decreases, the measured C and k values will be larger than those characteristic of the surface layer, $(Ck)^{\frac{1}{2}}$ will be overestimated and, hence, $\beta_\uparrow$ will be underestimated.

The seasonal pattern exhibited by soil $\beta_\uparrow$ is primarily a result of seasonal changes in thermal properties, with decreasing soil moisture, rather than a response to change in energy input or surface temperature. Unfortunately, there is no justification for transferring this conclusion to the vegetated surfaces. However, it should be noted that the very high values of grass $\beta_\uparrow$ in September may be a response to low thermal admittance, resulting from the "mulch" of dead and dried plant material at the surface. It is unlikely that the energy input would be independent of soil moisture in the case of living vegetation; hence, an inverse relationship between x_w and the proportion of R_n used in the "substrate" heat flux might be

expected.

6.4: Estimation of the Outgoing Longwave Parameters.

The variables used in correlation and regression analysis with the $L_\uparrow$ parameters, selected as surrogates for the factors discussed in section 2.6, are listed in Tables 6.5 (grass), 6.6 (soil) and 6.7 (cornfield). The only variable which gave significant correlations for all surfaces was soil moisture and, in all cases, the dependence implied is an inverse one, in accordance with theoretical expectation. Cornfield $\beta_\uparrow$ and $\lambda_\uparrow$ are less closely related to soil moisture variations than are the soil and grass parameters because the surface property changes exhibited by this plot were more complex, and variations in thermal response were controlled by other factors at different times during the season.

The only other significant bivariate correlations were those between $\beta_\uparrow$ and plant height (r only) and $\lambda_\uparrow$ and wind speed (r_p only) for grass. In both cases the inverse dependence satisfies theoretical expectation, if both variables are considered as surrogates for turbulent intensity. However, the proportion of $L_\uparrow$ coefficient variance "explained" by h and $\bar{u}$ is small relative to that accounted for by x_w.

For no surface would use of the seasonal mean provide an adequate estimate of either $L_\uparrow$ parameter; neither $\beta_\uparrow$ nor $\lambda_\uparrow$ can be considered as surface constants, therefore.

TABLE 6.5

CORRELATION AND STANDARD ERROR STATISTICS FOR GRASS $L_\uparrow$ PARAMETERS

Variable(s)	$\beta_\uparrow$			$\lambda_\uparrow$		
	r,R	s	r_p	r,R	s	r_p
Mean	-	.089	-	-	.082	-
$\bar{u}$	-0.391	.083	-0.481	-0.424	.075	-0.559*
$\bar{T}_a^3$	0.174	.089	0.112	0.201	.081	0.225
x_w	-0.954*	.027	-0.924*	-0.945*	.028	-0.921*
h	-0.680*	.066	-0.035	-0.669	.062	0.003
x_w and $\bar{u}$	0.968*	.025	-	0.966*	.023	-

Key: $\bar{u}$ mean daily wind speed ($m\ s^{-1}$)

$\bar{T}_a$ mean daily air temperature (K)

h crop height (m)

* R, r or r_p significant at 0.05 level.

TABLE 6.6

CORRELATION AND STANDARD ERROR STATISTICS FOR SOIL $L_\uparrow$ PARAMETERS

Variable(s)	$\beta_\uparrow$			$\lambda_\uparrow$		
	r, R	s	r_p	r, R	s	r_p
Mean	-	.049	-	-	.048	-
$\bar{u}$	-0.380	.046	-0.168	-0.432	.044	-0.299
$\bar{T}_a^3$	0.435	.045	0.521	0.419	.045	0.525
x_w	-0.787*	.031	-0.817*	-0.797*	.030	-0.831*
x_w and $\bar{T}_a^3$	0.869*	.027	-	0.877*	.026	-

Key: $\bar{u}$ mean daily wind speed (m s^{-1})

$\bar{T}_a$ mean daily air temperature (K)

h crop height (m)

* R, r or r_p significant at 0.05 level.

TABLE 6.7

CORRELATION AND STANDARD ERROR STATISTICS

FOR CORNFIELD $L_{\uparrow}$ PARAMETERS

Variable(s)	$\beta_{\uparrow}$			$\lambda_{\uparrow}$		
	r,R	s	r_p	r,R	s	r_p
Mean	-	.035	-	-	.030	-
$\bar{u}$	-0.092	.035	0.095	-0.176	.030	0.012
$\bar{T}_a^3$	0.180	.034	0.256	0.245	.029	0.347
x_w	-0.494*	.031	-0.415	-0.571*	.025	-0.444
h	0.141	.035	-0.045	0.224	.029	-0.009
F_c	-0.355	.033	-0.226	-0.288	.029	-0.263
F_d	0.353	.033	-0.253	-0.396	.028	-0.288
x_w and h	0.698*	.027	-	0.728*	.023	-

Key:

F_c crop ground cover fraction

F_d estimated fraction of canopy material dessicated

$\bar{u}$ mean daily wind speed (m s^{-1})

$\bar{T}_a$ mean daily air temperature (K)

h crop height (m)

* R, r or r_p significant at 0.05 level.

For grass, the significant simple and multiple regression relationships are:

$$\beta_{\uparrow} = 0.600 - 5.711\ x_w \ , \tag{6.1}$$

$$\lambda_{\uparrow} = 0.556 - 5.209\ x_w \ , \tag{6.2}$$

$$\beta_{\uparrow} = 0.634 - 5.494\ x_w - 0.014\ \bar{u} \ , \tag{6.3}$$

$$\lambda_{\uparrow} = 0.596 - 4.955\ x_w - 0.017\ \bar{u} \ . \tag{6.4}$$

In (6.3) and (6.4), the signs of the regression coefficients are as expected, since both increased soil moisture and higher wind speed should result in reduced surface heating.

For the soil plot, the equivalent equations are:

$$\beta_{\uparrow} = 0.381 - 2.508\ x_w \ , \tag{6.5}$$

$$\lambda_{\uparrow} = 0.381 - 2.515\ x_w \ , \tag{6.6}$$

$$\beta_{\uparrow} = -0.073 - 2.433\ x_w + 0.018\ (\bar{T}_a{}^3 \times 10^{-6}) \ ,$$

$$\lambda_{\uparrow} = -0.066 - 2.442\ x_w + 0.017\ (\bar{T}_a{}^3 \times 10^{-6}) \ .$$

The regression coefficients again agree with the expected effects

of the independent variables.

Finally, for the cornfield:

$$\beta_{\uparrow} = 0.247 - 1.149\ x_w \ , \qquad (6.7)$$

$$\lambda_{\uparrow} = 0.243 - 1.155\ x_w \ , \qquad (6.8)$$

$$\beta_{\uparrow} = 0.407 - 2.536\ x_w - 0.037\ h \ ,$$

$$\lambda_{\uparrow} = 0.369 - 2.247\ x_w - 0.029\ h \ .$$

Increasing soil moisture and crop height will thus lead to a reduction in the intensity of surface heating.

6.5: Seasonal Behaviour of the Incoming Longwave Parameters.

The parameters $\beta_{\downarrow}$ and $\lambda_{\downarrow}$, for all surfaces, are listed in Table 6.8. Statistical data for the defining relationships are tabulated in Appendix 3. It is apparent that these terms are not insignificant components of the net longwave coefficients, which cannot be considered exclusively as surface parameters. The large range of values explains the difficulty experienced in previous work in establishing any useful relationships between β or λ and surface properties.

On August 28, a day effectively free of cloud, mean $\beta_{\downarrow}$ = 0.156 and mean $\lambda_{\downarrow}$ = 0.147, suggesting that the postulate of

TABLE 6.8

INCOMING LONGWAVE PARAMETERS

Date		Grass		Soil		Cornfield	
		$\beta_{\downarrow}$	$\lambda_{\downarrow}$	$\beta_{\downarrow}$	$\lambda_{\downarrow}$	$\beta_{\downarrow}$	$\lambda_{\downarrow}$
July	6	.032	.033	.035	.032	.032	.030
	7	.088	.097	.098	.091	.095	.088
	8	.074	.074	.084	.074	.078	.070
	11	.090	.087	.096	.089	.090	.079
	13	.087	.088	.095	.089	.088	.078
	22	.107	.107	.114	.110	.100	.099
August	7	.090	.091	.106	.098	.087	.081
	11	.126	.124	.137	.132	.114	.113
	12	.145	.141	.163	.149	.134	.129
	27	.141	.129	.153	.143	.124	.115
	28	.156	.146	.174	.163	.138	.132
	29	.179	.169	.191	.183	.156	.150
September	1	.131	.119	.132	.123	.113	.104
	2	.213	.192	.229	.206	.184	.176
	3	.200	.187	.211	.200	.171	.168
	4	.109	.087	.119	.095	.093	.079
	9	.132	.096	.131	.103	.127	.084
	10	.168	.150	.176	.166	.142	.134
Mean		.126	.118	.136	.125	.115	.106
Standard Dev.		.045	.040	.048	.045	.036	.036
Coeff. of Var.		.359	.342	.350	.363	.311	.341

diurnal constancy of $L_{\downarrow}$ on cloudless days requires revision. If these values are typical of clear days, the low values of β and λ encountered in the literature are readily explicable. Mean grass β and λ reported in past investigations for clear sky conditions are 0.055 and -0.041 respectively. Using $\beta_{\downarrow} = 0.156$ and $\lambda_{\downarrow} = 0.146$ (August 28, for grass), $\beta_{\uparrow} = 0.211$ and $\lambda_{\uparrow} = 0.187$, values which fall within the range of determinations encountered in this study (Fig. 6.4) and which imply a thermal regime more in keeping with the known temperature response of this surface.

Histograms of the $L_{\downarrow}$ parameters are shown in Fig. 6.8. Though the magnitudes of $\beta_{\downarrow}$ and $\lambda_{\downarrow}$ vary slightly between surfaces, in general terms the frequency distributions are of similar shape. Since $L_{\downarrow}$ is constant between surfaces, the $L_{\downarrow}$ parameters are inversely proportional to the diurnal amplitude of Q_n and R_n. As $\alpha(\text{soil}) > \alpha(\text{grass}) > \alpha(\text{cornfield})$, $\lambda_{\downarrow}(\text{soil}) > \lambda_{\downarrow}(\text{grass}) > \lambda_{\downarrow}(\text{cornfield})$. On average, longwave loss from the soil is greatest and that from the cornfield is least, so an identical ranking by surface applies to the $\beta_{\downarrow}$ coefficient. However, the coefficients of variation for $\beta_{\downarrow}$ and $\lambda_{\downarrow}$ for all three surfaces are similar (Table 6.8), suggesting that the fluctuations in these parameters observed during the measurement season were largely determined by atmospheric longwave factors, rather than surface ones.

6.6: Estimation of the Incoming Longwave Parameters.

Mean air temperature ($\overline{T}_a$) and vapour pressure ($\overline{e}_a$) and

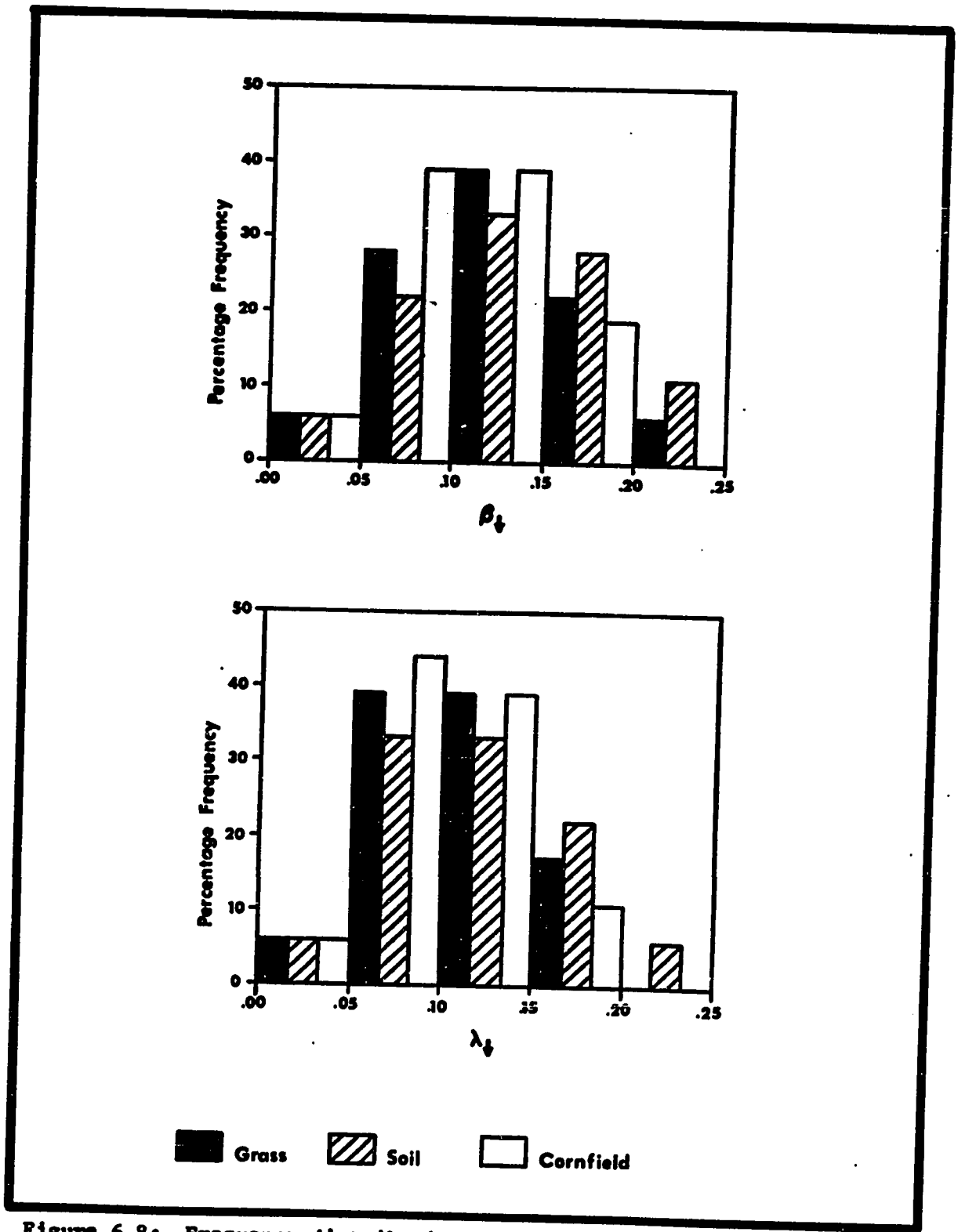

Figure 6.8: Frequency distributions of the incoming longwave parameters for each surface.

cloud type and amount have been used in previous studies (e.g. Ångström, 1916; Brunt, 1932; Bolz, 1949; Swinbank, 1963; Idso and Jackson, 1969; Kondrat'yev, 1969) as readily available surrogates for the emissive properties of the atmosphere. This practice has been justified by Lönnquist (1954) and Sellers (1965), who show that the accuracy of numerous charts and empirical equations is apparently unrelated to the amount of pure theory inherent in the method. Correlations were sought between these variables and the observed values of $\beta_{\downarrow}$ and $\lambda_{\downarrow}$. In addition, since these coefficients are a measure of diurnal change in $L_{\downarrow}$, the amplitude of screen temperature (ΔT_a) was also used in correlation and regression analysis. A weighted cloud cover c_w was computed from

$$c_w = c_l + 0.84c_m + 0.27c_h \; . \qquad (6.9)$$

Fractional cloud cover in the lowest atmospheric layer (c_l), the middle layer (c_m) and the upper layer (c_h) were derived from the hourly cloud data collected at the Simcoe meteorological station. The coefficients in (6.9) are proportional to those employed in the empirical equation of Bolz (1949) and purport to reflect the relative radiative efficiency of cloud in each layer. For this analysis, the daily mean value $\bar{c}_w$ was calculated.

Table 6.9 lists standard errors of the estimate for linear regression relationships with $\bar{T}_a$, $\bar{e}_a$, ΔT_a and $\bar{c}_w$. In no case could a simple or multiple correlation coefficient significant

TABLE 6.9

STANDARD ERRORS OF THE ESTIMATE ASSOCIATED WITH VARIOUS PREDICTIVE FUNCTIONS FOR β_ψ AND λ_ψ

Function	Grass		Soil		Cornfield	
	β_ψ	λ_ψ	β_ψ	λ_ψ	β_ψ	λ_ψ
L_ψ parameter = seasonal mean	0.047	0.041	0.049	0.047	0.037	0.037
L_ψ parameter = $f(\overline{e}_a)$	0.048	0.042	0.050	0.047	0.038	0.038
L_ψ parameter = $f(\overline{T}_a)$	0.047	0.041	0.049	0.046	0.037	0.037
L_ψ parameter = $f(\Delta T_a)$	0.047	0.042	0.050	0.047	0.037	0.038
L_ψ parameter = $f(\overline{c}_w)$	0.048	0.043	0.050	0.048	0.038	0.038

at the 0.05 level be found. Moreover, use of these regression equations failed to provide significantly better estimates of the $L_{\downarrow}$ parameters than those provided by the seasonal mean.

Accordingly, an attempt was made to search for empirical regularities in the $L_{\downarrow}$ coefficients, and in the residuals from regression, in terms of qualitative descriptions of the days upon which the data were collected. No correlation was found with predominant cloud types or with synoptic situation. An attempt was made to relate the coefficients and regression residuals to daily patterns of weighted cloud cover, which could be hypothesised to give rise to contrasting regimes of atmospheric longwave emission. Though the resulting means were intuitively reasonable, it could not be demonstrated that they were significantly different from each other at the 0.05 level.

On statistical grounds alone, $\beta_{\downarrow}$ and $\lambda_{\downarrow}$ can only be treated as random variables, to be represented in the net radiation estimation equations by their mean values.

Clearly, considerable difficulty attaches to the problem of making independent estimates of these terms and, by implication, of β and λ too. The errors associated with the use of the mean values of $\beta_{\downarrow}$ and $\lambda_{\downarrow}$ are far larger, both on an absolute basis and as a percentage of the mean of the predictand, than those associated with estimation of α, $\beta_{\uparrow}$ and $\lambda_{\uparrow}$.

6.7: Seasonal Behaviour of the L_o Parameter.

The parameter L_o, computed as the intercept of the regression

equation of R_n on $Q_\downarrow$, represents net radiation at zero insolation. Values of this term, for all surfaces, are listed in Table 6.10. In general, the L_o values found in this investigation are somewhat larger (less negative) than those previously evaluated (see Table 6.11). However, the measurement periods used in the above studies were either entirely or mainly clear. The more cloudy atmospheric conditions encountered in this investigation would tend to reduce longwave loss by increasing $L_\downarrow$ and, possibly, reducing surface heating.

A good correspondence was found between L_o and the mean of the actual values of L_n at sunrise and sunset. The correlation coefficients and slopes of the regression relations between L_o and L_n at sunrise, L_n at sunset and the mean of these two are presented in Table 6.12. Only for the mean is both the correlation high and the slope not significantly different from unity. Fig. 6.9 shows the relationship between L_o and mean L_n ($\overline{L}_n$).

Monteith and Szeicz (1961) found that the value of L_o, derived statistically, overestimated the actual longwave loss at sunset and sunrise. Fig. 6.9 indicates that the opposite is the case in this study, but that the error involved is small, being approximately 5 W m^{-2} at all values of L_o.

No clear seasonal trend is apparent in the data. For all surfaces, an analysis of the sequence of values above and below the median indicates that the sequence cannot be regarded as significantly different from a random one, at the 0.05 level.

TABLE 6.10

THE PARAMETER L_o ($W\ m^{-2}$)

Date		Grass L_o	Soil L_o	Cornfield L_o
July	6	-57.2	-67.7	-60.0
	7	-78.9	-73.3	-64.2
	8	-55.1	-57.2	-57.9
	11	-42.6	-44.7	-51.0
	13	-51.7	-69.8	-62.8
	22	-45.4	-53.7	-52.3
August	7	-35.6	-30.0	-25.8
	11	-51.0	-64.2	-62.1
	12	-56.5	-55.1	-65.6
	27	-48.9	-55.1	-53.0
	28	-50.3	-51.0	-58.6
	29	-39.8	-43.3	-46.8
September	1	-30.7	-34.9	-38.4
	2	-33.5	-39.1	-41.9
	3	-51.0	-57.9	-62.8
	4	-19.5	-25.1	-23.7
	9	-27.2	-39.1	-37.7
	10	-54.4	-71.2	-69.1
Mean		-46.1	-51.7	-51.7
Standard Dev.		14.0	14.7	13.3
Coeff. of Var.		-0.30	-0.28	-0.26

TABLE 6.11

EXAMPLES OF L_o VALUES FROM PREVIOUS INVESTIGATIONS

Source	Surface	Mean L_o ($W\ m^{-2}$)
Ekern (1965)	Various	-115.9
Fritschen (1967)	Various	-89.3
Gay (1971)	Various	-111.7
Idso et al (1969)	Various	-77.5
Impens and Lemeur (1969)	Various	-46.2
Kalma and Stanhill (1969)	Orange Plantation	-79.6
Kyle (1971)	Corn	-39.8
Lemon (1963)	Corn	-130.5
Monteith and Szeicz (1961)	Various	-64.9
Stanhill et al (1968)	Corn	-74.0
Stanhill and Fuchs (1968)	Cotton	-106.8
Stanhill et al (1966)	Various	-115.9
MEAN		-87.7

TABLE 6.12

RELATIONSHIPS BETWEEN L_o AND ACTUAL NET LONGWAVE FLUXES

Surface	Sunrise L_n		Sunset L_n		Mean L_n	
	r	slope	r	slope	r	slope
Grass	0.787*	0.59	0.399	0.36	0.954*	1.06**
Soil	0.758*	0.61	0.678*	0.71**	0.897*	0.90**
Cornfield	0.681*	0.52	0.597*	0.60**	0.932*	1.01**

* r significant at 0.05 level

** slope not significantly different from 1.0 at 0.05 level.

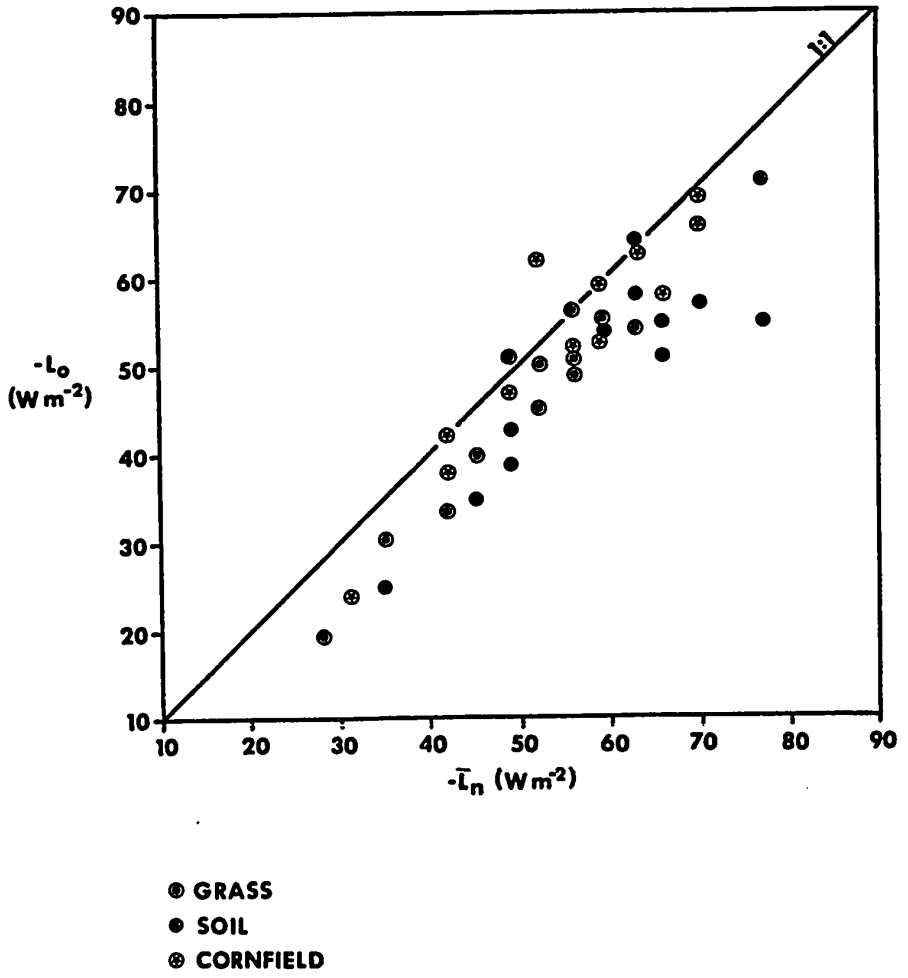

Figure 6.9: Relationship between L_o and mean L_n at sunrise and sunset.

Between surfaces, the coefficients are highly correlated (grass-soil, 0.888; soil-corn, 0.929; corn-grass, 0.855), suggesting that the origins of the fluctuations in L_o must be sought in atmospheric variations, or influences which are characteristic of all three surfaces. The similarity of the means and standard deviations suggests the attractive generalisation that L_o is independent of surface and largely determined by atmospheric properties. The rationalisation for this assumption may be that the same processes and surface properties which might be expected to result in strong surface heating during the day would tend to cause strong surface cooling during the nighttime hours. The effect on mean $L_\uparrow$ (and, hence, mean L_n) at sunrise and sunset might thus be largely independent of surface type.

6.8: Estimation of L_o.

An attempt was made to estimate L_o by the method of Monteith and Szeicz (1962), using the equation of Idso and Jackson (1969) to calculate atmospheric emission. The correspondence obtained was poor (Table 6.13, estimate 1). Use of the Galperin (1949) formula to correct the computed net longwave fluxes for cloud type and amount improved the performance of the technique somewhat (Table 6.13, estimate 2), but still gave errors in excess of those resulting from use of the surface mean.

Since procedures intended to make use of variables characteristic of the sunset and sunrise hours failed to provide adequate estimates of L_o, an attempt was made to relate the

TABLE 6.13

STATISTICAL DATA FOR L_o ESTIMATION PROCEDURE OF MONTEITH AND SZEICZ (1962)

Surface	Estimate 1		Estimate 2	
	r	s ($W\ m^{-2}$)	r	s ($W\ m^{-2}$)
Grass	0.426	41.9	0.490*	22.3
Soil	0.594*	36.3	0.552*	18.1
Cornfield	0.492*	36.3	0.644*	16.8

* r significant at 0.05 level.

Estimate 1: equation of Idso and Jackson (1969) used to calculate $L_\downarrow$, using screen temperatures for hours nearest sunrise and sunset. L_n computed for each and meaned.

Estimate 2: as for estimate 1, but L_n values corrected for cloud by equation of Galperin (1949) before being meaned.

parameter to daily mean variables. Screen temperature and daily values of the cloud parameter c_w were used in this analysis. To test the hypothesis of a surface-independent parameter, correlation and regression analyses were also performed using an aggregated data set from all three surfaces. Table 6.14 lists r values for the surface and aggregate analysis, along with two standard error of the estimate terms, s_1 and s_2. The former refers to the error inherent in the use of the relationship derived for the surface alone, while s_2 results from use of the "mean" equation.

Only $\bar{c}_w$ yielded significant correlations for all surfaces. The regression equations are:

(grass)

$$L_o = -63.5 + 46.8\ \bar{c}_w\ , \qquad W\ m^{-2} \qquad (6.10)$$

(soil)

$$L_o = -67.7 + 42.6\ \bar{c}_w\ , \qquad W\ m^{-2} \qquad (6.11)$$

(cornfield)

$$L_o = -69.1 + 46.1\ \bar{c}_w\ . \qquad W\ m^{-2} \qquad (6.12)$$

In each case, the smallest L_o values are encountered with clear skies and the term increases as cloud cover increases and/or cloud height decreases. For a complete cloud cover of high, medium and low clouds, characteristic L_o values are -54, -28 and -21 W m^{-2} respectively. The intercepts and regression coefficients of (6.10) - (6.12) are not significantly different. Use of aggregated data

TABLE 6.14

STATISTICAL DATA FOR L_o ESTIMATION FROM DAILY MEAN VARIABLES

Independent Variable	r Grass	r Soil	r Corn	r Aggregated	Grass s_1	Grass s_2	Soil s_1	Soil s_2	Cornfield s_1	Cornfield s_2
Mean L_o	-	-	-	-	14.0	14.0	14.7	14.0	13.3	13.3
$\overline{T}_a$	0.365	0.489*	0.362	0.399*	13.3	13.3	13.3	12.6	13.3	12.6
$\overline{c}_w$	0.702*	0.606*	0.702*	0.655*	9.8	10.5	11.9	11.2	9.8	9.8
$\overline{c}_w + \overline{T}_a$	0.763*	0.746*	0.762*	0.738*	9.1	9.8	10.5	9.8	9.1	9.1

s data in W m^{-2}

* r significant at 0.05 level.

gave

$$L_o = -66.3 + 45.4\ \bar{c}_w \ . \qquad W\ m^{-2} \qquad (6.13)$$

A comparison of s_1 and s_2 in the $\bar{c}_w$ column of Table 6.14 reveals that use of this equation will not lead to a marked reduction in the accuracy of the L_o estimate. Accordingly, it is recommended that (6.13) be used, and L_o be regarded primarily as a surface-independent parameter, responding most closely to the effects of fluctuations in cloud type and amount on net longwave loss.

6.9: Significance of Results.

The values of the net longwave coefficients were similar to those found in many previous investigations and were considerably smaller than those hypothesised as typical by Monteith and Szeicz, several being negative. Comparison of the magnitudes of the incoming and outgoing longwave parameters provides a convenient, quantitative method of estimating the degree to which β and λ are functions of surface properties; on average, $\beta_\downarrow$ and $\lambda_\downarrow$ are between 70 and 85% of $\beta_\uparrow$ and $\lambda_\uparrow$. Hence, seasonal fluctuations in the net longwave coefficients are strongly determined by atmospheric influences. This conclusion is valid for clear as well as cloudy periods and explains the failure of previous studies to establish useful predictive relationships between surface type and surface properties and β or λ, as

well as the large proportion of small and negative L_n coefficients. The unmodified forms of the Monteith and Szeicz and Gay equations cannot be regarded as useful models for net radiation estimation.

The parameters $\beta\uparrow$ and $\lambda\uparrow$ may be regarded as indices of surface dessication. For soil and grass, which exhibited relatively simple seasonal changes in surface properties, they were highly correlated with, and predictable from, soil moisture, a surrogate for several theoretically relevant variables. For the unvegetated plot, it was demonstrated that the seasonal regime of $\beta\uparrow$ and $\lambda\uparrow$ was brought about primarily by the effect of soil moisture content on substrate thermal properties. For the cornfield, which exhibited complex changes in surface configuration during the measurement period, the relationship between the outgoing longwave parameters and soil moisture was somewhat weaker.

The incoming longwave parameters were variable in magnitude and were unrelated to any simple atmospheric variables. The usefulness of (2.14) and (2.15) as net radiation estimators must be impaired by the unpredictable behaviour of these terms.

Seasonal patterns of L_o were similar for all surfaces and little predictive advantage results from preserving this term's surface dependence. Cloud height and amount were shown to determine L_o most strongly, through their influence on daily average atmospheric longwave emission.

In terms of the a priori predictability of the input parameters, no superior characteristics of either the Monteith

and Szeicz or the Gay forms of the basic model are apparent.

CHAPTER 7

THE ESTIMATION OF NET RADIATION

7.1: Model Sensitivity Analysis.

Mean values of the long- and shortwave parameters discussed in Chapters 5 and 6 are summarised in the first column of Table 7.1, in addition to mean day length and insolation. Substitution of these values in (2.14) and (2.15) yields the following regression-type equations. In each case, the equation derived from the Monteith and Szeicz model precedes that from the Gay model:

(grass)

$$[R_n] = 0.705[Q_\downarrow] - (228.73 \times 10^4), \quad J\ m^{-2} \qquad (7.1)$$

$$[R_n] = 0.702[Q_\downarrow] - (228.73 \times 10^4), \quad J\ m^{-2} \qquad (7.2)$$

(bare soil)

$$[R_n] = 0.654[Q_\downarrow] - (256.45 \times 10^4), \quad J\ m^{-2} \qquad (7.3)$$

$$[R_n] = 0.646[Q_\downarrow] - (256.45 \times 10^4), \quad J\ m^{-2} \qquad (7.4)$$

(cornfield)

$$[R_n] = 0.767[Q_\downarrow] - (256.45 \times 10^4), \quad J\ m^{-2} \qquad (7.5)$$

$$[R_n] = 0.762[Q_\downarrow] - (256.45 \times 10^4), \quad J\ m^{-2} \qquad (7.6)$$

TABLE 7.1

SUMMARY OF MODEL PARAMETERS AND ERROR DATA USED IN SENSITIVITY ANALYSES

Term	Mean	20% Error	"Best estimate" error	"Best estimate error as percentage of mean
Surface independent				
$[Q_{\downarrow}]$ J m^{-2} x 10^{-4}	1930.23	386.05	57.91	3.0
P s x 10^{-2}	497	-	-	-
Grass				
α	0.280	0.056	0.009	3.2
L_o W m^{-2}	-46.1	9.1	9.8	21.2
$\beta_{\uparrow}$	0.148	0.030	0.025	16.9
$\beta_{\downarrow}$	0.126	0.025	0.037	29.4
$\lambda_{\uparrow}$	0.143	0.029	0.023	16.1
$\lambda_{\downarrow}$	0.118	0.024	0.034	28.8
Bare Soil				
α	0.311	0.062	0.013	4.2
L_o W m^{-2}	-51.7	10.5	11.9	23.0
$\beta_{\uparrow}$	0.189	0.038	0.027	14.3
$\beta_{\downarrow}$	0.136	0.027	0.039	28.7
$\lambda_{\uparrow}$	0.187	0.037	0.026	13.9
$\lambda_{\downarrow}$	0.125	0.025	0.038	30.4

TABLE 7.1 (continued)

Cornfield					
α		0.202	0.040	0.014	6.9
L_o	W m^{-2}	-51.7	10.5	9.8	18.9
$\beta_\uparrow$		0.156	0.031	0.027	17.3
$\beta_\downarrow$		0.115	0.023	0.029	25.2
$\lambda_\uparrow$		0.151	0.030	0.023	15.2
$\lambda_\downarrow$		0.106	0.021	0.031	29.2

The slight differences between the regression coefficients of the equations for each surface are due to the previously discussed inequality in the β parameters computed by different methods.

The mean relationships were used to assess the significance of error in the various terms on the right-hand side of (2.14) and (2.15). Two analyses were performed. Firstly, the sensitivity of the $[R_n]$ estimate to a 20% error in each parameter was computed. These error terms are tabulated in the second column of Table 7.1. Secondly, the analysis was repeated with a variable error for each term, representing the "best estimate" available. For insolation, this was taken as 3%; for the long- and shortwave parameters, the standard error of the estimate or standard deviation of the mean, where appropriate, was used. These values are presented in the third column of Table 7.1, and as percentages of the mean in column four. In both analyses, no error was assumed in P.

The results of the first analysis are presented in Table 7.2. Both equations are clearly highly sensitive to error in the measurement of the incoming solar radiation total and, to a lesser extent, to poor estimation of the reflection coefficient. Of the longwave parameters, L_o is the most significant, errors in the other terms leading to relatively small inaccuracies in net radiation estimation. In summary, the sensitivity of the estimate to a fixed percentage error in single input variables is, in order of decreasing significance, $[Q_\downarrow]$, α, L_o, $\beta_\uparrow(\lambda_\uparrow)$, $\beta_\downarrow(\lambda_\downarrow)$.

TABLE 7.2

PERCENTAGE ERROR IN $[\underline{R}_n]$ ESTIMATE RESULTING FROM 20% ERROR IN INPUT VARIABLES

Variable	Grass		Bare Soil		Cornfield	
	(2.14)	(2.15)	(2.14)	(2.15)	(2.14)	(2.15)
α	9.4	9.4	11.3	11.3	6.1	6.1
L_o	4.0	4.0	5.2	5.3	4.3	4.3
$\beta_\uparrow, \lambda_\uparrow$	3.5	3.6	4.5	5.0	3.6	3.8
$\beta_\downarrow, \lambda_\downarrow$	2.9	3.0	3.2	3.4	2.7	2.7
$[\rho_\downarrow]$	24.1	24.1	25.1	25.2	24.2	24.2
root-sum-square	26.5	26.5	28.6	28.8	25.7	25.8

The cumulative effect of 20% error in each of the parameters is indicated by the root-sum-square error value, tabulated in the bottom row of Table 7.2. Clearly, in this rather unrealistic situation, total error is dominated overwhelmingly by error in the $[Q_\downarrow]$ measurement.

The error data from the second analysis are presented in Table 7.3. Because of the varying degree of accuracy with which the various terms can be measured or estimated, the ranking by sensitivity to error is altered substantially. In order of decreasing significance, it becomes L_o, $\beta_\downarrow(\lambda_\downarrow)$, $[Q_\downarrow]$, $\beta_\uparrow(\lambda_\uparrow)$, α. Overestimates of net radiation will occur when L_o, $\beta_\downarrow(\lambda_\downarrow)$ and $[Q_\downarrow]$ are overestimated, while underestimates will result from excessively high values of $\beta_\uparrow(\lambda_\uparrow)$ and α. Absolute root-sum-square errors are largest for the soil and least for the grass. However, because of the differences in net radiation for each surface, the cornfield estimates show slightly less error than do those for the grass on a percentage basis.

It is apparent from Table 7.3 that the net radiation equations can accomodate easily temporal changes in the surface properties of landscape elements, but are subject to larger errors in allowing for seasonal changes in atmospheric (incoming flux) properties. No advantage of one form of the model over the other is apparent.

7.2: Net Radiation Estimation Error.

Actual errors in $[R_n]$ estimation, resulting from use of

TABLE 7.3

PERCENTAGE ERROR IN $[R_{-n}]$ ESTIMATE RESULTING FROM "BEST ESTIMATE" ERROR IN INPUT VARIABLES

Variable	Grass		Bare Soil		Cornfield	
	(2.14)	(2.15)	(2.14)	(2.15)	(2.14)	(2.15)
α	1.5	1.5	2.4	2.4	2.1	2.1
L_o	4.3	4.3	5.9	6.0	4.0	4.0
$\beta_\uparrow, \lambda_\uparrow$	2.9	2.8	3.2	3.5	3.1	2.9
$\beta_\downarrow, \lambda_\downarrow$	4.4	4.2	4.6	5.1	3.4	3.9
$[Q_d]$	3.6	3.6	3.8	3.8	3.6	3.6
root-sum-square	7.8	7.7	9.3	9.7	7.4	7.6

several of the models described in Chapter 2, were evaluated using the data collected in this study. Three error terms were computed:

(i) the mean error,

(ii) the mean absolute error,

(iii) the standard error of the estimate.

Expressed as percentages of the mean actual $[R_n]$, these errors are designated E_m, E_a and E_s respectively.

Estimate 1 made use of the actual values of B, P and L_o determined for each run. This analysis is not intended as an assessment of the operational accuracy of the regression equations, but is rather a means of determining the minimum error possible. Residual error is an expression solely of the degree to which

$$\int_{t_1}^{t_2} E\,dt \neq 0.$$

This error is automatically incorporated into the other estimation equations.

Estimates 2 and 3 are basically the regression equations (7.1) - (7.6), although the P value incorporated into the intercept term is permitted to vary. However, B and L_o are the mean values. These estimates, therefore, represent the error inherent in the use of "fixed parameter" regression equations for each surface. Estimate 2 uses the equations derived from the Monteith and Szeicz model; estimate 3 uses those from the Gay version.

Owing to the inequality in the results of the two methods of calculating β, it might be expected that the former would be less accurate.

Estimate 4 uses the same "fixed parameter" technique as estimates 2 and 3, but employs B and L_o values derived from aggregated data from all surfaces. The equation is

$$[R_n] = 0.706[Q_\downarrow] - 49.8\,P\,. \qquad J\,m^{-2}$$

Estimates 5 and 6 are the modified Monteith and Szeicz and Gay models respectively, i.e. "variable parameter" regression equations. The techniques used to estimate the appropriate parameters are listed in Table 7.4. These techniques are not necessarily those "explaining" the largest proportion of the variance in the predictands, but are regarded as potentially the most useful for routine estimation. Again, estimate 6 might be expected to be most accurate as the net longwave parameter obtained by direct regression and that related to b are identical.

For comparative purposes, two previously described methods of $[R_n]$ estimation were used with the data from this investigation. Estimate 7 uses the equation of Davies (1967):

$$[R_n] = 0.617[Q_\downarrow] - (P/\overline{P})(100.56 \times 10^4)\,. \qquad J\,m^{-2}$$

Unfortunately, this equation, derived for a variety of surfaces

TABLE 7.4

PREDICTIVE PROCEDURES FOR MODEL PARAMETERS FOR ESTIMATES 5 AND 6

	Grass	Bare Soil	Cornfield
α	$\alpha = \overline{\alpha}$ Eqn. (5.2)	$\alpha = f(x_w)$ Eqn. (5.3)	$\alpha = f(x_w)$ Eqn. (5.4)
$\beta_\uparrow$ and $\lambda_\uparrow$	$\beta_\uparrow = f(x_w)$ and $\lambda_\uparrow = f(x_w)$ Eqns. (6.1) and (6.2)	$\beta_\uparrow = f(x_w)$ and $\lambda_\uparrow = f(x_w)$ Eqns. (6.5) and (6.6)	$\beta_\uparrow = f(x_w)$ and $\lambda_\uparrow = f(x_w)$ Eqns. (6.7) and (6.8)
$\beta_\downarrow$ and $\lambda_\downarrow$	$\beta_\downarrow = \overline{\beta_\downarrow}$ and $\lambda_\downarrow = \overline{\lambda_\downarrow}$ Table 6.8	$\beta_\downarrow = \overline{\beta_\downarrow}$ and $\lambda_\downarrow = \overline{\lambda_\downarrow}$ Table 6.8	$\beta_\downarrow = \overline{\beta_\downarrow}$ and $\lambda_\downarrow = \overline{\lambda_\downarrow}$ Table 6.8
L_o	$L_o = f$(cloud type, cloud amount) Eqn. (6.13)		

in many climatic zones, provides no allowance for day length in its original form. To permit useful estimates of error for the few incomplete days, therefore, the intercept value was multiplied by $(P/\bar{P})$, $\bar{P}$ being mean (complete) day length (497×10^2 s).

Estimate 8 employs the unmodified form of the Monteith and Szeicz model, with parameter values obtained from the literature (Table 7.5).

The three errors defined above are presented, for each surface and estimation technique, in Table 7.6. The statistics for estimate 1 justify the assumption that the integrated error term is zero, even for runs of less than a complete day. Error contributed by this source is of negligible significance in net radiation estimation.

The modified Monteith and Szeicz and Gay models (estimates 5 and 6) do not give significantly better accuracy than the "fixed parameter" regression-type equations for each surface. Indeed, in a few cases, the error is slightly larger. Despite the inequality $\beta \neq \beta'$, estimates 3 and 6 are not markedly more accurate than 2 and 5. In general, the error resulting from all of these techniques is similar in magnitude to that expected from instrumental considerations alone. Furthermore, for all equations, $|E_m| \ll E_a$, suggesting that error is random and that accuracy will improve with the length of the period for which net radiation estimates are required.

The regression equation derived from aggregated data

TABLE 7.5

MAGNITUDES AND SOURCES OF PARAMETERS USED IN ESTIMATE 8

	Grass	Bare Soil	Cornfield
α	$\alpha = 0.26$ Monteith (1959)	$\alpha = 0.125$ Mean value from Table 2.2	$\alpha = 0.192$ Mean value from Table 2.2
β	$\beta = 0.15$ Monteith and Szeicz (1962)	$\beta = 0.35$ Monteith and Szeicz (1962)	$\beta = 0.138$ Table 2.3
L_o	Calculated from sunrise and sunset air temperature and cloud type and amount by method of Monteith and Szeicz (1962), modified after Galperin (1949).		

TABLE 7.6

ERROR DATA FOR VARIOUS NET RADIATION ESTIMATION PROCEDURES

Estimate	Grass			Bare Soil			Cornfield		
	E_m	E_a	E_s	E_m	E_a	E_s	E_m	E_a	E_s
1	0	0.1	0.1	0	0.1	0.1	0	0.1	0.1
2	0.3	4.7	5.7	-1.6	6.6	7.2	-1.8	6.3	8.1
3	0.7	4.7	5.7	-0.1	6.3	6.9	-1.1	6.1	7.8
4	1.5	4.9	5.8	-12.2	12.3	15.0	7.0	8.3	9.2
5	-0.5	6.2	7.3	-4.3	6.9	8.5	-2.1	5.0	6.8
6	0.9	5.6	6.3	-2.6	6.5	7.7	-1.4	5.2	6.6
7	5.1	6.9	8.3	-8.1	8.6	10.7	10.4	10.4	11.1
8	17.4	17.4	19.1	5.1	6.4	8.3	11.6	11.9	13.4

$E_m > 0$: method underestimates $[R_n]$ on average.

$E_m < 0$: method overestimates $[R_n]$ on average.

(estimate 4) performs well only for the grass plot. This is a result of the fact that both the long- and shortwave response of this surface was, on average, between that of the other two plots. For the soil, this method consistently overestimates and, for the cornfield, underestimates. The performance of the Davies equation is similar, as might be expected, since the majority of the data used in its derivation were measured over grass. However, even these estimates do show some systematic bias toward underestimation, as do those for the cornfield. Soil net radiation totals are overestimated.

Estimate 8 shows errors within instrumental accuracy only for the soil. This is fortuitous as the literature parameter values used led to overestimation of both $(1 - \alpha)$ and $(1 + \beta)$, so that error in B was, consequently small. While the net radiation totals estimated are relatively accurate, the implications of the parameters regarding the spectral make-up of this flux are entirely erroneous. For the other two surfaces, this method underestimates considerably, primarily by overestimating net longwave loss (β too large, L_o too small).

7.3: Significance of Results.

The data of Table 7.6 suggest that the additional measurements and computation necessary to make use of the "variable parameter" regression-type equations do not appear to be justified by the extra accuracy achieved in net radiation totals. This does

not imply that the observed fluctuations in the component parameters are not real, but rather that the estimate is not particularly sensitive to these fluctuations. It has previously been shown (section 7.1) that the equations are highly insensitive to changes in the outgoing and incoming longwave coefficients. Furthermore, reflection coefficient changes were relatively conservative (compared to changes in $\beta\uparrow$ and $\lambda\uparrow$, for example) and the intercept term is strongly dependent on P, which is known.

The use of equations with no surface-dependent parameters, however, cannot be justified, except for grass and, perhaps, similar low-growing, freely-transpiring green vegetation, with a complete ground cover. The longwave and shortwave differences between surfaces necessitate separate equations if estimates are to be made within measurement error, although as indicated above, it is apparently not necessary for the parameters of these equations to be dependent upon time changes in surface and substrate properties.

Use of published values of α, β etc. cannot be justified without experiments to verify their local applicability.

It should be borne in mind that the errors resulting from estimates 2-6 are probably minimal, since the models were tested with the same data initially used to evaluate the parameters. In general, it might be expected that an equation derived for a given surface, location and season would give more accurate

results than one computed from data for other combinations of factors. However, if the models were tested with an independent data set and larger errors were found, this would presumably effect both the "fixed" and "variable parameter" equations similarly and thus not alter the basic conclusion of the above analysis.

CHAPTER 8

SUMMARY AND CONCLUSIONS

In section 8.1, the results of the investigation are summarised and conclusions relating specifically to the objectives of research outlined in section 2.7 are presented. In the following section, the broader implications and contributions of this research to the problem of net radiation estimation are treated.

8.1: Summary of Results.

Objective 1: Data Acquisition. The data collected show that significant differences exist between the net radiant energy inputs to a grass, bare soil and cornfield, with identical incident fluxes of short- and longwave radiation. These differences originate in variations in the surface-dependent component fluxes of R_n, not only between surfaces but also for one surface at different times during the season. Both longwave and shortwave factors may be responsible for variations in available radiant energy between landscape elements, a fact given scant attention in previous studies, which have tended to stress the dominance of the shortwave reflection process over differences in longwave loss.

Objective 1.1: The data collected are of high quality and constitute the first simultaneous determinations of the complete radiation budget for three surfaces, over an extended measurement

season. In the absence of any generally-accepted standards with which field instruments can be compared, data quality can only be evaluated by indirect means. This evidence is encouraging. Independent checks on the accuracy of the outgoing longwave flux, the least accurate flux evaluated, but one of fundamental significance in this study, suggest that a systematic error of between 8% and 15% is being achieved with the measurement system described.

Objective 2: Evaluation of Net Radiation Estimation Models.

Objective 2.1: On average, the magnitude of the incoming longwave parameters ranged between 70% and 85% of the outgoing longwave parameters. Seasonal fluctuations in β and λ are thus strongly determined by atmospheric influences and these terms cannot be regarded solely as surface parameters. The limited amount of evidence available suggests that this conclusion is as applicable to clear days as cloudy ones. Previous studies have discussed diurnal fluctuations in $L_{\downarrow}$, but have failed to demonstrate the quantitative significance of this fluctuation to the assumption that the net longwave coefficients are surface-controlled. This evidence explains the lack of success achieved in previous work in establishing any useful relationships between surface types and properties and β, as well as the large number of small and negative values obtained. The unmodified forms of the Monteith and Szeicz and Gay models cannot be regarded as useful methods of estimating net radiation, therefore.

Objective 2.2.1: The dependence of hourly values of the reflection coefficient on solar zenith angle was marked, leading to some divergence in the daily values computed by different methods. The conventional use of the proposed net radiation models prescribes use of the integrated flux or $Q_{\downarrow}$-intensity weighted mean methods of daily α computation. Although it is demonstrated that at least part of the zenith angle dependence is real, the effect of potential instrumental error on the daily α value is also minimised by use of these methods.

Objective 2.2.2: Grass α showed negligible, random seasonal fluctuations which were independent of plant height and colour and soil moisture. Soil α exhibited a simple inverse dependence on moisture content. Cornfield reflectivity showed a more complex seasonal regime which could not be related easily to any single variable, although it could be estimated from soil moisture. For no surface could any dependence of daily α on environmental variables be demonstrated.

Objective 2.2.3: $\beta_{\uparrow}$ and $\lambda_{\uparrow}$ behaved as indices of surface dessication. For simple seasonal regimes (grass and soil), these parameters were inversely related to, and predictable from, soil moisture, a surrogate for several relevant physical variables. The change brought about in the thermal response of grass with soil moisture stress and plant death is particularly noteworthy. For the cornfield, the correlation with soil moisture content was reduced by the complex seasonal changes in surface characteristics

which this plot underwent.

Objective 2.2.4: Virtually independent evaluations of soil properties provided theoretically-derived values of $\beta_{\uparrow}$ which compared favourably with those derived empirically from the radiation measurements. The systematic deviations encountered are explicable by reference to error in the measurement of soil thermal admittance. The analysis shows that the seasonal trend in the thermal response of the soil plot is due almost entirely to the decrease in the thermal admittance; no systematic trend in the proportion of net radiation used in the soil heat flux could be detected. The effect of changes in soil emissivity was small and that of surface temperature was random through time.

Objective 2.2.5: The incoming longwave parameters were variable in magnitude and were unrelated to either quantitative or qualitative atmospheric variables. The poor predictability of these parameters possibly reflects the obscurity of the physical processes which relate their component fluxes. In the net radiation estimation equations in which they are incorporated, $\beta_{\downarrow}$ and $\lambda_{\downarrow}$ can only be represented by their seasonal means. Since the range encountered was large (approximately 0.03 to 0.22), this will greatly impair the sensitivity of the $[R_n]$ estimates to surface controls.

Objective 2.2.6: The seasonal regimes of L_o for all surfaces were similar. Little predictive advantage was found in recognising the surface dependence of the term, which was most strongly

determined by, and predictable from, cloud type and amount, through their influence on daily avarage atmospheric emission.

Objective 2.2: A necessary condition to be met in establishing the usefulness of (2.14) and (2.15) is that the input parameters should be known a priori, with an appropriate level of accuracy. This is achievable for α, $\beta_{\uparrow}$, $\lambda_{\uparrow}$ and L_o but could not be demonstrated for the incoming longwave parameters.

Objective 2.3.1: No practical advantage of either the β- or λ-derived model over the other is apparent. In particular, the deviation between the two methods of calculating β is not large enough to significantly reduce the level of accuracy of (2.14) below (2.15).

Objective 2.3.2: Use of daily estimates of the predictable longwave and shortwave parameters in the "variable parameter" equations (2.14) and (2.15) failed to provide significantly better estimates of net radiation than are provided by seasonal mean values (i.e. "fixed parameter", regression-type equations), evaluated for each surface. This does not imply that the observed fluctuations are not real, but is rather a result of the insensitivity of the equations to such fluctuations, when considerable random error is associated with the use of seasonal mean values of the incoming longwave coefficients.

Objective 2.3.3: The long- and shortwave differences between the three surfaces studied were sufficiently marked, however, that use of surface dependent B values was essential.

The accuracy of equations computed from aggregated data was inadequate.

Objective 2.3: The accuracy of the $[R_n]$ estimates of both the "variable" and "fixed parameter" equations was similar to, or slightly larger than, that expected from instrumental considerations. Use of existing regression relations and published values of α and β to compute B cannot be recommended without local verification of their applicability.

8.2: Concluding Remarks.

The fundamental micrometeorological importance of surface net radiation, and its significance in agricultural, hydrological and macrometeorological studies of evaporation, has been stressed in the introductory chapter of this investigation. The following chapter discussed a group of net radiation models, using incoming shortwave radiation as the major predictive variable, which contain parameters intended to represent the factors which determine net radiation for a particular surface, under particular environmental conditions. The models discussed constitute a "family" of increasing complexity, which essentially resolve the slope coefficient of the linear regression equation relating R_n to $Q_\downarrow$ into parameters of increasing physical specificity. Such relations are useful, for routine estimation of net radiation, only if they undergo seasonal fluctuations which are sufficiently marked to effect the magnitude of $dR_n/dQ_\downarrow$.

This investigation was unable to demonstrate that $dR_n/dQ_\downarrow$ underwent significant predictable fluctuations within the period of a growing season, suggesting that linear regression equations employing $Q_\downarrow$ as the independent variable, the least physically satisfying of the equations, will give $[R_n]$ estimates as good or better than those yielded by the other methods. In the opinion of the author, no previous studies have adquately demonstrated the redundancy of the parameters α, β etc. and the consequent superiority of (2.1) over the more complex equations, if predictive accuracy alone is the criterion for evaluation.

It should be noted that the data upon which this conclusion is based were collected over a plant growing season, and, hence, it should be considered applicable only in agricultural studies, rather than hydrological and macrometeorological ones, in which interest is in the whole year. Over this longer period, more significant changes in surface properties of landscape elements will occur, which will effect α, $\beta_\uparrow$ and $\lambda_\uparrow$, a larger range of atmospheric conditions will be encountered, which may give rise to larger, predictable variations in $\beta_\downarrow$, $\lambda_\downarrow$ and L_o and variations in day length will become marked. Under such circumstances, the variable parameter approach to net radiation estimation could yield better estimates than the simple model proposed. The extension of this investigation to such longer periods would be a valid objective of future research in this field.

The recommendation regarding $[R_n]$ estimation method would

also have to be modified if a suitable means of predicting the incoming longwave parameters could be devised. This objective should be pursued in future studies of the components of the surface radiation balance, under various atmospheric conditions.

Nevertheless, it is felt that this study has provided a sounder basis for the use of the recommended procedure than hitherto existed. This is primarily a result of the acquisition of high quality radiation data, which have permitted more specific identification of the atmospheric and surface controls on the relationship between net radiation and incoming shortwave radiation. Emphasis has been given to surface controls and their variations between landscape elements and over time, mainly because such data have been less readily available in the past. For the same reason, emphasis has also been on longwave radiation exchanges. Specific mention may be made of the insight into the meaning of the "heating coefficient" concept, brought about by the resolution of the net longwave parameters into their unidirectional components, and to the analysis of the outgoing longwave parameters in terms of surface and substrate radiative and thermal properties. In some applications, particularly when net radiation totals are being estimated for more than one surface from measured $Q_{\downarrow}$, it might be considered desirable to expand the regression coefficient in terms of the component parameters defined in this study, if only to identify the controls on net radiation for each surface and to reflect the spectral make-up of the flux.

Future work in this field might seek to amass a larger body of data on total surface radiation budgets, ideally evaluated simultaneously for several landscape elements and for extended periods of time. This study has demonstrated that the radiation balance method is a sufficiently accurate one for obtaining such data, with modern instruments, carefully calibrated and exposed in the field. These data, if accompanied by detailed information on the relevant properties of the surfaces, will not merely provide increased understanding of the processes of radiative energy exchange at the earth-atmosphere interface, but will permit more thorough testing of the conclusions of this study regarding appropriate methods of estimating surface net radiation.

APPENDIX 1

SOURCES OF EVALUATIONS OF THE COEFFICIENTS B AND b

Source	Coefficients Evaluated*		No. of Determinations	No. of Surfaces
	B	b		
1 Berger-Landfeldt (1964)		x	5	5
2 Chang (1961)	x		1	1
3 Davies (1963)	x		1	1
4 Davies (1967)	x	x	2	1
5 Davies and Buttimor (1969)	x	x	26	8
6 de Boer (1959)	x	x	1	1
7 Decker (1966)**	x	x	39	2
8 Ekern (1965)	x	x	7	5
9 Fleischer (1953/54)	x	x	1	1
10 Fritschen (1967)	x	x	7	7
11 Gay (1971)	x	x	3	3
12 Idso (1968)		x	32	1
13 Idso (1971)	x	x	125	3
14 Idso et al (1969)	x	x	13	4
15 Impens and Lemeur (1969)	x	x	6	5
16 Kalma and Stanhill (1969)	x	x	13	1
17 Kyle (1971)	x	x	7	1

(continued overleaf)

18 Lemon (1963)		x	3	1
19 Monteith and Szeicz (1961)		x	9	4
20 Monteith and Szeicz (1962)		x	1	1
21 Nakagawa (1960)	x	x	1	1
22 Orvig (1961)	x		1	1
23 Polavarapu (1970)	x	x	6	1
24 Rider and Robinson (1951)**	x	x	1	1
25 Scholte Ubing (1961)	x	x	2	1
26 Shaw (1956)	x	x	2	1
27 Stanhill et al (1968)	x	x	8	1
28 Stanhill and Fuchs (1968)	x	x	14	2
29 Stanhill et al (1966)	x	x[4]	57	11
30 Viswanadham and Ramanadham (1967)		x	1	1

Total number of evaluations of B 344

Total number of evaluations of b 391

Number of surface types for which evaluations available 34

Notes:

* Where either B or b was not computed but an α value was available, the missing coefficient was derived from

$$B = (1 - \alpha)b \quad \text{or}$$

$$b = B/(1 - \alpha)$$

** These sources do not contain evaluations of the coefficients but tabulate data which permit such evaluations.

APPENDIX 2

SUMMARY OF MEAN HOURLY RADIATION BUDGET COMPONENTS FOR THE EXPERIMENTAL SURFACES

The data in the following tables are means of evaluations of radiant flux densities (W m^{-2}) at two minute intervals. All times are expressed as L.A.T.

The table columns are as follows:

(i) column A; $Q_{\downarrow}$

(ii) column B; $L_{\downarrow}$

(iii) column C; $Q_{\uparrow}$ for grass plot

(iv) column D; $Q_{\uparrow}$ for bare soil plot

(v) column E; $Q_{\uparrow}$ for cornfield

(vi) column F; $L_{\uparrow}$ for grass plot

(vii) column G; $L_{\uparrow}$ for bare soil plot

(viii) column H; $L_{\uparrow}$ for cornfield.

RUN NUMBER 01, JULY 6, 1969.

PERIOD	A	B	C	D	E	F	G	H
0850-0900	758.4	348.5	197.6	180.9	125.7	405.0	393.2	442.0
0900-1000	786.3	346.3	204.8	182.5	118.4	393.6	400.0	456.9
1000-1100	877.0	347.0	236.2	210.3	151.5	381.2	419.9	455.5
1100-1200	912.1	339.5	269.3	242.9	202.5	367.7	433.3	443.4
1200-1300	914.9	330.5	252.4	231.1	197.7	368.4	440.8	427.8
1300-1400	869.5	332.9	233.6	229.8	196.0	378.6	444.3	430.6
1400-1500	771.7	335.7	201.5	213.1	172.4	388.6	439.1	431.2
1500-1600	627.9	330.1	167.7	181.7	145.8	386.1	426.8	418.1
1600-1700	435.4	329.0	122.9	131.6	109.8	381.5	412.4	401.0
1700-1800	176.2	324.6	52.7	53.9	42.7	375.8	396.0	393.0
1800-1900	73.9	324.1	22.0	22.9	17.0	374.7	387.7	387.0
1900-2000	6.4	315.1	2.4	2.6	1.5	371.6	378.3	377.0
2000-2100	0.0	340.7	0.0	0.0	0.0	371.2	376.4	376.5
2100-2114	0.0	343.7	0.0	0.0	0.0	370.1	370.1	370.1

RUN NUMBER 02, JULY 7, 1969.

PERIOD	A	B	C	D	E	F	G	H
0824-0900	666.5	349.9	186.0	206.4	124.5	400.6	414.7	470.8
0900-1000	765.7	354.5	217.8	232.3	143.7	396.1	429.6	485.9
1000-1100	864.3	348.6	265.7	251.2	187.0	368.4	443.4	474.1
1100-1200	904.2	353.5	284.7	256.8	214.0	362.9	461.5	465.0
1200-1300	909.3	351.1	281.1	255.2	227.1	361.3	467.2	454.0
1300-1400	874.0	346.6	260.5	246.9	216.6	373.0	466.7	454.7
1400-1500	768.5	343.5	221.3	222.7	183.1	380.0	455.0	447.4
1500-1600	652.1	333.7	187.6	196.8	156.1	379.0	440.3	431.9
1600-1700	475.9	324.1	150.1	153.9	124.4	372.7	417.7	407.8
1700-1800	308.7	316.0	106.3	109.3	94.6	372.1	402.4	390.1
1800-1840	170.6	295.4	75.6	76.3	63.7	361.6	377.8	375.4

RUN NUMBER 03, JULY 8, 1969.

PERIOD	A	B	C	D	E	F	G	H
2234-2300	0.0	293.3	0.0	0.0	0.0	360.4	368.2	367.4
2300-0000	0.0	290.3	0.0	0.0	0.0	361.4	363.9	365.0
0000-0100	0.0	284.9	0.0	0.0	0.0	357.2	363.4	363.1
0100-0200	0.0	286.3	0.0	0.0	0.0	357.1	359.8	360.8
0200-0300	0.0	296.3	0.0	0.0	0.0	357.5	358.8	360.6
0300-0400	0.0	301.8	0.0	0.0	0.0	356.3	357.2	358.5
0400-0500	12.6	289.8	6.8	4.7	5.6	352.5	354.6	354.9
0500-0600	103.1	293.0	47.8	40.9	35.1	350.1	351.5	361.2
0600-0700	180.9	312.9	64.4	54.5	45.0	360.3	368.4	379.4
0700-0800	320.7	344.9	95.1	95.9	66.1	378.4	383.6	407.1

RUN 03 CONTINUED.

PERIOD	A	B	C	D	E	F	G	H
0800-0900	535.7	353.7	149.9	164.3	110.7	394.7	402.0	440.3
0900-1000	765.3	350.7	209.6	239.6	150.8	406.8	429.1	484.9
1000-1100	852.7	349.6	245.0	252.8	184.9	394.9	454.8	484.6
1100-1200	899.1	351.3	261.3	257.8	215.3	387.2	470.8	472.0
1200-1300	903.2	346.1	260.0	255.8	228.7	386.1	477.1	460.7
1300-1400	862.8	344.2	239.6	245.9	216.4	394.4	475.4	456.0
1400-1500	759.9	350.6	202.9	222.9	181.9	409.9	470.3	457.5
1500-1600	636.4	347.5	173.4	193.1	156.0	405.3	455.9	444.0
1600-1700	472.7	342.1	139.3	151.5	129.5	390.5	437.7	416.9
1700-1800	290.9	331.1	98.6	103.5	92.6	381.6	417.5	401.4
1800-1900	105.3	308.1	42.9	45.0	39.1	368.5	399.0	388.9
1900-2000	16.5	314.4	7.4	8.0	7.8	377.7	395.7	389.6
2000-2100	0.0	319.7	0.0	0.0	0.0	376.8	389.1	387.5
2100-2200	0.0	314.6	0.0	0.0	0.0	372.4	382.6	383.0
2200-2234	0.0	307.5	0.0	0.0	0.0	369.3	377.1	377.1

RUN NUMBER 04, JULY 11, 1969.

PERIOD	A	B	C	D	E	F	G	H
0534-0600	144.5	343.3	64.2	52.4	47.0	392.7	393.5	401.0
0600-0700	273.2	359.3	104.9	85.5	70.3	406.0	412.8	426.9
0700-0800	449.8	380.0	134.0	135.7	78.3	434.5	434.7	479.5
0800-0900	603.0	397.2	155.7	184.7	93.9	458.8	461.7	522.6
0900-1000	707.8	410.0	187.5	214.2	117.7	454.0	484.5	538.2
1000-1100	583.9	435.3	159.2	157.5	93.5	451.0	502.5	520.4
1100-1200	825.1	419.1	233.1	237.1	173.7	435.4	509.9	525.1
1200-1300	787.5	415.9	222.9	226.3	171.3	434.5	512.9	512.6
1300-1400	705.2	406.3	197.3	201.0	152.9	430.9	498.8	501.8
1400-1500	738.6	406.1	198.2	214.9	156.4	441.8	497.6	503.1
1500-1600	324.1	395.1	94.2	97.9	69.9	425.2	470.4	469.5
1600-1648	60.1	401.3	18.2	19.9	11.9	427.0	453.3	449.7

RUN NUMBER 05A, JULY 13, 1969.

PERIOD	A	B	C	D	E	F	G	H
0650-0700	362.4	359.6	125.0	118.7	90.8	399.4	409.9	430.9
0700-0800	465.9	369.3	136.2	149.6	91.9	419.1	424.7	463.1
0800-0900	625.1	379.9	164.7	197.7	107.9	437.5	448.6	499.9
0900-1000	748.0	393.0	192.9	228.5	125.0	448.0	474.6	527.8
1000-1100	855.0	395.5	230.3	248.0	158.9	441.6	502.2	533.2
1100-1200	802.2	403.5	225.2	235.6	167.9	439.3	514.2	510.0
1200-1300	865.5	396.4	240.1	243.4	178.7	430.8	520.8	508.3
1300-1400	765.3	399.4	201.0	222.0	157.7	453.6	521.2	508.7

RUN 05A CONTINUED.

PERIOD	A	B	C	D	E	F	G	H
1400-1500	694.6	400.3	177.0	207.3	144.7	456.6	512.9	505.4
1500-1600	470.2	385.7	119.5	142.2	93.3	438.7	486.6	474.2
1600-1700	346.6	382.1	99.2	110.9	80.1	430.1	464.3	453.5
1700-1800	167.9	382.0	51.3	55.9	40.7	424.6	452.9	443.8
1800-1900	84.5	339.5	35.7	38.9	28.9	392.7	418.2	404.2
1900-1932	19.4	348.5	12.4	13.7	10.9	402.2	426.6	417.0

RUN NUMBER 05B, JULY 14, 1969.

PERIOD	A	B	C	D	E	F	G	H
0424-0500	16.5	326.1	9.3	9.1	8.3	378.5	380.6	381.4
0500-0600	124.4	326.7	59.2	53.0	50.6	373.3	373.7	381.9
0600-0700	282.7	357.9	103.7	96.3	80.5	395.8	403.2	417.0
0700-0800	451.5	383.6	127.0	144.4	81.8	436.6	436.6	472.2
0800-0900	609.8	392.7	151.3	190.8	94.0	459.6	462.2	510.6
0900-1000	730.1	404.7	176.7	223.4	112.7	470.8	491.2	535.9
1000-1100	825.8	411.7	209.2	238.2	141.2	465.7	519.7	540.2
1100-1140	803.6	417.4	213.3	229.9	145.1	456.4	533.0	531.8

RUN NUMBER 06, JULY 22, 1969.

PERIOD	A	B	C	D	E	F	G	H
0428-0500	8.9	345.5	3.3	3.7	2.0	390.4	388.7	391.9
0500-0600	70.4	351.8	21.3	17.9	17.3	395.6	391.9	398.2
0600-0700	179.8	358.8	43.6	33.6	35.0	397.4	399.6	405.6
0700-0800	391.5	373.3	113.1	99.5	91.9	411.9	414.5	433.3
0800-0900	418.0	385.0	109.3	105.7	85.8	421.8	423.1	439.0
0900-1000	701.9	394.9	176.7	196.1	132.6	438.7	453.0	473.2
1000-1100	737.1	395.6	193.4	195.3	135.7	429.4	478.0	457.1
1100-1200	769.0	402.7	201.1	216.1	167.9	436.1	490.8	442.2
1200-1300	528.8	404.2	143.0	147.7	130.2	441.5	485.2	432.9
1300-1400	308.0	398.4	85.3	90.7	70.3	428.7	456.5	430.5
1400-1500	693.2	407.7	163.1	190.8	151.0	463.1	491.2	451.0
1500-1600	504.4	390.6	127.2	142.8	111.8	441.5	470.2	438.2
1600-1700	436.8	383.3	120.5	136.8	117.4	434.2	452.6	424.4
1700-1800	230.2	366.4	71.8	76.6	66.1	416.1	438.4	427.0
1800-1900	113.7	338.9	46.0	47.4	42.9	396.2	412.7	403.4
1900-1946	8.2	335.8	5.3	6.2	5.0	399.0	415.2	405.9

RUN NUMBER 07, JULY 23, 1969.

PERIOD	A	B	C	D	E	F	G	H
0502-0600	90.5	332.7	38.2	36.4	34.3	378.1	378.8	386.3
0600-0700	240.0	350.6	87.1	83.7	77.3	392.8	399.0	405.1
0700-0800	416.3	368.8	122.1	137.2	100.4	419.5	422.8	438.3
0800-0900	580.9	384.7	146.5	185.6	120.2	446.6	450.8	462.8
0900-1000	703.9	399.8	169.2	214.7	130.1	469.7	482.2	480.7
1000-1100	794.4	404.9	197.0	228.7	153.4	468.8	509.2	474.6
1100-1200	831.1	410.9	218.2	236.6	178.2	469.6	524.6	455.7
1200-1300	763.4	407.2	193.4	213.5	163.5	468.2	528.9	449.6

RUN NUMBER 08, JULY 30, 1969.

PERIOD	A	B	C	D	E	F	G	H
0640-0700	309.0	356.1	112.8	88.7	91.8	396.3	399.1	424.2
0700-0800	432.4	367.0	130.9	116.7	98.1	412.8	409.1	457.8
0800-0900	586.0	385.1	149.8	149.1	101.1	442.4	428.7	511.2
0900-1000	712.9	404.5	173.1	171.4	112.7	461.1	452.1	548.3

RUN NUMBER 09, JULY 31, 1969.

PERIOD	A	B	C	D	E	F	G	H
0652-0700	307.3	364.0	104.7	88.2	82.1	412.0	412.0	444.3
0700-0800	394.0	376.1	117.4	114.2	88.9	420.3	418.4	463.3
0800-0900	547.1	391.1	146.6	154.2	103.4	434.0	430.5	497.6
0900-0932	645.5	405.0	169.8	177.0	119.4	436.9	440.8	513.7

RUN NUMBER 10, AUGUST 7, 1969.

PERIOD	A	B	C	D	E	F	G	H
0542-0600	74.1	379.0	24.8	22.5	42.7	412.4	407.7	398.4
0600-0700	105.8	377.9	30.6	29.3	43.8	415.5	413.5	405.1
0700-0800	226.1	385.0	66.9	69.9	68.7	424.2	420.2	422.0
0800-0900	477.5	407.2	134.7	152.7	108.1	434.5	440.1	453.8
0900-1000	636.1	412.6	170.4	208.0	128.5	444.4	461.4	477.2
1000-1100	688.6	416.6	187.3	218.2	136.9	435.3	475.7	473.1
1100-1200	757.1	416.0	207.9	237.1	167.0	431.7	486.6	459.6
1200-1300	558.9	420.7	156.8	178.2	126.9	428.7	478.4	451.5
1300-1400	520.8	424.4	144.2	166.0	116.9	433.5	474.2	452.1
1400-1500	455.5	420.5	127.1	146.2	104.5	434.6	468.2	451.5
1500-1532	414.0	410.9	117.0	133.8	96.7	432.3	464.8	449.1

RUN NUMBER 11, AUGUST 11, 1969.

PERIOD	A	B	C	D	E	F	G	H
0502-0600	73.9	296.6	41.7	34.8	31.8	351.9	353.5	358.1
0600-0700	217.2	321.6	92.1	79.5	76.7	370.9	372.6	381.6
0700-0800	387.0	349.5	124.2	125.6	101.3	402.4	403.8	418.9
0800-0900	555.3	361.9	147.7	181.6	120.5	429.2	429.0	446.9
0900-1000	628.2	377.4	159.6	203.2	112.9	439.9	450.4	456.1
1000-1100	710.9	387.5	184.7	211.7	127.7	439.9	485.1	461.9
1100-1200	698.4	398.7	182.8	213.6	127.4	444.3	493.0	447.3
1200-1300	759.9	384.0	206.4	233.1	161.2	429.5	486.7	430.4
1300-1400	552.8	385.8	141.6	170.9	119.4	435.2	472.2	429.9
1400-1500	588.5	380.2	158.5	187.5	130.2	430.5	460.9	429.8
1500-1600	313.6	361.9	83.1	103.7	77.2	417.5	445.7	411.7
1600-1700	284.9	371.9	85.2	95.6	75.2	415.5	438.2	425.6
1700-1800	132.8	348.1	46.0	52.7	40.0	402.7	420.2	413.2
1800-1900	45.6	346.5	20.4	22.7	18.0	396.1	409.0	399.3
1900-1948	0.7	351.9	1.0	1.0	0.4	392.8	410.4	397.6

RUN NUMBER 12A, AUGUST 12, 1969.

PERIOD	A	B	C	D	E	F	G	H
0504-0600	71.0	293.3	41.0	33.4	28.8	352.4	357.1	363.8
0600-0700	215.4	320.2	97.0	84.3	72.0	374.2	374.1	389.4
0700-0800	391.6	345.7	127.9	131.4	96.5	405.0	405.1	426.1
0800-0900	564.0	362.1	154.1	183.2	112.7	432.0	435.5	458.0
0900-1000	691.3	378.6	176.8	218.2	123.0	454.7	469.4	479.3
1000-1100	772.6	396.4	185.9	220.6	124.4	473.4	514.3	495.6
1100-1200	800.2	412.2	191.9	204.5	128.6	479.9	555.9	490.6
1200-1300	805.8	412.7	192.7	205.8	138.2	473.8	547.6	483.9
1300-1400	770.4	399.9	184.8	210.1	146.5	470.1	528.1	467.5
1400-1500	690.1	388.4	169.9	199.1	142.3	458.7	504.3	452.9
1500-1600	556.1	378.4	142.8	169.3	129.8	448.2	482.3	438.4
1600-1700	377.7	375.4	112.1	120.7	103.7	432.0	465.0	428.4
1700-1800	197.5	362.1	69.9	73.0	60.9	419.8	441.6	425.9
1800-1900	45.9	339.0	22.7	23.2	17.1	400.7	422.4	410.5
1900-2000	0.0	336.5	0.0	0.0	0.0	388.0	418.4	397.7
2000-2100	0.0	333.2	0.0	0.0	0.0	382.0	411.7	392.0
2100-2200	0.0	329.3	0.0	0.0	0.0	375.0	403.4	384.3
2200-2300	0.0	326.8	0.0	0.0	0.0	368.5	398.3	382.1
2300-0000	0.0	337.4	0.0	0.0	0.0	380.9	405.4	393.5

RUN NUMBER 128, AUGUST 13, 1969.

PERIOD	A	B	C	D	E	F	G	H
0000-0100	0.0	333.7	0.0	0.0	0.0	376.4	399.3	386.2
0100-0200	0.0	327.6	0.0	0.0	0.0	368.1	389.8	374.4
0200-0300	0.0	328.2	0.0	0.0	0.0	370.0	385.1	369.9
0300-0400	0.0	327.2	0.0	0.0	0.0	368.6	384.2	370.2
0400-0500	0.6	332.1	0.0	0.6	0.0	368.3	383.0	369.1
0500-0600	36.3	333.0	13.6	14.2	8.4	371.2	378.4	369.2
0600-0700	197.7	340.4	85.8	71.8	60.2	383.5	388.0	388.6
0700-0800	356.7	377.0	125.8	114.9	89.9	418.0	426.3	435.9
0800-0900	512.0	399.4	146.6	161.7	107.1	448.9	454.6	472.9
0900-0924	500.5	414.6	138.2	154.5	90.8	452.5	464.7	469.3

RUN NUMBER 13, AUGUST 14, 1969.

PERIOD	A	B	C	D	E	F	G	H
1134-1200	721.4	446.9	191.0	202.8	131.9	489.4	538.3	573.4
1200-1300	649.6	438.4	171.0	182.8	120.1	489.4	535.6	564.1
1300-1400	555.1	432.2	145.8	158.3	100.0	480.5	519.0	544.7
1400-1500	567.2	419.8	152.6	169.7	106.7	474.3	511.5	539.3
1500-1544	274.7	410.6	77.3	82.1	55.2	455.3	485.0	483.9

RUN NUMBER 14, AUGUST 27, 1969.

PERIOD	A	B	C	D	E	F	G	H
0516-0600	22.4	302.0	11.4	12.9	6.5	349.5	357.9	352.5
0600-0700	110.0	316.2	44.1	44.7	31.3	365.2	366.4	372.1
0700-0800	282.7	340.9	99.0	101.6	68.6	395.4	392.8	408.9
0800-0900	474.7	355.7	138.6	164.0	91.9	431.8	421.9	443.4
0900-1000	621.3	371.4	162.7	208.7	100.7	464.3	450.7	470.2
1000-1100	717.2	388.2	177.0	229.3	102.9	490.2	483.6	493.0
1100-1200	756.4	400.3	189.9	230.5	109.2	500.4	509.4	501.5
1200-1300	757.3	403.8	188.3	229.9	112.5	504.4	519.2	499.2
1300-1400	719.4	394.6	179.9	228.5	119.8	490.6	502.0	480.1
1400-1500	636.3	380.7	158.8	212.6	119.2	475.4	480.9	460.2
1500-1600	498.1	370.1	136.5	174.7	109.5	452.4	460.9	436.8
1600-1700	318.7	368.0	102.5	113.7	78.6	434.0	452.2	427.5
1700-1800	140.0	351.4	56.7	60.2	42.5	415.5	426.8	414.9
1800-1900	13.2	340.6	8.0	8.0	5.0	402.0	418.7	408.6
1900-1936	0.0	335.2	0.0	0.0	0.0	388.2	412.0	399.0

RUN NUMBER 15A, AUGUST 28, 1969.

PERIOD	A	B	C	D	E	F	G	H
0504-0600	16.5	339.1	6.2	6.7	5.1	387.1	389.6	391.8
0600-0700	126.3	353.0	55.2	51.3	38.5	399.1	398.3	410.0
0700-0800	289.8	376.1	105.9	109.6	74.1	418.4	423.7	437.3
0800-0900	458.0	391.6	140.6	169.1	95.6	453.3	445.9	467.2
0900-1000	590.3	408.1	162.1	207.1	105.4	485.8	473.8	492.0
1000-1100	680.1	421.4	179.5	225.0	113.5	500.4	500.8	510.1
1100-1200	720.1	432.3	183.8	225.1	113.8	516.2	524.0	520.4
1200-1300	723.9	433.3	182.5	222.1	113.2	515.3	528.8	518.4
1300-1400	693.8	418.3	176.2	222.3	120.3	507.6	509.2	501.1
1400-1500	607.9	402.5	153.7	207.3	117.6	496.2	485.9	483.1
1500-1600	488.3	382.8	137.0	177.4	113.5	469.9	459.9	457.4
1600-1700	309.0	378.8	102.4	112.5	82.1	449.8	452.9	446.5
1700-1800	132.3	366.6	53.1	57.4	40.4	434.5	435.3	438.1
1800-1900	14.5	351.1	7.9	7.9	5.8	414.3	430.4	424.2
1900-2000	0.0	341.5	0.0	0.0	0.0	402.9	421.3	414.1
2000-2100	0.0	328.8	0.0	0.0	0.0	392.2	410.7	405.4
2100-2200	0.0	333.0	0.0	0.0	0.0	381.9	405.0	394.4
2200-2300	0.0	339.3	0.0	0.0	0.0	383.7	404.2	394.0
2300-0000	0.0	350.9	0.0	0.0	0.0	388.2	402.1	395.4

RUN NUMBER 15B, AUGUST 29, 1969.

PERIOD	A	B	C	D	E	F	G	H
0000-0100	0.0	387.2	0.0	0.0	0.0	402.9	411.0	405.8
0100-0200	0.0	370.2	0.0	0.0	0.0	401.9	407.7	409.1
0200-0300	0.0	374.0	0.0	0.0	0.0	401.2	407.6	406.8
0300-0400	0.0	375.6	0.0	0.0	0.0	401.8	407.7	407.5
0400-0500	0.0	367.2	0.0	0.0	0.0	401.1	405.1	406.5
0500-0600	7.7	370.6	3.1	3.5	1.5	405.4	406.1	408.2
0600-0700	87.6	375.8	30.5	31.0	20.6	413.2	412.1	420.3
0700-0800	206.4	397.8	65.2	70.6	43.4	432.6	430.6	441.9
0800-0900	372.3	409.8	111.8	128.1	73.9	464.7	457.6	470.8
0900-1000	523.9	432.6	148.9	178.0	95.6	495.6	488.7	496.4
1000-1100	617.4	448.8	169.9	204.6	105.3	514.6	511.3	516.0
1100-1200	507.6	451.0	139.2	160.7	86.9	505.9	513.5	508.3
1200-1300	572.9	450.1	156.8	177.8	98.5	510.2	522.9	513.2
1300-1400	522.2	442.4	143.0	171.3	97.8	505.5	511.5	500.7
1400-1500	475.6	431.1	134.7	160.5	95.0	490.8	496.4	487.4
1500-1600	372.3	412.8	112.5	131.2	82.5	471.7	476.1	470.6
1600-1700	219.5	401.9	71.3	79.1	51.4	456.1	462.9	457.6
1700-1800	89.0	391.1	30.6	35.5	20.9	442.4	447.4	447.2
1800-1856	10.6	384.5	4.5	5.6	2.2	433.2	439.9	437.6

RUN NUMBER 16, SEPTEMBER 1, 1969.

PERIOD	A	B	C	D	E	F	G	H
0552-0600	25.3	365.8	7.9	7.9	4.4	405.0	405.0	408.5
0600-0700	90.8	368.4	29.4	32.0	19.1	411.0	408.8	417.8
0700-0800	227.4	394.0	70.4	74.6	47.4	435.4	432.5	448.4
0800-0900	378.6	412.4	111.8	124.0	71.6	459.5	454.1	473.0
0900-1000	482.9	428.2	137.0	152.6	82.5	487.1	481.5	492.4
1000-1100	569.1	446.5	153.2	171.9	88.5	514.8	508.4	514.9
1100-1200	655.2	455.4	171.8	188.3	100.4	526.9	539.3	532.9
1200-1300	654.5	452.6	170.3	185.5	109.1	521.4	543.2	524.8
1300-1400	439.5	446.4	117.4	133.6	76.0	496.6	516.4	499.4
1400-1500	336.5	435.4	89.7	103.2	55.5	484.2	496.3	486.2
1500-1600	189.6	428.8	50.4	58.9	31.1	472.0	480.8	475.3
1600-1700	97.4	422.1	26.4	32.6	15.0	457.8	465.0	462.8
1700-1800	35.1	415.5	11.3	13.4	6.1	445.8	454.8	451.5
1800-1900	5.5	403.8	3.0	3.8	1.5	433.5	445.0	438.7

RUN NUMBER 17, SEPTEMBER 2, 1969.

PERIOD	A	B	C	D	E	F	G	H
0528-0600	17.9	356.4	5.9	7.2	6.3	393.9	397.4	395.0
0600-0700	103.2	362.3	34.0	37.6	22.9	401.4	400.7	408.2
0700-0800	122.9	392.0	33.2	39.1	20.1	414.9	413.8	418.3
0800-0900	182.1	413.8	49.5	55.4	28.9	426.0	427.1	428.8
0900-1000	300.6	429.4	79.0	89.3	48.8	442.2	445.0	445.0
1000-1100	230.7	428.0	60.9	67.9	33.5	439.9	446.2	443.9
1100-1200	336.5	432.7	90.0	99.5	53.4	452.8	459.2	454.7
1200-1300	428.7	435.5	116.7	131.2	72.7	462.9	471.7	460.7
1300-1400	491.5	425.2	129.2	149.6	89.0	475.4	485.0	467.0
1400-1500	435.3	408.6	117.3	136.6	80.5	467.7	473.8	458.5
1500-1600	336.2	393.3	94.9	110.0	67.9	449.1	458.7	445.4
1600-1700	207.3	377.8	63.4	70.4	47.6	433.2	443.9	432.0
1700-1800	68.3	364.2	23.6	26.9	16.6	419.6	427.5	422.0
1800-1900	14.4	355.7	6.3	7.2	3.8	405.6	419.6	413.1
1900-1932	0.0	349.2	0.0	0.0	0.0	398.1	411.8	405.0

RUN NUMBER 18, SEPTEMBER 3, 1969.

PERIOD	A	B	C	D	E	F	G	H
0600-0700	84.5	346.3	28.7	30.8	20.5	390.7	387.9	397.7
0700-0800	230.6	364.5	77.2	80.3	54.2	406.5	406.8	420.0
0800-0900	396.3	381.2	120.2	133.5	81.5	437.7	430.9	445.3
0900-1000	376.4	403.3	106.4	117.7	66.0	452.2	449.1	454.4
1000-1100	597.8	416.8	162.4	186.7	102.8	488.5	483.1	486.9
1100-1200	605.3	428.9	159.7	184.1	105.3	497.7	501.8	491.5

RUN 18 CONTINUED.

PERIOD	A	B	C	D	E	F	G	H
1200-1300	646.5	427.7	169.6	193.7	106.5	507.3	513.2	494.8
1300-1400	608.6	418.1	158.4	186.0	106.7	499.7	508.3	486.5
1400-1500	529.2	403.9	140.7	166.8	100.6	491.5	497.1	473.0
1500-1600	429.0	381.9	122.7	145.6	97.0	465.2	471.6	450.8
1600-1700	272.8	368.7	89.0	93.9	69.6	442.9	457.8	438.7
1700-1800	112.4	347.7	44.1	47.0	33.5	418.1	429.1	422.8
1800-1900	11.1	332.9	5.4	6.2	3.6	401.0	418.7	414.3
1900-1940	0.0	319.7	0.0	0.0	0.0	387.4	408.2	401.2

RUN NUMBER 19, SEPTEMBER 4, 1969.

PERIOD	A	B	C	D	E	F	G	H
0546-0600	12.5	391.1	0.0	0.0	0.0	391.6	398.0	392.1
0600-0700	33.4	399.9	5.9	5.7	2.8	401.4	404.0	402.8
0700-0800	124.2	408.1	31.4	35.0	19.7	415.9	413.4	418.7
0800-0900	169.6	415.9	46.2	50.6	26.8	425.8	423.5	428.3
0900-1000	375.4	424.2	102.5	118.8	63.9	454.3	444.7	455.8
1000-1100	405.5	409.1	112.8	129.2	67.7	455.8	455.5	463.0
1100-1200	510.0	425.2	134.9	154.6	82.1	474.7	473.4	477.2
1200-1300	464.6	428.2	126.0	146.9	75.3	482.3	482.0	476.4
1300-1400	574.0	416.9	150.3	180.8	102.9	485.5	488.0	477.1
1400-1500	439.9	401.7	118.6	143.0	85.8	465.3	470.8	460.8
1500-1600	379.4	392.8	107.1	129.5	83.5	456.7	459.7	448.3
1600-1700	228.5	390.3	69.6	81.8	52.0	445.2	450.1	441.6
1700-1800	91.6	371.5	32.5	37.4	24.4	426.3	431.2	427.6
1800-1900	7.1	362.8	3.7	3.8	2.2	414.0	422.8	418.9
1900-1914	0.0	371.1	0.0	0.0	0.0	411.5	421.0	414.0

RUN NUMBER 20, SEPTEMBER 9, 1969.

PERIOD	A	B	C	D	E	F	G	H
0600-0700	113.6	294.3	54.1	48.3	33.4	348.6	348.2	365.3
0700-0800	285.3	325.1	103.6	98.3	76.0	370.9	375.6	393.0
0800-0900	377.1	336.7	109.5	120.0	76.2	391.5	396.2	411.9
0900-1000	608.6	350.7	157.2	196.3	105.8	432.6	422.8	446.1
1000-1100	459.9	385.8	118.6	135.0	67.6	431.6	438.9	445.7
1100-1200	157.0	382.2	42.2	47.3	22.3	407.8	417.8	412.4
1200-1300	300.9	394.6	74.7	85.9	43.2	424.7	427.5	425.6
1300-1346	293.9	395.2	75.1	84.7	42.7	425.2	433.0	428.7

RUN NUMBER 21, SEPTEMBER 10, 1969.

PERIOD	A	B	C	D	E	F	G	H
1842-1900	0.0	279.3	0.0	0.0	0.0	363.1	370.1	370.1
1900-2000	0.0	276.2	0.0	0.0	0.0	361.0	364.8	367.1
2000-2100	0.0	267.6	0.0	0.0	0.0	353.1	358.6	359.1
2100-2200	0.0	265.4	0.0	0.0	0.0	343.6	353.7	352.1
2200-2300	0.0	265.4	0.0	0.0	0.0	331.8	348.4	341.5
2300-0000	0.0	296.3	0.0	0.0	0.0	341.8	352.0	345.9
0000-0100	0.0	340.7	0.0	0.0	0.0	355.0	363.1	356.1
0100-0200	0.0	341.1	0.0	0.0	0.0	356.5	363.1	356.8
0200-0300	0.0	328.3	0.0	0.0	0.0	356.3	361.6	357.2
0300-0400	0.0	327.9	0.0	0.0	0.0	354.8	360.6	356.5
0400-0500	0.0	340.1	0.0	0.0	0.0	357.0	363.1	360.7
0500-0600	3.3	314.7	2.0	2.0	1.3	352.0	357.9	355.6
0600-0700	112.7	319.8	50.4	46.6	33.5	363.0	360.7	374.9
0700-0800	256.4	332.8	93.2	94.5	66.0	387.2	379.7	392.1
0800-0900	436.6	328.7	134.8	154.7	93.1	410.9	405.8	423.4
0900-1000	588.3	349.7	153.1	192.2	100.1	453.1	441.7	455.4
1000-1100	464.3	379.7	123.6	146.6	76.2	444.5	446.7	449.4
1100-1200	519.3	384.0	123.5	161.1	91.6	471.7	466.8	454.5
1200-1300	655.4	390.0	174.7	207.9	105.3	474.7	486.2	466.8
1300-1400	543.0	371.5	147.5	170.2	90.3	456.8	473.6	451.9
1400-1500	589.5	352.9	162.7	191.5	118.6	448.7	466.4	435.6
1500-1600	495.7	338.0	153.6	172.4	119.8	424.5	446.4	412.5
1600-1700	272.8	330.0	98.3	98.3	70.8	404.0	429.6	404.8
1700-1800	116.0	297.1	55.9	56.3	43.6	378.6	389.8	381.4
1800-1900	3.1	284.6	2.0	2.3	1.4	369.4	384.0	377.0
1900-1942	0.0	274.8	0.0	0.0	0.0	357.0	373.6	366.6

APPENDIX 3

STATISTICAL DATA SUMMARY FOR LONGWAVE PARAMETERS

Tabulated below are the correlation coefficients and standard errors of the estimate for each of the relationships defining a longwave parameter. The r and s terms are identified by subscription with the appropriate slope coefficient. Tables are subdivided according to surface and longwave flux involved.

Contents:

(N.B. s data expressed in W m^{-2}).

TABLE A

1	July	6
2		7
3		8
4		11
5		13
6		22
7	August	7
8		11
9		12
10		27
11		28
12		29
13	September	1
14		2
15		3
16		4
17		9
18		10
19	Mean	
20	Standard Deviation	
21	Coefficient of Variation	

TABLE B

	r_b	r_β	r_λ	s_b	s_β	s_λ
1	.996	-.459	.413	12.6	11.9	12.6
2	.999	-.865	.836	9.8	9.1	9.8
3	.999	-.347	.306	10.5	9.8	10.5
4	.994	-.303	.219	16.8	16.8	16.8
5	.996	-.180	.121	13.3	13.3	13.3
6	.996	-.172	.107	13.3	13.3	13.3
7	.998	-.557	.503	11.2	10.5	11.2
8	.996	.058	-.111	11.9	11.9	11.9
9	.999	.587	-.613	7.0	7.0	7.0
10	.999	.926	-.939	7.0	7.7	7.0
11	.998	.729	-.769	10.5	11.9	10.5
12	.998	.676	-.718	8.4	9.1	8.4
13	.998	.861	-.884	7.0	7.7	7.0
14	.984	-.068	-.094	18.8	18.8	18.8
15	.995	.470	-.551	14.0	14.7	14.0
16	.986	.505	-.622	18.8	20.9	18.8
17	.980	.473	-.580	16.1	17.5	16.1
18	.990	.574	-.654	17.5	18.8	17.5
19	.994	.489	.502	12.6	12.6	12.6
20	.006	.258	.276	4.2	4.2	4.2
21	.006	.528	.550	.308	.325	.308

TABLE C

	r_b	r_β	r_λ	s_b	s_β	s_λ
1	.989	.338	-.416	19.5	20.2	19.5
2	.997	.451	-.526	14.7	15.4	14.7
3	.994	.598	-.679	21.6	23.7	21.6
4	.995	.652	-.711	13.3	14.7	13.3
5	.992	.387	-.486	22.3	23.7	22.3
6	.989	.242	-.343	20.2	20.9	20.2
7	.996	.523	-.592	11.9	12.6	11.9
8	.994	.279	-.372	19.5	20.2	19.5
9	.999	.768	-.823	16.1	18.1	16.1
10	.997	.760	-.806	12.6	14.0	12.6
11	.998	.661	-.715	11.9	12.6	11.9
12	.995	.479	-.553	11.9	12.6	11.9
13	.998	.736	-.786	11.9	12.6	11.9
14	.976	-.115	-.079	21.6	20.9	21.6
15	.989	.220	-.354	19.5	20.2	19.5
16	.976	.279	-.453	23.7	25.1	23.7
17	.983	.293	-.402	14.0	14.0	14.0
18	.985	.148	-.301	25.1	25.8	25.1
19	.991	.441	.522	17.5	18.1	17.5
20	.007	.210	.198	4.2	4.9	4.2
21	.007	.476	.379	.261	.252	.261

TABLE D

	r_b	r_β	r_λ	s_b	s_β	s_λ
1	.994	.740	-.774	12.6	13.3	12.6
2	.999	.742	-.784	11.2	12.6	11.2
3	.998	.833	-.864	13.3	14.0	13.3
4	.996	.709	-.769	16.1	18.1	16.1
5	.993	.635	-.702	20.2	21.6	20.2
6	.995	-.143	.061	18.1	17.5	18.1
7	.998	.430	-.493	12.6	13.3	12.6
8	.994	-.161	.085	18.1	18.1	18.1
9	.998	.305	-.363	14.0	14.0	14.0
10	.999	.845	-.867	9.1	9.8	9.1
11	.998	.826	-.843	6.3	6.3	6.3
12	.998	.520	-.562	8.4	9.1	8.4
13	.999	.795	-.821	7.7	8.4	7.7
14	.987	-.322	.200	16.8	16.8	16.8
15	.996	.061	-.121	10.5	10.5	10.5
16	.988	.401	-.513	19.5	20.9	19.5
17	.973	.327	-.472	21.6	23.0	21.6
18	.992	.146	-.240	18.8	19.5	18.8
19	.994	.497	.530	14.0	14.7	14.0
20	.006	.266	.282	4.9	4.9	4.9
21	.006	.536	.532	.324	.322	.324

TABLE E

	$r_{\beta\uparrow}$	$r_{\lambda\uparrow}$	$s_{\beta\uparrow}$	$s_{\lambda\uparrow}$
1	.093	.127	16.8	16.1
2	.033	.079	14.0	14.0
3	.712	.725	13.3	13.3
4	.539	.564	18.8	18.8
5	.620	.647	21.6	20.9
6	.753	.778	17.5	16.8
7	.614	.637	10.5	10.5
8	.824	.833	19.5	18.8
9	.918	.921	15.4	14.7
10	.934	.943	17.5	16.1
11	.947	.961	13.3	11.9
12	.944	.955	12.6	11.2
13	.888	.892	17.5	16.8
14	.932	.955	9.1	7.7
15	.933	.956	14.7	11.9
16	.893	.933	13.3	11.2
17	.777	.731	20.9	23.0
18	.891	.910	21.6	19.5
19	.736	.753	16.1	15.4
20	.268	.261	3.5	4.2
21	.364	.346	.226	.263

TABLE F

	$r_{\beta\uparrow}$	$r_{\lambda\uparrow}$	$s_{\beta\uparrow}$	$s_{\lambda\uparrow}$
1	.622	.673	19.5	18.1
2	.888	.920	12.6	10.5
3	.836	.882	23.0	20.2
4	.742	.771	25.8	24.4
5	.708	.766	29.3	26.5
6	.716	.773	25.8	23.7
7	.838	.866	14.7	14.0
8	.739	.784	30.0	27.2
9	.849	.889	32.1	27.9
10	.855	.889	25.8	22.3
11	.913	.938	17.5	14.7
12	.876	.908	18.1	16.1
13	.796	.829	25.1	23.0
14	.853	.911	14.0	11.2
15	.835	.897	22.3	18.1
16	.789	.874	17.5	14.0
17	.614	.575	25.8	26.5
18	.707	.783	32.1	28.6
19	.788	.829	23.0	20.2
20	.086	.093	6.3	5.6
21	.109	.112	.263	.286

TABLE G

	$r_{\beta\uparrow}$	$r_{\lambda\uparrow}$	$s_{\beta\uparrow}$	$s_{\lambda\uparrow}$
1	.775	.798	18.1	17.5
2	.883	.909	16.1	14.0
3	.938	.949	14.7	13.3
4	.834	.856	23.0	21.6
5	.864	.892	21.6	19.5
6	.722	.759	18.1	17.5
7	.872	.892	11.9	11.2
8	.733	.758	22.3	21.6
9	.914	.924	15.4	14.7
10	.939	.946	15.4	14.7
11	.956	.963	11.2	10.5
12	.939	.948	11.9	11.2
13	.904	.903	14.7	14.7
14	.903	.916	9.1	8.4
15	.947	.957	10.5	9.1
16	.877	.915	13.3	11.2
17	.879	.829	14.0	16.1
18	.840	.860	20.2	18.8
19	.873	.887	15.4	14.7
20	.068	.063	4.2	4.2
21	.078	.071	.260	.269

TABLE H

	r_{β_4}	r_{λ_4}	s_{β_4}	s_{λ_4}
1	.527	.522	12.6	12.6
2	.907	.914	7.7	7.7
3	.813	.804	12.6	12.6
4	.654	.621	20.2	20.9
5	.751	.749	17.5	17.5
6	.845	.836	14.0	14.7
7	.814	.794	11.2	11.9
8	.822	.813	19.5	19.5
9	.894	.891	15.4	15.4
10	.900	.905	12.6	12.6
11	.963	.960	7.7	8.4
12	.946	.942	9.1	9.8
13	.763	.756	17.5	17.5
14	.855	.770	16.1	18.8
15	.955	.941	9.1	10.5
16	.723	.640	14.0	15.4
17	.450	.353	32.8	34.9
18	.822	.796	20.2	21.6
19	.800	.778	14.7	15.4
20	.137	.155	5.6	6.3
21	.171	.199	.391	.395

TABLE I

	$\Sigma\beta_{\downarrow}$	$\Sigma\lambda_{\downarrow}$	$^{s}\beta_{\downarrow}$	$^{s}\lambda_{\downarrow}$
1	.549	.521	12.6	12.6
2	.919	.896	7.0	7.7
3	.817	.792	12.6	13.3
4	.612	.612	20.9	20.9
5	.743	.738	17.5	17.5
6	.829	.829	14.7	14.7
7	.799	.785	11.2	11.9
8	.796	.797	20.2	20.2
9	.867	.893	16.8	15.4
10	.886	.909	13.3	12.6
11	.962	.967	7.7	7.0
12	.936	.943	9.8	9.8
13	.733	.748	18.1	17.5
14	.868	.779	14.7	18.1
15	.953	.943	9.1	10.5
16	.752	.645	13.3	15.4
17	.418	.341	33.5	34.9
18	.804	.787	20.9	21.6
19	.791	.774	15.4	15.4
20	.140	.157	6.3	6.3
21	.177	.203	.402	.401

TABLE J

	r_{β_4}	r_{λ_4}	s_{β_4}	s_{λ_4}
1	.527	.526	12.6	12.6
2	.915	.921	7.0	7.0
3	.820	.805	12.6	12.6
4	.630	.607	20.9	20.9
5	.754	.728	16.8	18.1
6	.837	.818	14.0	14.7
7	.811	.787	11.2	11.9
8	.802	.785	20.2	20.9
9	.895	.881	15.4	16.1
10	.906	.904	12.6	12.6
11	.966	.968	7.7	7.0
12	.945	.942	9.1	9.8
13	.764	.749	17.5	17.5
14	.848	.784	15.4	18.1
15	.955	.945	9.1	9.8
16	.719	.644	14.0	15.4
17	.470	.333	32.8	34.9
18	.806	.774	20.9	22.3
19	.798	.772	14.7	15.4
20	.136	.158	6.3	6.5
21	.170	.205	.401	.412

REFERENCES

Aizenshtat, B.A. and M.V. Zuyev. 1952: Some features of the thermal balance of a sand desert. Trudy GGO No. 6(7), (cited in Kondrat'yev, 1965).

Allen, L.H. and K.W. Brown. 1965: Shortwave radiation in a corn crop. Agron. J. 57, 575-580.

Allen, L.H., C.S. Yocum and E.R. Lemon. 1964: Photosynthesis under field conditions. VII. Radiant energy exchanges within a corn crop and implications in water use efficiency. Agron. J. 56, 253-258.

Ångström, A. 1916: Über die Gegenstrahlung der Atmosphäre. Meteorol. Z. 33, 529-538.

Ångström, A. 1925: The albedo of various surfaces of ground. Geogr. Ann. 7, 323-342.

Anonymous. 1967: Unpublished soil map of the Horticultural Experiment Station, Simcoe.

Aslyng, H.C. and B.F. Nielsen. 1960: The radiation balance at Copenhagen. Arch. Meteorol. Geophys. Bioklimatol. B10, 342-358.

Barry, R.G. and R.E. Chambers. 1966: A preliminary map of summer albedo over England and Wales. Quart. J. Roy. Meteorol. Soc. 92, 543-548.

Berger-Landefeldt, U. 1964: Über der Strahlungshaushalt verschiedener Pflanzenbestande. Ber. Deut. Bot. Geschr. 77, 27-48.

Bolz, H.M. 1949: Die Abhangigkeit der infraroten Gegenstrahlung von der Bewölkung. Z. Meteorol. 3, 201-203.

Brooks, F.A. 1963: Investigation of energy and mass transfers near the ground including the influence of the soil-plant-atmosphere system. Final Report, University of California.

Brown, K.W. and W. Covey. 1966: The energy-budget evaluation of the micrometeorological transfer processes within a corn field. Agr. Meteorol. 3, 73-96.

Brown, K.W., N.J. Rosenberg and P. Doraiswamy. 1970: Shading inverted pyranometers and measurements of radiation reflected from an alfalfa crop. Water Resources Res. 6, 1782-1786.

Brunt, D. 1932: Notes on radiation in the atmosphere. Quart. J. Roy. Meteorol. Soc. 58, 389-420.

Budyko, M.I. 1956: The heat balance of the earth's surface. English translation by N.A. Stepanova, 1958. Office of Technical Services, U.S. Department of Commerce, Washington.

Businger, J.A. and K.J.K. Buettner. 1961: Thermal contact coefficient (a term proposed for use in heat transfer). J. Meteorol. 18, 422.

Canada, Environment Canada, Atmospheric Environment Service. 1972: Monthly Radiation Summary. Ottawa.

Carslaw, H.S. and J.C. Jaeger. 1959: Conduction of Heat in Solids. Clarendon Press, Oxford.

Chang, J.H. 1961: Microclimate of sugar cane. Hawaiian Planters Rec. 56, 195-225.

Davies, J.A. 1963: Net radiation studies in the Schefferville area. Arctic 16, 41-46.

Davies, J.A. 1967: A note on the relationship between net radiation and solar radiation. Quart. J. Roy. Meteorol. Soc. 93, 109-115.

Davies, J.A. and P.H. Buttimor. 1969: Reflection coefficients, heating coefficients and net radiation at Simcoe, Southern Ontario. Agr. Meteorol. 6, 373-386.

Davies, J.A., P.J. Robinson and M. Nunez. 1970: Radiation measurement over Lake Ontario and the determination of emissivity. First Report, Contract No. H081276, Department of Geography, McMaster University, Hamilton.

de Boer, H.J. 1959: Enkels metingen van de totale straligs-balans en zijn vier componenten op 1,60 m hoogte boven een grasmat te De Bilt. Koninkl. Ned. Meteorol. Inst. 46, 111-229.

Decker, W.L. 1959: Variation in the net exchange of radiation from vegetation of different heights. J. Geophys. Res. 64, 1617-1619.

Decker, W.L. 1964: Res. Bull. No. 854. Agr. Exp. Sta., Miss.

Decker, W.L. 1966: Climatology of the total energy budget of the earth-atmosphere interface. (A summary of results from December 1964 - December 1965). Final Report GP-1899 (N.S.F.).

de Vries, D.A. 1963: Thermal properties of soils. In van Wijk, 1963, pp. 210-235.

Ekern, P.C. 1965: The fraction of sunlight retained as net radiation in Hawaii. J. Geophys. Res. 70, 785-793.

Falckenberg, G. 1928: Die Absorptionskonstanten einiger meteorologisch wichtiger Körper für infrarote Wellen. Meteorol. Z. 45, 334-337.

Fleischer, R. von. 1953/54: Der Jahresgang der Strahlungsbilanz und ihrer Komponenten. Ann. Meteorol. 11/12, 357-364.

Fritschen, L.J. 1967: Net and solar radiation relations over irrigated field crops. Agr. Meteorol. 4, 55-62.

Fritschen, L.J. and C.H.M. van Bavel. 1964: Energy balance as affected by height and maturity of Sudangrass. Agron. J. 56, 201-204.

Fritz, S. 1948: The albedo of the ground and atmosphere. Bull. Amer. Meteorol. Soc. 29, 303-312.

Fuchs, M. and C.B. Tanner. 1968: Surface temperature measurements of bare soils. J. Appl. Meteorol. 7, 303-305.

Funk, J.P. 1959: Improved polythene-shielded net radiometer. J. Sci. Instrum. 36, 267-270.

Gadd, A.J. and J.F. Keers. 1970: Surface exchanges of sensible and latent heat in a 10-level model atmosphere. Quart. J. Roy. Meteorol. Soc. 96, 297-308.

Galperin, B.M. 1949: The radiation balance at the Lower Volga during the warm season. Trudy GGO No. 18(80), (cited in Kondrat'yev, 1965).

Gates, D.M. 1965: Radiant energy, its receipt and disposal. Meteorol. Monogr. 6, 1-26.

Gay, L.W. 1971: The regression of net radiation upon solar radiation. Arch. Meteorol. Geophys. Bioklimatol. B19, 1-14.

Graham, W.G. and K.M. King. 1961: Short-wave reflection coefficient for a field of maize. Quart. J. Roy. Meteorol. Soc. 87, 425-428.

Grulois, J. 1968: La variation annuelle du coefficient d'albedo des surfaces superieures du Peuplement. Bull. Soc. Roy. Bot. Belg. 101, 141.

Haise, H.R., R.J. Hanks and M.E. Jensen. 1967: Solar reflectance for soil and crop surfaces. Unpublished report, (cited in Stanhill et al, 1968).

Hall, F.H. 1968: The effect of cirrus clouds on 8-13μ infrared sky radiance. Appl. Opt. 7, 891-898.

Haltiner, G.J. and F.L. Martin. 1957: Dynamical and Physical Meteorology. McGraw-Hill, New York.

Idso, S.B. 1968: An analysis of the heating coefficient concept. J. Appl. Meteorol. 7, 716-717.

Idso, S.B. 1971: Relations between net and solar radiation. J. Meteorol. Soc. Jap. 49, 1-12.

Idso, S.B., D.G. Baker and B.L. Blad. 1969: Relations of of radiation fluxes over natural surfaces. Quart J. Roy. Meteorol. Soc. 95, 244-257.

Idso, S.B. and R.D. Jackson. 1969: Thermal radiation from the atmosphere. J. Geophys. Res. 74, 5397-5403.

Impens, I. and R. Lemeur. 1969: The radiation balance of several field crops. Arch. Meteorol. Geophys. Bioklimatol. B17, 261-268.

Johnson, J.E. 1954: Physical Meteorology. John Wiley and Sons, New York.

Kalitin, N.N. 1930: The measurements of the albedo of a snow cover. Mon. Weather Rev. 58, 59-61.

Kalma, J.D. and G. Stanhill. 1969: The radiation climate of an irrigated orange plantation. Solar Energy 12, 491-508.

Kondrat'yev, K.Ya. 1965: Radiative Heat Exchange in the Atmosphere. (Translated by O. Tedder). Pergamon Press, London.

Kondrat'yev, K.Ya. 1969: Radiation in the Atmosphere. Academic Press, New York.

Kondrat'yev, K.Ya. and T.S. Holm. 1959: Some results of measurements of thermal atmospheric radiation in daytime. Meteorol. Hydrol. 11, (cited in Kondrat'yev, 1969).

Kuhn, P.M. and V.E. Suomi. 1958: Airborne observations of albedo with a beam reflector. J. Meteorol. 15, 172-174.

Kung, E.C., R.A. Bryson and D.H. Lenschow. 1964: Study of a continental surface albedo on the basis of flight measurements and structure of the earth's surface cover over North America. Mon. Weather Rev. 92, 543-564.

Kyle, W.J. 1971: Daytime radiation regimes within a corn canopy. McMaster University, Department of Geography, Publications in Climatology No. 2.

Lemon, E.R. (Editor). 1963: The energy budget at the earth's surface. I. U.S. Dept. Agr., Prod. Res. Rept. (Washington, D.C.). 71, 7-31.

Lettau, H.H. 1959: A Review of Research Problems in Micrometeorology. Final Report. Contract DA-36-039-SC-80063, Task 65-58-0026, USAEPG, Fort Huachuca, Arizona; University of Wisconsin, Madison, Wisc.

Linacre, E.T. 1968: Estimating the net-radiation flux. Agr. Meteorol. 5, 49-63.

List, R.J. 1966: Smithsonian Meteorological Tables. Smithsonian Institution Press, Washington.

Lönnquist, O. 1954: Synthetic formulae for estimating effective radiation to a cloudless sky and their usefulness in comparing various estimation procedures. Ark. Geofys. 2, 245-294.

McIlroy, I.C. and D.E. Angus. 1964: Grass, water and soil evaporation at Aspendale. Agr. Meteorol. 1, 201-224.

Monteith, J.L. 1959: The reflection of short-wave radiation by vegetation. Quart. J. Roy. Meteorol. Soc. 85, 386-392.

Monteith, J.L. 1964: Evaporation and environment. In: G.F. Fogg (Editor), The State and Movement of Water in Living Organisms. Cambridge University Press, Cambridge.

Monteith, J.L. and G. Szeicz. 1961: The radiation balance of bare soil and vegetation. Quart. J. Roy. Meteorol. Soc. 87, 159-170.

Monteith, J.L. and G. Szeicz. 1962: Radiative temperature in the heat balance of natural surfaces. Quart. J. Roy. Meteorol. Soc. 88, 496-507.

Nakagawa, Y. 1960: English title: Studies on the radiation balance in the paddy field and water temperature in the percolating paddy field (English summary included). J. Agr. Meteorol. (Tokyo) 15, 143-146.

Oguntoyinbo, J.S. 1970: Reflection coefficient of natural vegetation, crops and urban surfaces in Nigeria. Quart. J. Roy. Meteorol. Soc. 96, 430-441.

Orvig, S. 1961: Net radiation flux over sub-Arctic surfaces. J. Meteorol. 18, 199-203.

Penman, H.L. 1948: Natural evaporation from open water, bare soil and grass. Proc. Roy. Soc. London A193, 120-145.

Petterssen, S. 1959: On the influence of heat exchanges on motion and weather systems. Scientific Report No. 10, Contract AF-19(604)-2179; University of Chicago, Chicago.

Polavarapu, R.J. 1970: A comparative study of global and net radiation measurements at Guelph, Ottawa and Toronto. J. Appl. Meteorol. 9, 809-814.

Priestley, C.H.B. 1959: Turbulent Transfer in the Lower Atmosphere. University of Chicago Press, Chicago.

Priestley, C.H.B. and R.J. Taylor. 1972: On the assessment of surface heat flux and evaporation using large-scale parameters. Mon. Weather Rev. 100, 81-92.

Pruitt, W.O. and D.E. Angus. 1961: Comparison of evapotranspiration with solar and net radiation and evaporation from water surfaces. Chapter 6, First Annual Report, Investigation of Energy and Mass Transfers near the Ground, pp. 74-107. U.S. Army Proving Grounds Technical Program, University of California, Davis.

Rider, N.E. and G.D. Robinson. 1951: A study of the transfer of heat and water vapour above a surface of short grass. Quart. J. Roy. Meteorol. Soc. 77, 375-401.

Rijks, D.A. 1967: Water use by irrigated cotton in Sudan. I. Reflection of short-wave radiation. J. Appl. Ecol. 4, 561-568.

Scholte-Ubing, D.W. 1959: Over straling de warmtebalans en de verdamping van gras. Mededel. Landbouwhschool, Wageningen 59, 1-93.

Scholte-Ubing, D.W. 1961: Solar and net radiation, available energy and its influence on evapotranspiration from grass. Neth. J. Agr. Sci. 9, 81-93.

Sellers, W.D. 1965: Physical Climatology. University of Chicago Press, Chicago.

Shaw, R.H. 1956: A comparison of solar radiation and net radiation. Bull. Amer. Meteorol. Soc. 37, 205-206.

Shinn, J.H. and E.R. Lemon. 1962: Studies of water relations in a corn field in Ellis Hollow (Ithaca, New York). Interim Report 62-8. The energy budget at the earth's surface. USDA Research Report No. 356.

Siegel, S. 1956: Nonparametric Statistics for the Behavioural Sciences. McGraw-Hill, New York.

Skvortzov, A.A. 1928: On the problem of the climate in oasis and desert and some peculiarities of their heat balance. Trans. Agr. Meteorol. 20, (cited in Kondrat'yev, 1969)

Slatyer, R.O. and I.C. McIlroy. 1961: Practical Micrometeorology. C.S.I.R.O., Canberra.

Special Committee for the International Geophysical Year. 1958: Radiation instruments and measurements. Annals of the I.G.Y. 5 (part 6). Pergamon, London.

Stanhill, G., J.T.H. Cox and S. Moreshet. 1968: The effect of crop and climatic factors on the radiation balance of an irrigated maize crop. J. Appl. Ecol. 5, 707-720.

Stanhill, G, and M. Fuchs. 1968: The climate of the cotton crop: physical characteristics and microclimate relationships. Agr. Meteorol. 5, 183-202.

Stanhill, G., G.J. Hofstede and J.D. Kalma. 1966: Radiation balance of natural and agricultural vegetation. Quart. J. Roy. Meteorol. Soc. 92, 128-140.

Swinbank, W.C. 1963: Long-wave radiation from clear skies. Quart. J. Roy. Meteorol. Soc. 89, 339-348.

Tanner, C.B. 1960: Energy balance approach to evapotranspiration from crops. Soil Sci. Soc. Amer. Proc. 24, 1-9.

Tanner, C.B. and M. Fuchs. 1968: Evaporation from unsaturated surfaces: a generalised combination method. J. Geophys. Res. 73, 1299-1304.

Tanner, C.B. and E.R. Lemon. 1962: Radiant energy utilized in evapotranspiration. Agron. J. 54, 207-212.

Thornthwaite, C.W. and F.K. Hare. 1965: The loss of water to the air. Meteorol. Monogr. 6, 163-180.

Turner, J.C. 1968: Thermal response of a concrete slab to controlled daytime and nighttime cycles of radiation. Ph.D. Thesis, University of Wisconsin, Madison.

U.S., Department of Commerce, NOAA. 1972: Climatological Data, National Summary. Environmental Data Service, Ashville.

van Wijk, W.R. (Editor). 1963: Physics of Plant Environment. North-Holland Publishing Co., Amsterdam.

van Wijk, W.R. 1965: Soil microclimate, its creation, observation and modification. Meteorol. Monogr. 6, 59-73.

van Wijk, W.R. and W.J. Derksen. 1963: Sinusoidal temperature variation in a layered soil. In van Wijk, 1963, pp. 171-209.

Viswanadham, Y. and R. Ramanadham. 1967: The dependence of net radiation on short-wave radiation at Waltair. Indian J. Meteorol. Geophys. 18, 527-530.

World Meteorological Organisation. 1965: Measurement of radiation and sunshine. Guide to Meteorological Instrument and Observing Practices, Supplement No. 5 (chapter 9), WMO-No.8. TP.3.

Zuev, M.V. 1956: Formation of the microclimate of a cotton field. Hydrometeorol. Publ. House, Leningrad (in Russian).